Reply to the referee comments (RC1 and RC2) on "The non-hydrostatic global atmospheric model for CMIP6 HighResMIP simulations (NICAM16-S): Experimental design, model description, and sensitivity experiments" [gmd-2019-369], by C. Kodama et al.

Thank you for kindly reviewing the manuscript. We are pleased to have constructive and favorable comments from the two anonymous referees, that significantly improved the manuscript. Below we answer all the comments from the referees and show how the manuscript was revised following the referee comments.

In the followings, we show the revision in two steps: (1) changes suggested point-by-point by the referees (and some minor changes by us), as posted on 4 Aug 2020 as the AC1 (https://gmd.copernicus.org/preprints/gmd-2019-369/#discussion) and (2) changes to homogenize the manuscript and to improve English presentation, which are suggested by both referees. The former changes, explained in Page 2-43 in this response file, are the main part of the revision. Please see the above URL for the modified manuscript with the change history in (1). The latter changes, which do not affect the meaning of the manuscript, are summarized in Page 44 in this response file. The final revised manuscript with the change history from the original manuscript is attached in the end of this response file.

Step 1. Changes suggested point-by-point by the referees (and some minor changes by us)

In the following, the referee comments (RC1 and RC2) are shown in *maroon italic text* and the original and the revised texts are shown in *quoted purple italic text*. Note that some of the revised texts were overwritten in a minor way in the Step 2. All the section, page, line, figure and table numbers are based on the original manuscript except for authors' specific changes. References used in the responses are listed after the responses to RC1 and RC2.

In addition to the revisions suggested by the referees, we modified the manuscript to enhance its readability and clarity. Specifically, we

- added *"A double-moment cloud microphysics scheme is also available in NICAM.16 (Seiki and Nakajima, 2014; Seiki et al., 2014, 2015b; Satoh et al., 2018). However, the double-moment scheme was not used for the HighResMIP simulations and hence is not described in this paper."* in page 2, line 28 to contrast NICAM16-S with NICAM.16,

- replaceed title of the Section 2.2, *"Initial conditions"*, with *"HighResMIP simulations and sensitivity experiments"* to describe each experiment together in one place for readability,

- mooved *"As noted ... (see Section 3.6)"* in page 7, lines 2-5 to the second paragraph of Section 2.2 and slightly modify it as *"As noted in Section 3.7, we often prefer to use a slab ocean model with nudging toward the boundary SST rather than the fixed SST condition requested by the HighResMIP protocol because of better performance in the simulated precipitation pattern (Kodama et al., 2015), particularly with a horizontal mesh size of 14 km (Section 3.7). Therefore, both the fixed SST and slab ocean configurations (REFFIX and REFSLB runs, respectively) were tested in the sensitivity experiments."* (see **Response1-5** for the modified run name),

- deleted *"In the short-term sensitivity experiments ... unless explicitly specified."* in page 4, lines 30-33 to avoid duplication with the above sentences in Section 2.2,

- deleted *"Above the tropopause ... external conditions (Section 2.3)"* in page 10, lines 24-26 to avoid duplication with a sentence in Section 2.2,

- merged *"However, fixed SST simulation ... is often preferred."* in page 12, lines 21-22 and *"The introduction of the slab ocean model ... the cloud and precipitation system"* in page 12, lines 26-27, as *"However, the fixed SST simulation is known to cause severe bias in the horizontal distribution of clouds and precipitation system in the tropics (Kodama et al., 2015; Figure 13), and thus the use of the slab ocean model with a 7 day relaxation time is often preferred."* in page 12, line 26,

- replaced *"As the resolution increases, ... with different resolutions."* in lines 27-29, page 14 with

"As the resolution is increased, the percentage of the dynamics is increased and that of the cloud microphysics and turbulence processes is decreased because of their invariant time step interval among the models with different resolutions. An increase in the percentage of the land surface scheme in the simulations with higher resolution and with greater number of computational nodes seems to be caused by the node imbalance associated with land-ocean distribution." to add sufficient explanation on Figure 14 (Figure 18 in the revised manuscript),

- changed label of Figure 14 (e.g. *"gl8-p640"* -> *"NICAM16-8S (640 nodes)"*) for clarity, and
- removed the run name of the HighResMIP simulations (which is not used in the manuscript) and simplify Table 1, as shown below.

Table 1: List of HighResMIP simulations.

Source ID	HighResMIP Tier	Integration period	Initial atmospheric condition	Initial land condition
NICAM16-7S	1 & 3	1950–2050 (101-yr)	ERA-20C (Poli et al., 2016)	NICAM climatology
NICAM16-8S	1 & 3	1950–2050 (101-yr)	ERA-20C	NICAM climatology
NICAM16-9S	1	1950–1960 (11-yr)	ERA-20C	NICAM climatology
NICAM16-9S	1	2000–2010 (11-yr)	ERA-20C	NICAM climatology
NICAM16-9S	3	2040–2050 (11-yr)	The NICAM16-8S Tier 3 run	The NICAM16-8S Tier 3 run

In addition, we also did some minor modifications and updated the references.

Response to RC1

RC1-0) *The paper describes the new version of the global non-hydrostatic could-system resolving model, NICAM. The goal of the paper is twofold (1) evaluate several recent updates which brought the model from version NICAM.12 to the newest NICAM.16; (2) describe additional developments that were made necessary to adapt the model to the HighResMIP (CMIP6 endorsed MIP) protocol and that were introduced in the specific configuration NICAM16-S. The description and evaluation of those changes is valuable, and the paper will undoubtedly serve as a reference for NICAM16-S in studies analysing HighResMIP models. However, the paper does not investigate the impact of model resolution on the model climatology or only marginally. The reader understands only at the end of the paper that it is a deliberate decision and that the impact of resolution will be presented in another paper in preparation. This is a surprising choice, as most people would expect a reference paper of a new model configuration participating in HighResMIP to have horizontal resolution as its main focus. This makes me wonder if the present paper should not be limited to the description of the new model NICAM.16, leaving the developments for CMIP6 to another HighResMIP paper in which the impact of resolution would be investigated in more detail? The quality of the writing in unequal, some sections (e.g, abstract, introduction of section 3 and section 3.1) fall short of meeting the standards of a journal such as GMD, while other sections (e.g. 3.2, 3.3) are written in a very good english. I would recommend a collective effort to improve and homogenise the quality of the text throughout the manuscript. I believe the paper requires major revisions before being published and I would like the authors to answer more specifically the following comments :*

Response1-0) Thank you very much for your warm and constructive comments. We agree that horizontal resolution dependency is very interesting, and indeed the HighResMIP mainly focuses on it. However, we believe this paper should mainly focus on the description of the model updates and their impact on the simulated climatology (as suggested by RC2) for rapid publication as a reference of the model, considering many HighResMIP analysis papers will soon need such reference. So, we changed the title to show the focus more clearly (also see **Response1-2**). Also, we homogenized the whole manuscript and further use English proofreading service by native speakers (see the Step 2) after making the following modifications.

RC1-1) *Main comments :*

1) Could you please clarify both in the abstract and in the introduction to which MIP of CMIP6, NICAM will participate? Am I right to understand that they will only participate to HighResMIP and

Response1-1) Thank you for your comment that will clarify the position of NICAM in CMIP6. Your understanding is correct. NICAM group participates in HighResMIP but will not perform the DECK simulations in CMIP6. Though CMIP6 formally positions NICAM as a submodel of MIROC6 (Tatebe et al. 2019), two models are different in most ways and we will not introduce such formality to avoid further confusion. As suggested by the referee, we

- replaced most of the term *"CMIP6"* with *"HighResMIP"* (line 19 in page 1, lines 26 and 27 in page 2, lines 19 and 29 in page 5, line 14 in page 6, line 28 in page 13, line 15 in page 15, lines 2 and 4 in page 17, item name in page 30),
- deleted *"from CMIP6"* in page 12, line 11,
- added *"High Resolution Model Intercomparison Project (HighResMIP)"* after *"Coupled Model Intercomparison Project Phase 6 (CMIP6)"* in page 1, line 16 (instead of page 1, lines 19-20),
- inserted *"The DECK and CMIP historical simulations* (Eyring et al. 2016) *will not be performed at this time because NICAM is an atmosphere-only model while a coupled ocean-atmosphere model NICAM-COCO* (Miyakawa et al. 2017) *is being developed."* in page 2, line 28, and
- moved *"These model updates…as reported later"* in page 2, lines 28-29 to line 24 and replace *"often (but not always)"* with *"generally"* for logicality.

RC1-2) *2) My main issue is that the paper describes a new set-up for HighResMIP but there is absolutely no description of the impact of a change in resolution on the simulated climate. Even section 4, whose title announces an investigation of the dependency to horizontal resolution has only three lines about resolution (l. 7 to 10). Is there a convergence of those statistics when horizontal resolution is increased? I believe you need to inform the reader in the abstract that you do not discuss the impact of resolution.*

Response1-2) Thank you for your comments. As we have replied in **Response1-0**, this paper mainly aims to describe the model updates and their impacts on the simulated field. So, instead of rephrasing the abstract, we replaced *"sensitivity experiments"* with *"impacts of model updates"* in the title to clarify the main focus.

Even the resolution dependency is not a main focus of this paper, we admit the original description of

the resolution dependency was not satisfactory for many readers and needs improvement. First, we replaced Tables 5 and 6 with a new figure, Figure R1 below, in response to RC2 (see **Response2-1**). See Table 2 in **Response1-5** for revised run name shown in Figure R1. In the left part of Figure R1, the resolution dependency is graphically shown, although it is difficult to see convergence of the statistics in this narrow resolution range.

Following the referee comment and based on Figure R1 and Figure 11 (Figure 13 in the revised manuscript), we

- added more descriptions of the resolution dependency in Section 4, as *"As we have seen in Figure 13, precipitation pattern in the tropics is strongly resolution-dependent: more dominant double-ITCZ pattern and less intense local precipitation are simulated as the horizontal resolution is increased."* in page 14, line 9,

- further replaced *"Surface air temperature…in total cloud fraction"* in page 14, line 10-11 with *"Surface air temperature is slightly decreased as the resolution is increased (Figure 5a) in association with an increase in total cloud fraction (Figure 5g–i) and a decrease in net downward shortwave radiation at the surface (Figure 5k). Consistent with the precipitation, surface latent heat flux is decreased as the resolution is increased (Figure 5l). Dependency of surface sensible heat flux (Figure 5m) mostly cancels that of the surface latent heat flux."*, and

- added a brief description of precipitation intensity in Section 4, as shown in **Response1-6**.
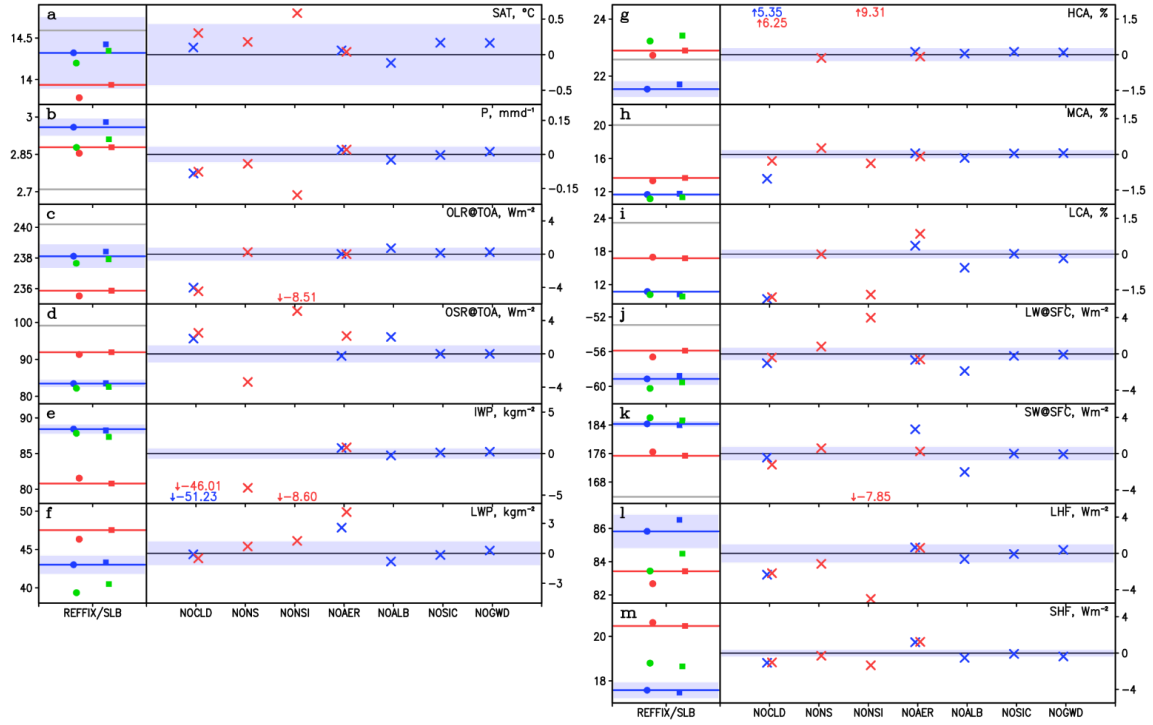
Figure R1 (Figure 5 in the revised manuscript): Global annual means of surface air temperature (a), precipitation (b), top-of-atmosphere (TOA) outgoing longwave radiation (OLR) (c), TOA outgoing shortwave radiation (OSR) (d), ice water path (e), liquid water path (f), high cloud amount (g), middle cloud amount (h), low cloud amount (i), surface net downward longwave radiation (j), surface net downward shortwave radiation (k), surface latent heat flux (l), and surface sensible heat flux (m). They are averaged over June 2004 – May 2005. Blue shading shows interannual variability (2σ, detrended) estimated from the HighResMIP NICAM16-7S run over 1950 – 2050 (Table 1). In the left part of each panel, global annual means simulated by NICAM16-7S (56 km mesh; blue), NICAM16-8S (28 km mesh; green), and NICAM16-9S (14 km mesh; red), which were performed under the fixed SST condition (filled circle; the REFFIX run in Table 2) and with the slab ocean condition (filled rectangle; the REFSLB run in Table 2), are plotted. Blue and red lines are the reference (REF) runs with 56 km mesh and 14 km mesh, respectively. Observational values taken from JRA-55 reanalysis (surface air temperature), GPCP (precipitation), CERES (radiation) and ISCCP (cloud amount) are shown as gray lines. In the right part of each panel, Differences between the REF run and each sensitivity run (the NOCLD, NONS, NONSI NOAER, NOALB, NOSIC, and NOGWD runs in Table 2) are shown. Those outside the value range are shown in digit.

RC1-3) *3) The HighResMIP protocol stipulates : "For a clean evaluation of the impact of horizontal resolution, additional tuning of the high-resolution version of the model should be avoided. The experimental set-up and de- sign of the standard resolution experiments will be exactly the same as*

for the high-resolution runs" (Haarsma et al., 2016). Have you performed specific retuning at each resolution? Please mention explicitly which resolution has been tuned first and what was the procedure and the parameters which were adjusted. In addition, mention any additional tuning specific of each resolution.

Response1-3) Thank you for pointing out the important aspect of the simulations. Of course, we agree to add these descriptions. Though we did not fine-tune the model due to heavy computational cost, we have tuned, albeit in a crude manner, parameters of sea ice thickness with 56 km mesh run and orographic gravity wave drag scheme with 14 km mesh run. All the other parameters in the physics schemes are the same as those described in their original scheme description papers. We did not retune the model at each resolution. Following the suggestions, we

- added *"Though we did not fine-tune the model due to heavy computational cost, we turned, albeit in a crude manner, parameters of sea ice thickness with NICAM16-7S (Section 3.7) and gravity wave drag scheme with NICAM16-9S (Section 3.8). We did not return the model at each resolution under the principles of the HighResMIP."* in page 6, line 29,

- replaced *"Based on an ocean model ... to diagnose ICE from SIC"* in page 12, lines 16-17 with *"Based on an ocean model result (H. Tatebe, personal communication), we performed a series of preliminary annual-scale experiments using NICAM16-7S, with SICCRT values of 1,600 and 3,200, respectively, to improve the surface air temperature over the Arctic. As a result of this crude tuning, SICCRT is set to 1,600 kg m⁻² in NICAM16-S. This leads to a significant reduction in the warm bias (Figure 11b vs. Figure 11c; blue vs. red lines in Figure 11d) and excess of TOA OLR (blue vs. red lines in Figure 12a) over the Arctic."*, and

- replaced *"it is roughly doubled as the horizontal mesh size is halved"* in page 13, lines 10-11 with *"was tuned first for NICAM16-9S to improve zonal mean zonal wind and then roughly halved as the horizontal mesh size is doubled."*

RC1-4) *4) You do not comment on the effect of changing the time step of the radiation scheme in NICAM16-7S to 9S (from 40 to 10min) and changing the time step of the dynamics from (240 to 60s) will have on the climatology (precipitation for instance in Table 6 and figure 11). In addition, and related to the previous question, how will changes in the time step be distinguished from the direct impact of increasing horizontal resolution in HighResMIP? Have you done additional sensitivity experiments? I believe the paper should address this issue.*

Response1-4) Thank you for your constructive comments. That's very interesting point. First, we modified the descriptions of the time integration for clarity following RC2 (**Response2-8**), as follows:

"The time step interval of the dynamics (Δt in Satoh et al. 2008) is set to 4, 2 and 1 min in NICAM16-7S, NICAM16-8S, and NICAM16-9S, respectively. The time loop in the model is based on the dynamics, and physics schemes with a time interval smaller or greater than that of the dynamics are subcycled or skipped, appropriately. Specifically, the time step interval of 30 s is used in the cloud microphysics scheme in NICAM16-7S, NICAM16-8S, and NICAM16-9S. The time interval of 1 min is used in the turbulence (mainly for planetary boundary layer) and land and ocean surface schemes in NICAM16-7S, NICAM16-8S, and NICAM16-9S. The radiation scheme, which requires considerable computational time, is executed every 40, 20, and 10 min in NICAM16-7S, NICAM16-8S, and NICAM16-9S, respectively. Gravity wave drag scheme is called at the same time step of the dynamics."

We additionally performed 56 km mesh sensitivity experiments, in which the time step interval of the dynamics (including gravity wave drag scheme) was set to 2 min (the DDT2M run) or 1 min (the DDT1M run) and that of radiation to 20 min (the RDT20M run) and 10 min (the RDT10M run) and analyzed their impacts, as Figure R2. We found the impact of the changes in the radiation time interval was negligible from the REFFIX, RDT20M and RDT10M runs. The impact of the time step interval of dynamics, as seen in Figure R2, was large in terms of the low cloud amount and shortwave radiation.
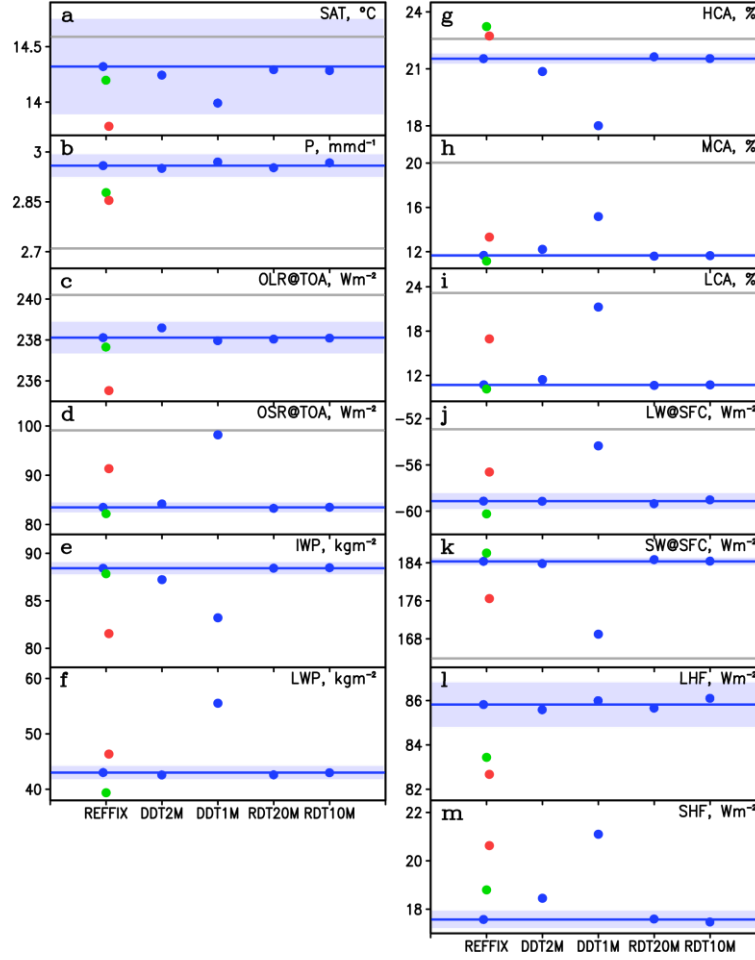
Figure R2 (Figure 16 in the revised manuscript): Same as the left part of Figure R1 but for the REFFIX, DDT2M, DDT1M, RDT20M, and RDT10M runs, respectively.

Based on these results, we inserted Figure R2 in the manuscript, added *"The DDT2M, DDT1M, RDT20M, and RDT10M runs were performed to check sensitivity of the simulated climate to the time interval of the model."* in the second paragraph of Section 2.2, and rephrased the overall Section 4, as followings:

"Understanding the dependency of horizontal resolution is a central interest of the HighResMIP. Figure 16 shows the global mean climate in NICAM16-7S (56 km mesh; blue circle), NICAM16-8S (28 km mesh; green circle), and NICAM16-9S (14 km mesh; red circle), along with a sensitivity of the time step interval of the dynamics (including gravity wave drag scheme) and the radiation scheme in the model. Note that dependency of the time step interval of the radiation scheme is negligible in terms of the global mean climate.

Global mean precipitation and TOA OLR are decreased as the horizontal resolution is increased (Figure 16b and c), consistent with a previous study using 3.5–14 km mesh NICAM (Miyakawa and Miura, 2019). The results do not strongly depend on the temporal resolution. As we have seen in Figure 13, precipitation pattern in the tropics is strongly resolution-dependent: more dominant double-ITCZ pattern and less intense local precipitation are simulated as the horizontal resolution is increased. The intense precipitation occurs less frequently in the higher-resolution runs (Figure 17), consistent with Noda et al. (2012) using older NICAM with 14–7 km mesh. The intense precipitation occurs more frequently in the model compared with the GPCP product (Noda et al., 2012), and it is consistent with Maher et al, (2018), who compared precipitation in GCMs without convection scheme with that in the GPCP product. Na et al. (2020) showed that the frequency of intense precipitation in the GPCP product is lower than that in the TRMM product, and 14-km mesh NICAM without convection scheme could realistically reproduce the intense precipitation observed by TRMM.

Low cloud amount is substantially underestimated, especially in the NICAM16-7S and NICAM16-8S runs (Figure 16i), leading to the underestimation of TOA OSR (Figure 16d). Consistently, the net downward shortwave radiation at the surface is decreased (Figure 16k) and the surface air temperature is slightly decreased (Figure 16a) as the horizontal resolution is increased. This horizontal resolution dependency of the low cloud amount and its related variables in terms of global mean could be reproduced, albeit overly, by changing the time step interval of the dynamics in the model. The low cloud amount is rather greater in the 56 km mesh run than that in the 14 km mesh run under the fixed time step interval of the dynamics (red circle in the REFFIX tun vs. blue circle in the DDT1M run in Figure 16). Also, the simulated TOA OSR is greater and closer to the CERES product in the 56 km mesh run compared with the 14 km mesh run with the same temporal resolution, though better performance in the simulated global mean TOA OSR in the 56 km mesh run is a result of a strong compensation between a negative bias off the subtropical west coasts of continents and the SH storm-track region and a positive bias in the rest of the lower latitudes (not shown). Such a result of horizontal resolution dependency under the fixed temporal resolution in TOA OSR is similar to Goto et al. (2020), who performed 14 km and 56 km mesh online-aerosol NICAM with the same time step interval of 60 s for the dynamics, turbulence, and surface schemes and 10 s for the cloud microphysics scheme. In HighResMIP, there is no protocol on the temporal resolution of the model, and the horizontal resolution dependency may include the effect of temporal resolution change in the HighResMIP models."

RC1-5) *5) There are four levels of labelling in the paper which makes it sometimes difficult to follow : (1) the different versions of NICAM.12 and 16, (2) the configuration for High-ResMIP NICAM16-S,*

(3) the various resolutions 7S, 8S, 9S, (4) and the sensitivity experiments (g, f, : : :). Labels are sometimes redundant NICAM16-S and g for instance refer to the same simulations. I believe you might need to keep both (to remain consistent with the naming already communicated to CMIP6) but you need to refer consistently to those different labels throughout the paper and I feel it is not always the case. -> NICAM.16-S rather than NICAM16-S is used in many places. -> Most sensitivity experiments are listed in Table 2 but not all. Could you give an experimental id to simulations described in section 3.5 and column Table 2e? -> The experimental id are not mentioned in the text after section 3.4 (only in tables and captions) whereas they are used in the text before section 3.3. Please can you at least recall once what they are (maybe when you list the sensitivity experiments at the beginning of the section).

Response1-5) Thank you for your constructive comment. In particular, the naming convention of *"g"*, *"f"*, which is internally used for computation and friendly only for us, was very confusing for the readers. So, we

- covered all the sensitivity experiments and rename the run names in more straightforward way such as *"REF"*, *"NOCLD"*, and *"NOAER"* runs, as shown in revised Table 2 below and
- useed these run names in Section 3 and 4, and Figure labels and captions.

"NICAM16-S" is the formal name for CMIP6 and all the *"NICAM.16-S"* are replaced with *"NICAM16-S"*.

Table 2: List of sensitivity experiments.

Run name	Descriptions
REFFIX	Same as NICAM16-S (with the fixed SST condition; Section 3.7).
REFSLB	Same as NICAM16-S but with the slab ocean model and nudging (Section 3.7).
REF	Alias name of the REFFIX run for 56 km mesh and the REFSLB run for 14 km mesh.
NOCLD	Same as the REF run but for using the previous cloud microphysics scheme used in NICAM.12 (Table 5; Section 3.2).
NONS	Same as the REF run but for considering only the spherical particle in the radiation table (Section 3.3).
NONSI	Same as the NONS run but for removing the interaction between radiation and cloud microphysics (Section 3.3).
NOAER	Same as the REF run but for prescribing zero natural and anthropogenic aerosol mass concentration for the radiation scheme and constant CCN of 50 cm^{-3} for the cloud microphysics scheme (Section 3.4).
NOANTAER	Same as the REF run but for prescribing zero anthropogenic aerosol mass concentration for the radiation scheme (Section 2.3).
NOLND	Same as the REF run but for omitting the effects of wetland and water accumulation on land ice (Section 3.5).
NOALB	Same as the REF run but for using the previous surface albedo values (Table 6; Section 3.6).
NOSIC	Same as the REF run but for using the previous SICCRT value of 300 kg m^{-2} (Section 3.7).
NOGWD	Same as the REF run but for switching off the subgrid-scale orographic gravity wave drag scheme (Section 3.8).
DDT2M	Same as the REF run but for setting the time step interval of the dynamics and gravity wave drag scheme to 2 min.
DDT1M	Same as the REF run but for setting the time step interval of the dynamics and including gravity wave drag scheme to 1 min.
RDT20M	Same as the REF run but for setting the time step interval of the radiation scheme to 20 min.
RDT10M	Same as the REF run but for setting the time step interval of the radiation scheme to 10 min.

RC1-6) *6) You make the choice not to use a convection scheme. This has been tested in several models at resolutions where convective processes are not yet resolved : please cite references which have tested a similar approach (see for instance Hohenegger et al 2020, https://www.jstage.jst.go.jp/article/jmsj/98/1/98_2020-005/_html/-char/en and references therein). You explain that not having a convective parameterization results in more patchy precipitation (page 6, line 27) and it would be interesting to illustrate that (see for instance Figure 2 in Maher et al, 2018, https://agupubs.onlinelibrary.wiley.com/doi/full/10.1002/2017GL076826)*

Response1-6) Thank you for your constructive comment. Agree to modify as suggested. We also made a plot of tropical precipitation intensity, Figure R3, and found more frequent intense precipitation in a coarser resolution model as expected from Noda et al. (2012) using 7-14km NICAM. Also, we confirmed that the frequency of occurrence of precipitation in NICAM is comparable with ConvOff in Figure 2 of Maher et al, (2018). Based on these results, we

- added *"Such approach has also been tested in other researchers besides the NICAM users (Maher et al., 2018; Hohenegger et al., 2020)."* in page 6, line 25,
- inserted Figure R3 after Figure 13, and
- added explanation of Figure R3 as *"The intense precipitation occurs less frequently in the higher-resolution runs (Figure 17), consistent with Noda et al. (2012) using older NICAM with 14–7 km mesh. The intense precipitation occurs more frequently in the model compared with the GPCP product (Noda et al., 2012), and it is consistent with Maher et al, (2018), who compared precipitation in GCMs without convection scheme with that in the GPCP product. Na et al. (2020) showed that the frequency of intense precipitation in the GPCP product is lower than that in the TRMM product, and 14-km mesh NICAM without convection scheme could realistically reproduce the intense precipitation observed by TRMM."* in Section 4.
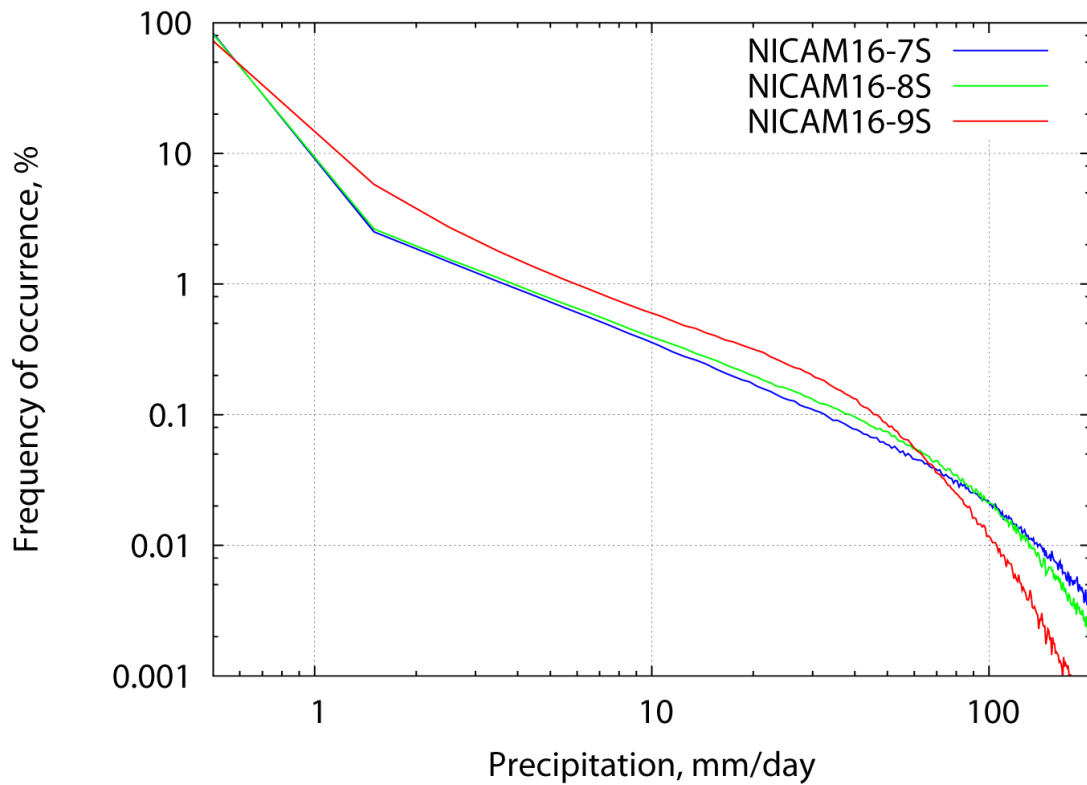

Figure R3 (Figure 17 in the revised manuscript): Frequency of occurrence (%) of daily mean precipitation binned with an interval of 1 mm day^{-1} during 01 June 2004 – 31 May 2005 averaged over 15°S–15°N. The REFFIX runs with NICAM16-7S, NICAM16-8S, and NICAM16-9S are shown in black, green, and red lines. The data are re-gridded to 1 degree in longitude and latitude before sampling.

RC1-7) *7) The beginning of the introduction is a bit confused, both climate sensitivity and climate*

impacts are mentioned and it is unclear why. What not saying from the beginning that the accurate treatment of cloud requires high-resolution cloud resolving models. You could also cite the review paper by Bony et al. 2015, https://www.nature.com/articles/ngeo2398) in this paragraph.

Response1-7) Agree. We simplified the beginning of the introduction by replacing *"Natural disasters ... Shukla et al. 2009)"* in page 2, lines 1-6 with *"The accurate treatment of such interaction between clouds and circulation requires high-resolution global cloud resolving models (Bony et al., 2015; Satoh et al. 2019). <PARAGRAPH GAP> This as well as an increasing demand from society to project tropical cyclones and extremes motivated us to perform…"*

RC1-8) *8) Section 2.2: Please be more specific on the initial land conditions in NICAM16-7S and NICAM16-8S. Are they derived in a similar way as NICAM16-9S? this is not clear.*

Response1-8) Agree. We replaced *"The initial land condition in the past and present-day simulations was taken from ..."* in page 4, lines 4-5 with *"For the simulations starting from 1 January 1950 or 1 January 2000, the initial land condition prescribed for NICAM16-7S, NICAM16-8S, and NICAM16-9S was taken from ..."*.

RC1-9) *9) The change of SICCRT between the AMIP and slab experiments is very large (a factor 5!). Could you please explain if there is any resulting inconsistency between the AMIP and slab experiments for SIC, which I believe is a standard diagnostic of CMIP6?*

Response1-9) Sorry for the confusion here. Our original description was not exact and we made clear description of the ocean treatment. The sea ice was fixed to the boundary condition not only in the AMIP experiment but also in the slab experiments. In this study, SICCRT value of 1,600 was used for both Eq. (2) and Eq. (3) in both the AMIP and the slab experiments. So, the SIC is equivalent between the two types of experiments by definition. Only a difference between the AMIP and the slab experiments in this study is the nudging relaxation time of SST (0 for AMIP and 7 days for the slab experiments). Based on these, we

- replaced *"A simple nudging technique ... 7 days"* in page 12, lines 6-7 with *"A simple nudging technique is used to force the predicted SST and ICE toward their reference states with a relaxation time of τ_{SST} and τ_{ICE}, respectively. Specifically, τ_{SST}=7 days and τ_{ICE}=0 (i.e., ICE was fixed to the boundary condition) were used in the slab ocean experiments of this study and in the previous climate simulation with NICAM.12 (Kodama et al., 2015). Both τ_{SST} and τ_{ICE} were set to*

zero in the fixed SST/ICE experiments including the HighResMIP simulations. <PARAGRAPH GAP> In the slab ocean model implemented ...",

- deleted *"This fixed SST/SIC ... in the slab ocean model."* in page 12, lines 19-21,
- replaced *"where SICCRT is set to 300 kg m^{-2}."* in page 12, line 9 with *"where SICCRT is a parameter in kg m^{-2}.",*
- replaced "for Eq. (3), the same as that used in Eq. (2)." in page 12, lines 14-15 with *", considering Eq. (2).",* and
- replaced *"for Eq. (3) in NICAM16-S to diagnose ICE from SIC."* in page 12, line 7 with *"in NICAM16-S".*

RC1-10) *10) Page 15 : you indicate that you will share regridded data with CMIP6 at resolution of 1degree or coarser. Will you be able to provide higher-resolution fields on demand? HighResMIP has a special focus at fine scale features, such as tropical cyclones, extreme precipitation, for which high-resolution data might be needed.*

Response1-10) Sorry also for the confusion here. The high-resolution data requested by HighResMIP are available through ESGF, and low-resolution data are provided on demand. So, we added *"Note that the high-resolution data requested by HighResMIP are or will be available through the Earth System Grid Federation (ESGF). All the other data (low-resolution, monthly-mean, special variables and so on) are or will be available on request from the corresponding author."* after page 15, line 25. We also found a small error in the code and data availability section and replaced *"HighResMIP Tier 1 (3) simulation data are (and will be)"* in page 16, lines 25-26 with *"HighResMIP product run data are or will be".*

RC1-11) *Specific comments :*
page 1, line 2 : Experimental -> experimental
page 1, line 6 : the Coupled Model Intercomparison Project Phase 6

Response1-11) Agree. We modified them as suggested.

RC1-12) *page 1, line 17 : the land surface model (and everywhere thereafter)*

Response1-12) Agree. We inserted *"surface"* as suggested, specifically, at line 17 in page 1, line 21

in page 2, lines 4, 5, and 12 in page 11, line 7 in page 16, and line 2 in page 45.

RC1-13) *page 1, line 18 : an improvement of the coupling*

page 1, line 19 : and the radiation schemes; ... to follow the protocol of the CMIP6 High ...

page 1, line 21 : the impacts of the various model updates

page 1, line 23 : over Africa and South Asia

page 1, line 29 : redistributes mass

page 2, line 22 : non-sphericity of ice particles

Response1-13) Agree. We changed them as suggested.

RC1-14) *page 2, line 26 : "That is, the interfaces" => unclear, please rephrase*

Response1-14) Agree. We replaced *"NICAM.16 has been further modified ... have been implemented"* in page 2, lines 24-27 with *"NICAM.16 has been further modified to support the external forcings of natural and anthropogenic aerosols and the solar cycle defined in the Coupled Model Intercomparison Project Phase 6 (CMIP6) High Resolution Model Intercomparison Project (HighResMIP) protocol (Haarsma et al., 2016)."* for clarity and simplicity.

RC1-15) *page 3, line 9 : NICAM17-nS -> NICAM16-nS.*

page 3, line 15: including tropical cyclones

page 3, line 31: using -> with

page 4, line 4: The initial land conditions ... were

page 4, line 6: under present-day conditions ... the last 5 years of data

page 4, line 14 : are derived from "g" ... 1 une 2004 to ensure consistency with previous NICAM studies

Response1-15) Thank you! Agree. We changed them as suggested. For the last suggestion, we rephrased *"These experiments ... in the previous NICAM studies"* in page 4, lines 14-16 with *"These sensitivity experiments were started from 1 June 2004 and integrated for 1 year. An exception was the NOLND and the REF runs, which were performed for 4 years to make land surface state settle down. The initial date was chosen to ensure consistency with previous NICAM studies"* in association with RC2 (**Response2-9**).

RC1-16) *page 4, line 19 : Is SST an external forcing? I don't think it is what people mean by external forcing.*

Response1-16) Agree. We replaced *"External forcings"* with *"External forcings and boundary conditions"* in page 4, lines 19 and 20. Also, we replaced *"external conditions"* with *"boundary conditions"* in page 12, line 19.

RC1-17) *page 4, line 32 : fixed SST conditions ere used in the 56km meh run*
page 4, line 33 : was used in the 14 km mesh runs

Response1-17) Agree, but we deleted this part to avoid duplication (see the additional modification in page 3 of this response).

RC1-18) *page 5, line 4 : Future change in SST is somewhat similar to the El Nino pattern => personally I don't think so, there is a warming everywhere! You could mention with a larger warming in the equatorial Pacific.*

Response1-18) Thank you for your comments. Our description here was crude and necessary to be improved. We replaced *"Future change in SST ... the polar regions."* in page 5, lines 4-6 with *"The SST in the 2040s has larger values almost everywhere compared with that in the 2000s, especially in the midlatitudes, the equatorial eastern Pacific, the tropical Atlantic Ocean, and the edge of the Arctic regions."*

RC1-19) *page 5, line 9 : ICE is nearly*
page 5, line 11 : prescribed in the model
page 6, line 8 : a smoother is applied -> a spatial filter is applied to smooth

Response1-19) Agree. We changed them as suggested.

RC1-20) *page 6, line 18: could you give a reference for the various schemes?*

Response1-20) Agree. We added not only references but also brief descriptions of each scheme following RC2. Please see **Response2-11** for details of the changes.

RC1-21) *page 6, line 21 : sentence is too long.*

Response1-21) Agree. We simplified page 6, lines 21-25 as *"While most climate models use convection and large-scale condensation schemes even for a mesh size around 14 km, we use the cloud microphysics scheme to represent interactions between clouds and circulation in an explicit way. This not only lowers the cost of development, but also reduces the uncertainty of the results arising from highly arbitrary tuning."*

RC1-22) *page 6, line 32 : global means -> global mean climate*

Response1-22) Agree. We changed it as suggested.

RC1-23) *page 7, line 10 : We used ... -> the sentence is unclear. Do you use it to show improvements or because it shows improvements?*

Response1-23) Thank you for your comment. Agree. We replaced *"to show the improvements in the climatology of the NICAM simulation"* in page 7, lines 10-11 with *"and found improvements in the climatology of the NICAM simulation, as will be shown later."*

RC1-24) *page 7, line 13 : was originated -> originated*
page 7, line 21 : is the key -> represent a significant change
page 7, line 26 : comparing -> compared
page 7, line 32 : accounts for the snow category [this is a typical example where a simple grammar mistake can loose the reader. I thought a new special category was created.]
page 8, line 5 : midlatitude storm-track
page 8, line 7 : 399¥%, respectively
page 8, line 10 : the accretion
page 8, line 15 : In addition, the decrease

page 8, line 21 : The low cloud amount is increased as a result of a compensation ... in medium and thick clouds and a decrease in thin clouds.

page 8, line 28 : check punctuation

page 8, line 31 : consistent assumptions of coupling ..... can reduce the model biases

Response1-24) Agree. We changed them as suggested.

RC1-25) *page 10, line 8-9 : reference needed.*

Response1-25) Agree. For the sake of accuracy and completeness of description, we

- replaced *"Finally, ... high pressure belt"* in page 10, lines 8-9 with *"Finally, NICAM16-S still shows strong negative biases in TOA OLR over the tropical to subtropical regions and TOA OSR over the subtropical high-pressure belt compared with the CERES product (Figure 8, black vs. red lines), and these biases are qualitatively similar to those simulated by NICAM.12 (Kodama et al. 2012).",*

- added *"Unlike NICAM.12, a strong negative bias of TOA OSR is also prominent over the Arctic region, and this seems to relate to an update (reduction) of the surface albedo introduced in Section 3.6."* in page 10, line 14,

- inserted a new figure, Figure R4, after Figure 10 (as Figure 12 in the revised manuscript) and insert *"In terms of the TOA radiation budget, OSR is worsen by a few watt per square meter (Figure 5d), that arises from the polar regions (Figure 12b; green vs. red lines)."* after page 11, line 32, and

- fixed typo by deleting *"become stronger"* in page 10, line 12 and by replacing *"the increased net upward shortwave"* in page 11, line 26 with *"the resulting decreased net upward shortwave"*.
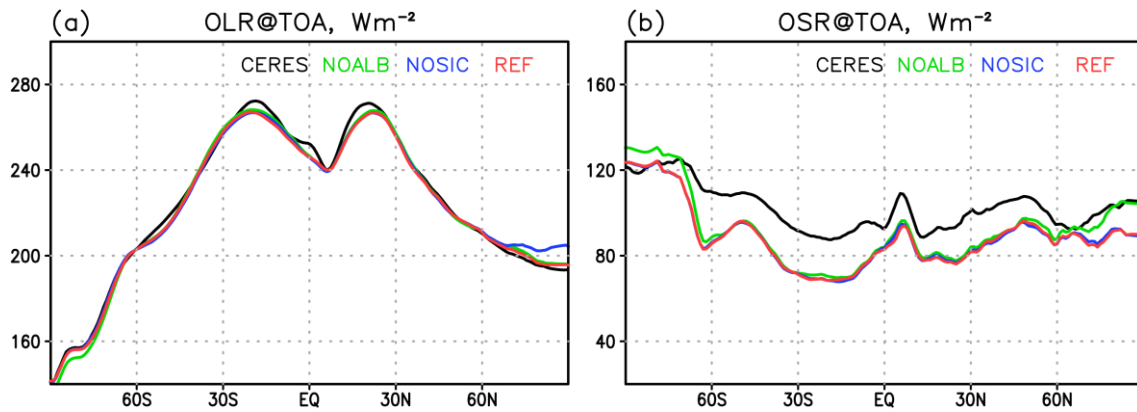
Figure R4 (Figure 12 in the revised manuscript): Same as Figure 8 (Figure 7 in the original manuscript) but for the NOALB run (green), the NOSIC run (blue), and the REF run (red), respectively, by NICAM16-7S.

RC1-26) *page 11, line 5 : capital letters for the model name.*

Response1-26) Thank you. In association with **Response2-11** and **Response1-12**, we replaced *"A land model named as minimal advanced treatments of surface interaction and runoff (MATSIRO; Takata et al. 2003), ..."* with *"The land surface land model, MATSIRO (Takata et al. 2003), ..."*.

RC1-27) *page 11, line 7 and line 10 : the model name is NICAM16-S not NICAM.16-S (the same mistake occurs in other places)*

Response1-27) Thank you for pointing out the typo. We changed them as suggested.

RC1-28) *Figure 9 : is it possible to have an idea of the fractional reduction of the bias?*

Response1-28) At this stage, it is difficult to say reduction of the bias only by our results here because of the short integration period, as we had written in page 11, line 16. The only clear result in Figure 9 was an increase in soil moisture, which is consistent with Nitta et al. (2017). The impacts of precipitation and temperature were not so clear. Based on these, we
- deleted Figures 9b and c,
- rephrased the second paragraph of Section 3.4 as *"Figure 10 shows an impact of the land surface model update on soil moisture in boreal summer. The soil moisture is increased over most of the*

Eurasian and the North American continents as expected from Nitta et al. (2017), particularly in the Siberia and around the Great Lakes. Though it is expected from Nitta et al. (2017) that the increased soil moisture leads to an increase in precipitation and a decrease in surface air temperature, the resulting impacts on the precipitation and surface air temperature are still unclear (not shown). It is difficult to show robust reduction of the biases at this stage, and longer integration is needed to assess these impacts appropriately.", and

- replaced *"Overall, ... over the continent"* page 16, line 7 with *"Overall, the soil moisture increases over most of the Eurasian and the North American continents."*

RC1-29) *page 12, line 5 : The depth of the slab*

Response1-29) Could you please comment it again? Seemingly the comment was broken due to a technical reason.

RC1-30) *End of section 3.6 : please mention when a result is not shown.*

Response1-30) Also, could you please comment it again?

RC1-31) *page 13, line 2,3 : the precipitation -> precipitation; line 5 : remove coma*
page 13, line 8 : is tested -> is used / or / introduced in the model (and please mention that no gravity wave drag was used in NICAM.12)
page 13, line 21 : it may not be a wise choice -> introducing such a gravity wave drag scheme will not necessarily lead to an improvement of the simulated climate.

Response1-31) Agree. We changed them as suggested. Also, we added *"No gravity wave drag scheme is used in NICAM.12."* in page 13, line 8.

RC1-32) *page 14, line 3-7 : this is a repetition of things which have already been introduced in previous sections.*

Response1-32) Agree. We removed this and also removed *"The most noticeable change from the previous simulation in terms of the global mean is the IWP. As described in Section 3.1, IWP is*

drastically increased by the update of cloud microphysics scheme.” in page 14, line 11-12 to avoid repetition. We changed name of Section 4 from *“Preliminary evaluations with observations including dependency of horizontal resolution”* to *“Horizontal and temporal resolution dependency”* to reflect the above change as well as changes in **Response1-6** and **Response1-4**.

RC1-33) *page 14, line 9 : NICAM-7S -> NICAM16-7S*

Response1-33) Agree. We changed it as suggested.

RC1-34) *page 14, line 19 : greater than SYPD ??? How many?*

Response1-34) We replaced *“The actual wall clock time ... the Earth Simulator 3”* in page 14, lines 18-20 with *“In NICAM16-8S and NICAM16-9S, the actual SYPD was a few times smaller than the SYPD shown in Table 7 for NICAM16-8S and NICAM16-9S.”* Also see **Response1-35**.

RC1-35) *page 14, line 20 : please mention the number of cores per node (I guess 4 from the table 9?)*

Response1-35) Yes and agree. Following the suggestion and considering readability, we rephrased the first paragraph of Section 5.1 as *“Table 7 shows computational setting and the simulation year per wall-clock day (SYPD) of the simulations by NICAM16-S on the Earth Simulator 3 (NEC SX-ACE). The Earth simulator 3 has 5,120 nodes in total for computation and each computation node has 4 cores. We often use 10, 40, and 160 computation nodes to run NICAM16-7S, NICAM16-8S, and NICAM-9S, respectively, considering a balance between computational efficiency and wall clock time. An exception was NICAM16-8S for the HighResMIP simulation, in which 160 computation nodes were used to finish the 101-year product run within a realistic time. A file staging option ...”*.

RC1-36) *page 15, line 2 : in an icosahedral grid -> on the model’s native icosahedral grid ?*

Response1-36) Yes. We changed it as suggested.

RC1-37) *page 15 : Summary section : no capital after “ : “ in this section*

Response1-37) Agree. We changed them as suggested and removed *"description"* in page 15, line 28 to follow the suggestion. For page 29, line 4, the overall footnote in Table 2 was deleted, as replied in **Response1-5** and **Response2-1**.

RC1-38) *page 32 : global mean impacts -> difference of global mean variables between control "g" and sensitivity experiments*

Response1-38) Thank you for your comment. Table 5 in page 32 is deleted, as replied in **Response2-1** and **Response1-2**.

RC1-39) *page 32 : it would be nice if you could highlight in bold where the difference is statistically significant?*

Response1-39) Thank you for your constructive comment. Instead of performing a formal statistical test, we calculated an interannual variability using 101-year NICAM16-7S HighResMIP run (Table 1) and added them as shadings in Figure R1 (Figure 5 in the revised manuscript; see **Response1-2**).

RC1-40) page 33 : NICAM.16-S -> NICAM16-S and phrase the legend similarly to Tab 5.

page 34 : NICAM.16-S -> NICAM16-S

Response1-40) Thank you. We changed them as suggested.

RC1-41) *page 34 : line 5, rephrase the end of the sentence. What does ad hoc mean here?*

Response1-41) Thank you. Agree. We replaced *"to reproduce ... ad hoc"* in page 34, lines 5-6 with *"to tune the model to the observed high cloud signals over the tropics."* for clarity.

RC1-42) *page 36 : what does Output size in latitude-longitude grid per year TB means here?*

Response1-42) Thank you. We deleted it from the table, since they were not used in the body text.

RC1-43) page 38 : The same as -> Same as
page 39 : prescribed in the model ; decadal running mean}

Response1-43) Agree. We changed them as suggested.

RC1-44) *page 40: NICAM16-7 -> NICAM16-7S. Could you add a reference in this figure?*

Response1-44) Agree. We
- added *"NOANTAER"* and *"Forcing"* to the title of Figure 4a and b, respectively,
- added a description of NOANTAER run in the revised Table 2 (see **Response1-2**) as *"Same as the REF run but for prescribing zero anthropogenic aerosol mass concentration for the radiation scheme (Section 2.3)."*, and
- modified the caption of Figure 4 as *"Annual mean natural aerosol optical thickness averaged for June 2004 – May 2005 simulated by NICAM16-7S (NOANTAER run in Table 2). ..."*.

RC1-45) *page 41 : line 3 : "g3 and g, respectively".*

Response1-45) Agree. We changed them as suggested.

RC1-46) *page 41 : units of the vertical axis?*

Response1-46) Thank you. The unit is kilometer. We added *"km"* in Figure 5 and added *"in km"* between *"altitude"* and *"above sea level"* at the end of the figure caption.

Response to RC2

RC2-0) *In this manuscript, the authors detail the particular configuration of NICAM used for the High Resolution Model Intercomparison Project (HighResMIP). This is using NICAM16 instead of NICAM12, a previous version used for CMIP-class experiments. Updates are described in components such as microphysics and the land surface. The mean climatology at three different resolutions (56, 28, and 14km) and a few basic sensitivity experiments are discussed. The authors finish by discussing computational performance and post-processing needs.*

I assume the primary purpose of this manuscript is to detail the particular configuration of NICAM that is used in HighResMIP so it can serve as a reference for scientific papers using such datasets. As such, the paper really doesn't describe any new science; rather, just discusses particular aspects of a specific model configuration. This seems acceptable for a journal such as GMD, even if the results are overly novel from a scientific perspective.

I find it to feel somewhat hastily thrown together. Some details regarding NICAM16 are discussed in detail, others are left to the reader to try and track down. Data isn't always presented in the cleanest manner, making jumping from figure to table a bit difficult. Some figures need work, including axis labels and resizing. In some ways, the manuscript feels approximately 75¥% finished, thrown together a bit quickly with some holes that need to be filled and smoothed over before publication. There also is a bit of a mix of 'model description' and then 'high-resolution evaluation,' although the authors then note that more formal climate evaluation is left for future work. I would perhaps focus most of the time in this manuscript on explicitly defining the precise design choices for the contributed runs.

I recommend major revisions to clean many pieces of this up and make it more useful as a basic reference for future users of HighResMIP data who wish to learn more about how NICAM operates.

The manuscript reads somewhat disjointed, as if multiple authors were e-mailed and asked to 'provide a paragraph or two' and it was eventually stitched together. Some passages are riddled with grammatical errors, while others are much more cleanly written. Although it didn't rise to the level of making the manuscript illegible, I recommend a thorough read-through by one or two proficient English speakers before submission to clean as many of these up before proofreading as possible. Even small corrections to tense and terminology would make for a much more pleasant read.

Response2-0) Thank you very much for your warm and constructive comments. Following the suggestions, we improved the presentation of figures and descriptions of the model as follows. We

tried to homogenize the whole manuscript and further used English proofreading service by native speakers (see the Step 2) after making the following modifications.

RC2-1) *Major comments*

Tables 5 and 6 need to be better presented. I am not sure why Table 5 only shows differences between model simulations and Table 6 shows a mean climatology for the three different resolutions. Without the mean values, the numbers in Table 5 are relatively meaningless, as it is tough to gauge how large the changes are relative to the base (reference) state and whether these changes are moving values towards or away from observations at the global level. The easiest thing to do here would be to effectively combine Tables 5 and 6, with mean climatology presented in additional columns, so it is trivial for the reader to mentally process what the difference in the sensitivity experiments (e.g., g-g3, etc.) actually mean.

Response2-1) Thank you for your constructive comments. We admit Tables 5 and 6 are very confusing and need improvement. One reason for the confusion may arise from the different reference experiments among different sensitivity test. So, we first rerun a few sensitivity experiments (f1d, f1, and f runs in the original manuscript) so that all the impacts could be seen as a deviation from the g runs (hereafter REF runs). Then, naming convention of the sensitivity experiments (e.g. g, g3, g6, …) in Table 2 was changed to more straightforward one such as REF, NOCLD, NOAER, etc., as shown in Table 2 below. We added *"we used the REFFIX run with 56 km mesh and the REFSLB run with 14 km mesh as the reference (REF) runs for the other sensitivity experiments."* and *"Impacts of the model updates described in Section 3 on the simulated climate states were individually tested by switching off each update."* in page 4, around line 13.

Table 2: List of sensitivity experiments

Run name	Descriptions
REFFIX	Same as NICAM16-S (with the fixed SST condition; Section 3.7).
REFSLB	Same as NICAM16-S but with the slab ocean model and nudging (Section 3.7).
REF	Alias name of the REFFIX run for 56 km mesh and the REFSLB run for 14 km mesh.
NOCLD	Same as the REF run but for using the previous cloud microphysics scheme used in NICAM.12 (Table 5; Section 3.2).
NONS	Same as the REF run but for considering only the spherical particle in the radiation table (Section 3.3).
NONSI	Same as the NONS run but for removing the interaction between radiation and cloud microphysics (Section 3.3).
NOAER	Same as the REF run but for prescribing zero natural and anthropogenic aerosol mass concentration for the radiation scheme and constant CCN of 50 cm^{-3} for the cloud microphysics scheme (Section 3.4).
NOANTAER	Same as the REF run but for prescribing zero anthropogenic aerosol mass concentration for the radiation scheme (Section 2.3).
NOLND	Same as the REF run but for omitting the effects of wetland and water accumulation on land ice (Section 3.5).
NOALB	Same as the REF run but for using the previous surface albedo values (Table 6; Section 3.6).
NOSIC	Same as the REF run but for using the previous SICCRT value of 300 kg m^{-2} (Section 3.7).
NOGWD	Same as the REF run but for switching off the subgrid-scale orographic gravity wave drag scheme (Section 3.8).
DDT2M	Same as the REF run but for setting the time step interval of the dynamics and gravity wave drag scheme to 2 min.
DDT1M	Same as the REF run but for setting the time step interval of the dynamics and including gravity wave drag scheme to 1 min.
RDT20M	Same as the REF run but for setting the time step interval of the radiation scheme to 20 min.
RDT10M	Same as the REF run but for setting the time step interval of the radiation scheme to 10 min.

Just merging Tables 5 and 6 leads to a large table and may cause another confusion. So, we instead inserted a new figure, Figure R5, after Figure 4 to graphically summarize impact of the updates in more straightforward way. We added *"Figure 5 (right part of each panel) summarizes impacts of the model changes on the global mean climate. All the significant impacts of the model changes shown here can be qualitatively reproduced even if the analysis period was limited to the last six months (not shown). The REFFIX and REFSLB runs with each horizontal mesh and the observations are shown at the left part of each panel in Figure 5. We will discuss these impacts along with the details of the model updates later in this section."* in page 6, line 31. Also see the related change in **Response2-2**.
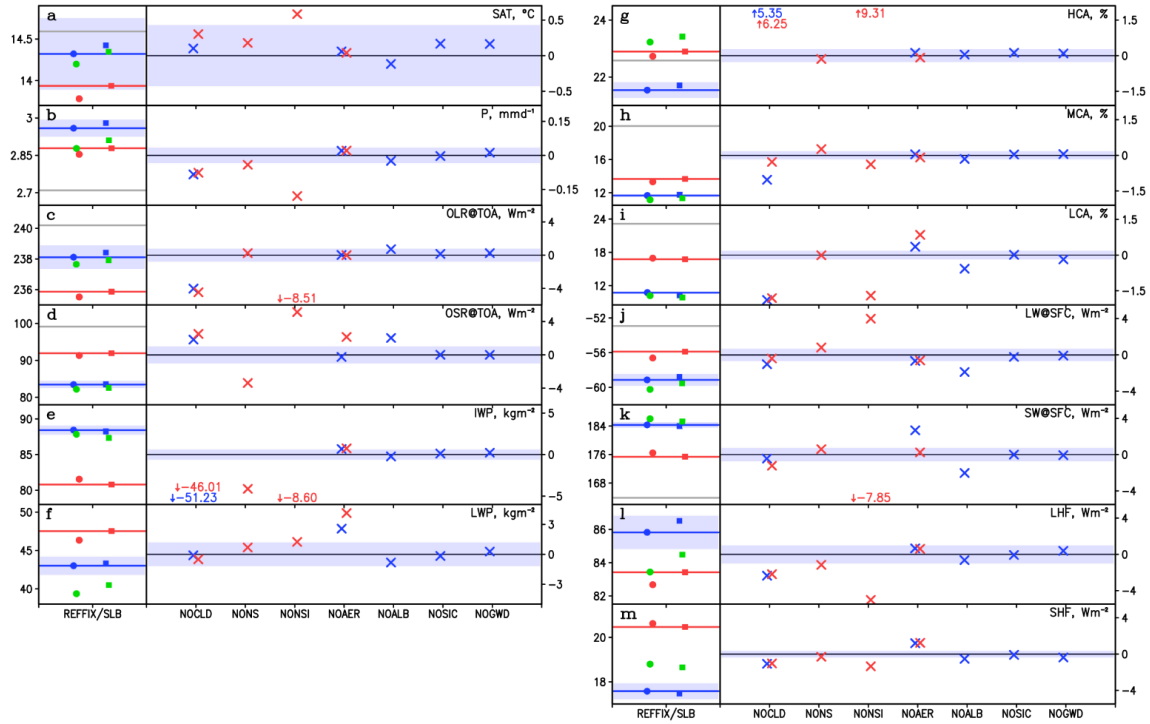
Figure R5 (Figure 5 in the revised manuscript): Global annual means of surface air temperature (a), precipitation (b), top-of-atmosphere (TOA) outgoing longwave radiation (OLR) (c), TOA outgoing shortwave radiation (OSR) (d), ice water path (e), liquid water path (f), high cloud amount (g), middle cloud amount (h), low cloud amount (i), surface net downward longwave radiation (j), surface net downward shortwave radiation (k), surface latent heat flux (l), and surface sensible heat flux (m). They are averaged over June 2004 – May 2005. Blue shading shows interannual variability (2σ, detrended) estimated from the HighResMIP NICAM16-7S run over 1950 – 2050 (Table 1). In the left part of each panel, global annual means simulated by NICAM16-7S (56 km mesh; blue), NICAM16-8S (28 km mesh; green), and NICAM16-9S (14 km mesh; red), which were performed under the fixed SST condition (filled circle; the REFFIX run in Table 2) and with the slab ocean condition (filled rectangle; the REFSLB run in Table 2), are plotted. Blue and red lines are the reference (REF) runs with 56 km mesh and 14 km mesh, respectively. Observational values taken from JRA-55 reanalysis (surface air temperature), GPCP (precipitation), CERES (radiation) and ISCCP (cloud amount) are shown as gray lines. In the right part of each panel, Differences between the REF run and each sensitivity run (the NOCLD, NONS, NONSI NOAER, NOALB, NOSIC, and NOGWD runs in Table 2) are shown. Those outside the value range are shown in digit.

by design choices and not internal variability. How are the authors confident they are not confounding these?

Response2-2) Thank you for pointing out an important issue. We added caution in the manuscript. In our experience using NICAM, even a monthly-scale integration is often valuable to see qualitative (and sometimes quantitative) features of the simulated key climatology such as cloud, precipitation, and radiation and their sensitivity to model changes (e.g., Noda et al. 2010; Kodama et al. 2012). Such idea has also been supported by many previous studies (e.g., Phillips et al. 2004; Williams et al. 2013; Hohenegger et al. 2020). Also, we tried to distinguish the impacts of the model changes from internal variability by diagnosing interannual variability simulated by NICAM16-7S. We further confirmed that Figure R5 is not significantly affected by limiting the analysis period to the last six months, as Figure R6 below. Based on these considerations, we

- added *"The integration period of 1 year and even less is sufficient to evaluate basic state of the atmosphere such as cloud, precipitation, radiation, and temperature   (e.g., Phillips et al., 2004; Noda et al., 2010; Kodama et al., 2012; Williams et al., 2013; Miyakawa et al. 2018; Miyakawa and Miura, 2019; Stevens et al., 2019; Hohenegger et al., 2020) and tropical variability including diurnal cycle, tropical cyclones, and MJO (e.g., Sato et al., 2009; Kinter et al., 2013; Stevens et al., 2019; Matsugishi et al., 2020). An interannual variability of the NICAM16-7S run (Table 1) over 101 years was diagnosed to distinguish the impacts of the model changes from internal variability in a rough manner."* in page 4, line 16,
- added interannual variability of the 56 km mesh NICAM simulation as shadings in Figure R5 (**Response2-1**), that was inserted in the manuscript as Figure 5 in the revised manuscript and
- added *"We confirmed that all the significant impacts of the model changes shown here can be qualitatively reproduced even if the analysis period was limited to the last six months (not shown)."* in page 7, around line 1.
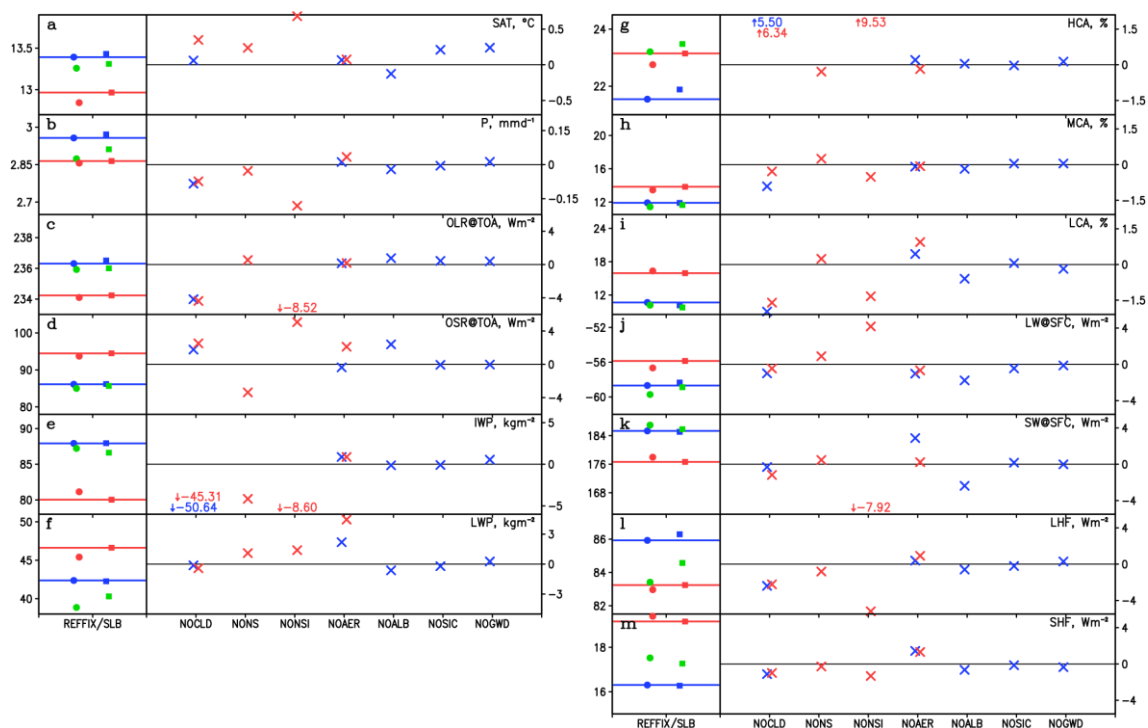
Figure R6: Same as Figure R5 but for limiting the analysis period to the last six months (December 2004– May 2005). Note that the shading in Figure R5 is omitted here.

RC2-3) *Page 9, Line 28. I cannot find the g9 simulations in the tables, is there a reason they are not included like the other sensitivity experiments?*

Response2-3) Originally, the g9 (and g9a) runs were not included in the Tables 5 and 6 to avoid confusion, because the impact of the model changes was very clear and they had been performed just for three months. Now, the g9 and g9a (the NONS and NONSI runs in the new version; see the revised Table 2 in **Response2-1**) runs were finished for one year, and we added them to Figure R5 and extended Figure 7 to annual mean, as shown below.
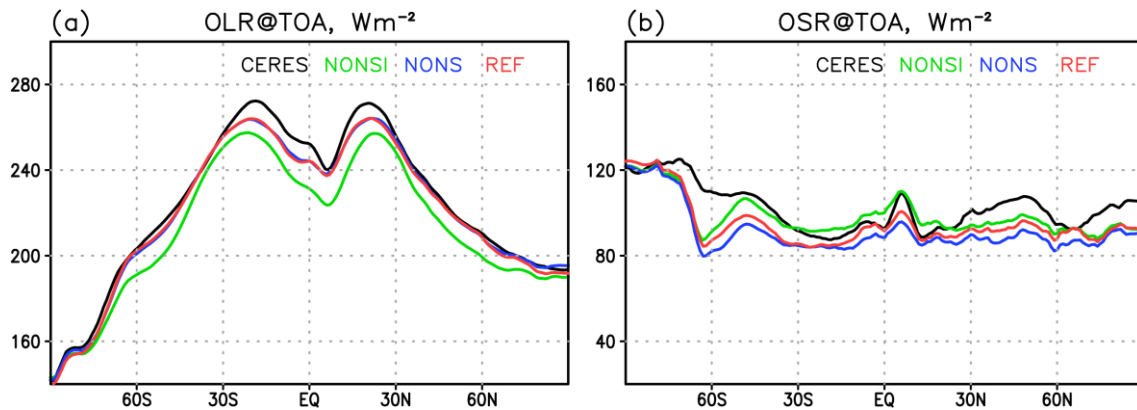
Figure 7 (Figure 8 in the revised manuscript): Annual mean of OLR (a) and OSR (b) at TOA, in W m⁻²,

for CERES product (black) and NICAM16-9S runs. Green, blue, and red lines show the NONSI, NONS,

RC2-4) *The naming convention is fairly confusing and there are times when names are redundant and refer to the same simulation (i.e., the 'g' simulation refers to a control run, which is occasionally referred to as NICAM16 or NICAM16-S). Is there a particular reason why these naming conventions are used. Are there ways to simplify this so that they are more clear 'in-text.'*

Response2-4) Thank you for your constructive comment. As we have replied in **Response2-1**, we changed the naming convention of the run name. *"NICAM16-S"* is the formal name for CMIP6 and *"NICAM.16-S"* was replaced with *"NICAM16-S"*.

RC2-5) *Minor comments*

Page 2, Lines 6-7. I am not sure exactly what is meant by 'cloud-system resolving climate simulations.' I'd argue cloud-resolving simulations really need to be O(1km). A cloud 'system' may be a larger feature, but I can't recall seeing this as common parlance.

Response2-5) Thank you. The term *"cloud-system resolving"* seems to be ambiguous, and we deleted *"the first cloud-system resolving"* in page 2, line 6.

RC2-6) *Page 2, Lines 26-30. Does this mean that NICAM16 is the first NICAM version to allow for transient CMIP forcing, or does this mean special code was added for only HighResMIP/CMIP6?*

Response2-6) The latter is correct. NICAM16-S is a special version of NICAM.16 to perform the HighResMIP simulations. We rephrased here for clarity following a comment by RC1 (**Response1-13**).

RC2-7) *Page 3, Line 14. 38 vertical levels seems low, particularly for a 14km experiment. Assuming the levels are not evenly spaced, this implies a dz of greater than 1km toward model top, which is really pushing the common notion that dx >> dz. The authors later discuss higher vertical resolution, more information should be added about the potential impact of this in HighResMIP, especially if prior work can be cited.*

Response2-7) Agree. We rephrased the 2nd paragraph of Section 2.1 as *"The number of vertical levels is 38, with a model top height of around 40 km, equivalent to the previous climate simulations (Kodama et al., 2015). The interval between each vertical layer increases from 160 m to 2 km as the altitude increases from the ground to 25 km (see K38 setting in Figure 1 of Ohno et al. 2019). Even at such a low vertical resolution, atmospheric phenomena of interests may be practically well simulated including tropical cyclones, MJO, and diurnal precipitation cycle, as we have confirmed in the previous study (Kodama et al., 2015). As a caveat, such coarse vertical resolution in the upper atmosphere leads to an overestimation of the cirrus cloud amount (Seiki et al., 2015b; Ohno et al., 2019) and may cause a different response of high cloud amount to warmer climate* (Ohno et al. 2019). *Also, it has been suggested that the vertical resolution should be increased when the horizontal resolution is increased in terms of atmospheric gravity wave* (Lindzen and Fox-Rabinovitz 1989; Polichtchouk et al. 2019). *Such coarse vertical resolution could overly produce vertical propagation of gravity wave and change zonal wind in the stratosphere* (Watanabe et al. 2015).*"*

RC2-8) *Page 3, Line 25. More information is needed about timestep of the gravity wave drag, boundary layer parameterization, etc. Are these called at the same timestep of the dynamics? Is the dynamics subcycled?*

Response2-8) Thank you for your comment. The time loop in the model is based on the dynamics, and physics schemes with the time step interval less than that in the dynamics are subcycled. Specifically, the boundary layer parameterization (turbulence) is called four times (NICAM16-7S), twice (NICAM16-8S), and once (NICAM16-9S) after the dynamics is executed. This means the time step interval of turbulence is 60 s for all the horizontal resolution. The gravity wave drag scheme is

called at the same timestep of the dynamics.

We rephrased page 3, lines 23-26 as *"The time step interval of the dynamics ("Δt" in Satoh et al. 2008) is set to 4, 2 and 1 min in NICAM16-7S, NICAM16-8S, and NICAM16-9S, respectively. The time loop in the model is based on the dynamics, and physics schemes with a time interval smaller or greater than that of the dynamics are subcycled or skipped, appropriately. Specifically, the time step interval of 30 s is used in the cloud microphysics scheme in NICAM16-7S, NICAM16-8S, and NICAM16-9S. The time interval of 1 min is used in the turbulence (mainly for planetary boundary layer) and land and ocean surface schemes in NICAM16-7S, NICAM16-8S, and NICAM16-9S. The radiation scheme, which requires considerable computational time, is executed every 40, 20, and 10 min in NICAM16-7S, NICAM16-8S, and NICAM16-9S, respectively. Gravity wave drag scheme is called at the same time step of the dynamics."*

RC2-9) *Page 4, Line 10. How quickly does the land spin up from this state? Within days, weeks, months? This may be important given the some of the short runs.*

Response2-9) As far as we experienced using legacy NICAM, it takes several years for surface air temperature and soil moisture over the land and OLR to settle down without initialization of land surface model. Even with the initialization adopted here, initial shock, albeit weak, seems to occur in some land variables such as soil moisture. Soil moisture and soil temperature at the uppermost layers of the land surface model in 56 km mesh HighResMIP simulation are shown as Figure R7 below for reference to the referees.
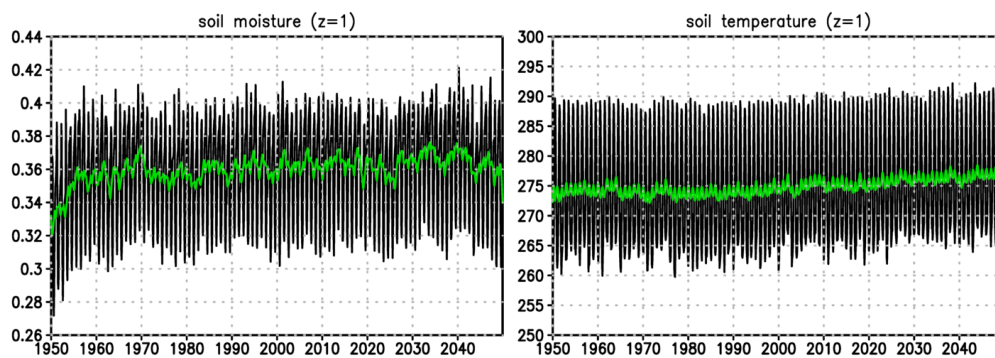

Figure R7: Soil moisture (left) and soil temperature (right) at the uppermost layers of the land surface model in the HighResMIP NICAM16-7S simulation (Table 1). These are averaged over 20°-120°E and 50°-70°N. Black and green lines show monthly mean and annual running mean, respectively.

We

- inserted *"This could partly reduce the initial shock of the land surface model, even though it may cost more than several years for some land variables such as soil moisture to fully settle down (not shown)."* in page 4, line 7 and

- added *"the NOLND and the REF runs were performed for 4 years to make land surface state settle down."* as a description of sensitivity experiments in page 4, around line 15.

RC2-10) *Page 4, Line 24. Is SST 'standardized' in HighResMIP (i.e., do all models use the same file?) or was this specific to NICAM16? I would also quibble that this is more of a boundary condition than an 'external forcing.'*

Response2-10) Yes, all the models including NICAM used the same SST files provided by the HighResMIP, and we deleted "basically" in line 20, page 4. We replaced *"External forcings"* with *"External forcings and boundary conditions"* in lines 19 and 20 in page 4.

RC2-11) *Page 6, Lines 18-22. Regarding the dynamical core, diffusion, boundary layer parameterization, etc. it is critical that they at least cite previous work when discussing these aspects where interested parties can get model details. Preferably, they would use 1-2 sentences to explain such components and then refer readers to more detailed publications for further information.*

Response2-11) Agree. We rephrased page 6, lines 18-21 as follows:

"Dynamical core and numerical filters in NICAM16-S are the same as those in NICAM.12. NICAM adopts a fully compressible non-hydrostatic system as governing equations of the dynamics (Tomita and Satoh, 2004; Satoh et al., 2008). The horizontal discretization is icosahedral grid system modified with spring dynamics for homogeneity on the sphere (Tomita et al. 2002). Divergence damping and second order Laplacian horizontal diffusion are used to stabilize the integration (Satoh et al., 2008). Additionally, first order Laplacian horizontal diffusion is applied above 20 km in altitude to avoid spurious wave reflection at the model top.

Table 4 shows a summary of the physics schemes used in NICAM16-S and NICAM.12 A single-moment bulk cloud microphysics scheme that solves mass concentrations of water vapor, liquid cloud, ice cloud, rain, snow, and graupel (Tomita, 2008; Roh and Satoh, 2014; Roh et al., 2017) is used instead of a combination of convection and large-scale condensation schemes".

Also, we will insert the following lines in page 6, line 28: "A modified version of Mellor-Yamada level 2 scheme (Nakanishi and Niino, 2006; Noda et al., 2010) is used to simulate planetary boundary layer. The radiation scheme, mstrnX (Sekiguchi and Nakajima, 2008), is a broadband model with 29 radiation bands here. The land surface model, Minimal Advanced Treatments of Surface Interaction and RunOff (MATSIRO; Takata et al, 2003) solves land states such as soil temperature, soil moisture, and land surface fluxes. Ocean surface fluxes are calculated following Louis (1979) with a modification of roughness length for strong surface wind conditions (Fairall et al., 2003; Moon et al., 2007). The conventional orographic gravity wave drag scheme (McFarlane, 1987) is used to introduce the effect of vertically-propagating subgrid-scale orographic gravity wave on the momentum tendency of the atmosphere."

RC2-12) *Page 6, Lines 22-25. 'Although most climate models... in the future.' I am not sure I philosophically agree with the notion of removing convective parameterization even at 56km (this would imply extremely large grid point updrafts in my experience). That said, this sentence is long and preferably requires further justification. Has anyone from the NICAM team published a paper regarding their philosophy around the lack of convective parameterizations, even coarser than 20km?*

Response2-12) In NICAM team, Seiki et al. (2015) performed 28 and 14 km mesh simulations to study an impact of the vertical resolution on the simulated cirrus cloud. They found a similar vertical resolution dependency between 14 and 28 km mesh simulations. Ohno et al. (2019) also used 28 km mesh model and found a reasonable result on the high cloud response to SST increase. For the 56 km mesh, Takasuka et al. (2018) performed an aqua planet experiment with 56 km mesh NICAM to investigate MJO-like disturbances. As you expected, 56 km simulation produces extremely large grid point updrafts and leads to very intense precipitation as seen in Figure R8 below requested by RC1 (see **Response1-6** for details). Meanwhile, pattern of the time-mean precipitation is well simulated, as shown in Figure 11 in the original manuscript, and such results are also found in Maher et al. (2018) using GCMs with 50 km – a few degrees mesh size. Also see **Response1-21**. Based on these and other previous studies, we replaced *"Although ... (see Section 4)"* in page 6, lines 21-29 with the followings:

"While most climate models use convection and large-scale condensation schemes even for a mesh size around 14 km, we use the cloud microphysics scheme to represent interactions between clouds and circulation in an explicit way. This not only lowers the cost of development, but also reduces the uncertainty of the results arising from highly arbitrary tuning. Such approach has also been tested in other researchers besides the NICAM group (Maher et al., 2018; Hohenegger et al., 2020). Global

mean precipitation is constrained by radiative cooling in large-scale clear-sky regions, which can be captured by the relatively coarse resolution model without the convection and large-scale condensation schemes. The simulated climatology of the precipitation pattern, even with the lowest resolution setting (NICAM16-7S), is comparable with the observation, as shown later, although our choice leads to a patchy behaviour of precipitation and dry/wet bias in the middle/lower troposphere in the simulation (Miyakawa et al., 2018). Similar precipitation behaviour was also reported in a climate model study with a mesh size of around $O(10^2$ km) without convection scheme (Maher et al., 2018). In terms of clouds, Seiki et al. (2015b) performed NICAM simulations with 28 and 14 km mesh to study an impact of the vertical resolution on the simulated cirrus cloud. They found a similar vertical resolution dependency between 14 and 28 km mesh simulations. Ohno et al. (2019) used 28 km mesh NICAM and found a reasonable result on the high cloud response to SST increase compared with a result using 7–14 km mesh NICAM (Iga et al. 2007). *In terms of MJO, Takasuka et al. (2018) performed an aqua planet experiment with 56 km mesh NICAM to investigate MJO-like disturbances. Yoshizaki et al. (2012) and Takasuka et al. (2015) even performed NICAM with a mesh size larger than 100 km without the convection and large-scale condensation schemes and found MJO-like disturbances in the simulation."*
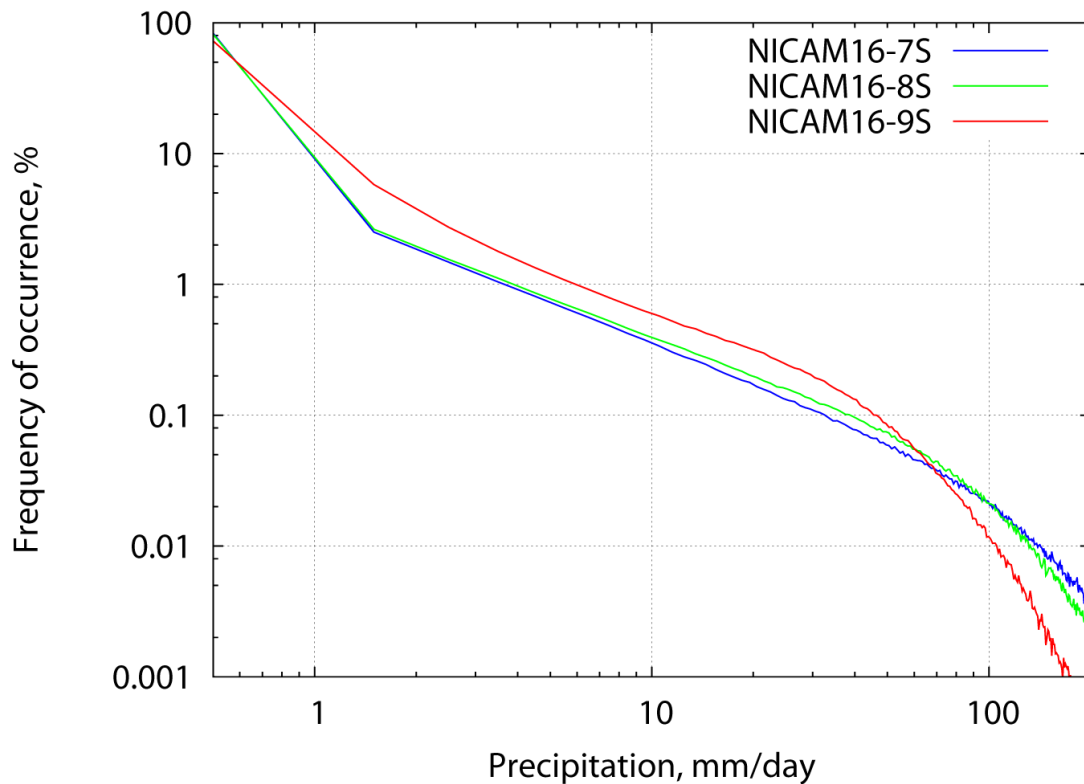
Figure R8 (Figure 17 in the revised manuscript): Frequency of occurrence (%) of daily mean precipitation binned with an interval of 1 mm day-1 during 01 June 2004 – 31 May 2005 averaged over 15°S–15°N. The REFFIX runs with NICAM16-7S, NICAM16-8S, and NICAM16-9S are shown in black, green, and red lines. The data are re-gridded to 1 degree in longitude and latitude before sampling.

RC2-13) *Page 7, Lines 32-33. I am not sure this is 'more than twice,' but this is where the aforementioned reformulation of Tables 5 and 6 would be quite helpful.*

Response2-13) Thank you. We believe *"more than twice"* becomes more apparent by Figure R5, which was inserted to the manuscript. Please see **Response2-1**.

RC2-14) *Page 8, Line 2. '... graupel in the simulation.' Which one, the reference?*

Response2-14) We replaced *"simulation"* in page 8, line 2 with *"NOCLD and REF runs"*.

RC2-15) *Page 8, Line 19. 'was replaced with zero ... whereas it was zero and unchanged in this study.' I'm a bit confused – the sentence makes it seem like the study applied something different than Roh et al. but it seems like it was zero in both cases?*

Response2-15) Thank you. We cleared misunderstanding by replacing *"The cloud ice terminal velocity ... in this study"* in page 8, lines 18-19 with *"Eventually, the cloud ice terminal velocity was set to zero in both Roh et al. (2017) and this study. Unlike this study, Roh et al. (2017) performed their reference run with non-zero cloud ice terminal velocity diagnosed by Heymsfield and Donner (1990), and their comparison before and after the scheme update includes the effect of reduction in cloud ice terminal velocity."*

RC2-16) *Page 11, Line 2. This is quite a large resolution sensitivity (the aerosol forcing completely changes sign going from 56km to 14km if I interpret this correctly).*

Response2-16) Yes, the sign of the aerosol impact on the net radiation reverses from 56 km to 14 km. This is a result of the compensation between longwave and shortwave components, and sign of the changes of each component seems to be reasonable. We added this explanation in the manuscript. Specifically, we

- added *"This links to a decrease in liquid water path (Figure 5f), which was also found in an online aerosol experiment by NICAM (Sato et al., 2018)."* in page 11, line 1 and
- added *"Such a sign reverse among the resolutions might be related to the resolution dependency of the low and middle cloud amount in the REF run (Figure 5h and i), and a detailed analysis is needed to properly understand the mechanism."* in page 11, line 2.

RC2-17) *Fig. 9. This needs to be bigger. Perhaps stack the three panels vertically?*

Response2-17) Agree. However, we removed (b) and (c) in response to RC1 (**Response1-28**).

RC2-18) *Typographical errors and grammar*

Page 3, Lines 17-18. Awkward grammar and typos.

Page 11, Line 5. The first letters used in the acronym should be capitalized.

Table 3. 'Laege' should be 'large.'

Fig. 4, The color bar should read 50 and not 50.01.

Fig. 5, Label the order of differencing for the lower three panels (e.g., g-g3).

Fig. 5., are the units on the vertical axis 'km?'

Response2-18) Agree. We changed them as suggested. For page 3, lines 17-18, we rewrote it as replied in **Response2-7**. For Figure 4, we also modified the caption as *"The lower bound of CCN, 50 cm^{-3} (Section 2.3), is shown in white shading."*. The units of the vertical axis in Figure 5 is km, and we added it to the figure.

Reference list to RC1 and RC2:

Eyring, V., S. Bony, G. A. Meehl, C. A. Senior, B. Stevens, R. J. Stouffer, and K. E. Taylor, 2016: Overview of the Coupled Model Intercomparison Project Phase 6 (CMIP6) experimental design and organization. *Geosci. Model Dev.*, **9**, 1937–1958, doi:10.5194/gmd-9-1937-2016. http://www.geosci-model-dev.net/9/1937/2016/.

Goto, D., Y. Sato, H. Yashiro, K. Suzuki, E. Oikawa, R. Kudo, T. M. Nagao, and T. Nakajima, 2020: Global aerosol simulations using NICAM.16 on a 14-km grid spacing for a climate study: Improved and remaining issues relative to a lower-resolution model. *Geosci. Model Dev. Discuss.*, doi:10.5194/gmd-2020-34.

Hohenegger, C., L. Kornblueh, D. Klocke, T. Becker, G. Cioni, J. F. Engels, U. Schulzweida, and B. Stevens, 2020: Climate statistics in global simulations of the atmosphere, from 80 to 2.5 km grid spacing. *J. Meteorol. Soc. Japan.*, **98**, 73–91, doi:10.2151/jmsj.2020-005. https://www.jstage.jst.go.jp/article/jmsj/98/1/98_2020-005/_article.

Iga, S., H. Tomita, Y. Tsushima, and M. Satoh, 2007: Climatology of a nonhydrostatic global model with explicit cloud processes. *Geophys. Res. Lett.*, **34**, L22814, doi:10.1029/2007GL031048.

Kodama, C., A. T. T. Noda, and M. Satoh, 2012: An assessment of the cloud signals simulated by NICAM using ISCCP, CALIPSO, and CloudSat satellite simulators. *J. Geophys. Res. Atmos.*, **117**, doi:10.1029/2011JD017317. http://dx.doi.org/10.1029/2011JD017317.

Lindzen, R. S., and M. Fox-Rabinovitz, 1989: Consistent vertical and horizontal resolution. *Mon. Weather Rev.*, **117**, 2575–2583, doi:10.1175/1520-0493(1989)117<2575:CVAHR>2.0.CO;2. http://journals.ametsoc.org/doi/abs/10.1175/1520-0493%281989%29117%3C2575%3ACVAHR%3E2.0.CO%3B2.

Maher, P., G. K. Vallis, S. C. Sherwood, M. J. Webb, and P. G. Sansom, 2018: The impact of parameterized convection on climatological precipitation in atmospheric global climate models. *Geophys. Res. Lett.*, **45**, 3728–3736, doi:10.1002/2017GL076826. http://doi.wiley.com/10.1002/2017GL076826.

Miyakawa, T., H. Yashiro, T. Suzuki, H. Tatebe, and M. Satoh, 2017: A Madden-Julian Oscillation event remotely accelerates ocean upwelling to abruptly terminate the 1997/1998 super El Niño. *Geophys. Res. Lett.*, **44**, 9489–9495, doi:10.1002/2017GL074683.

Na, Y., Q. Fu, and C. Kodama, 2020: Precipitation probability and its future changes from a global cloud-resolving model and CMIP6 simulations. *J. Geophys. Res. Atmos.*, **125**, doi:10.1029/2019JD031926. https://onlinelibrary.wiley.com/doi/abs/10.1029/2019JD031926.

Nitta, T., K. Yoshimura, and A. Abe-Ouchi, 2017: Impact of Arctic Wetlands on the Climate System: Model Sensitivity Simulations with the MIROC5 AGCM and a Snow-Fed Wetland Scheme. *J. Hydrometeorol.*, **18**, 2923–2936, doi:10.1175/JHM-D-16-0105.1. http://journals.ametsoc.org/doi/10.1175/JHM-D-16-0105.1.

Noda, A. T., K. Oouchi, M. Satoh, H. Tomita, S. Iga, and Y. Tsushima, 2010: Importance of the subgrid-scale turbulent moist process: Cloud distribution in global cloud-resolving simulations. *Atmos. Res.*, **96**, 208–217, doi:10.1016/j.atmosres.2009.05.007. http://linkinghub.elsevier.com/retrieve/pii/S0169809509001550.

——, ——, ——, and ——, 2012: Quantitative assessment of diurnal variation of tropical convection simulated by a global nonhydrostatic model without cumulus parameterization. *J. Clim.*, **25**, 5119–5134, doi:10.1175/JCLI-D-11-00295.1. http://journals.ametsoc.org/doi/abs/10.1175/JCLI-D-11-00295.1.

Ohno, T., M. Satoh, and A. Noda, 2019: Fine vertical resolution radiative-convective equilibrium experiments: roles of turbulent mixing on the high-cloud response to sea surface temperatures. *J. Adv. Model. Earth Syst.*, **11**, 1637–1654, doi:10.1029/2019MS001704. https://onlinelibrary.wiley.com/doi/abs/10.1029/2019MS001704.

Phillips, T. J., and Coauthors, 2004: Evaluating Parameterizations in General Circulation Models: Climate Simulation Meets Weather Prediction. *Bull. Am. Meteorol. Soc.*, **85**, 1903–1916, doi:10.1175/BAMS-85-12-1903. https://journals.ametsoc.org/bams/article/85/12/1903/104943/Evaluating-Parameterizations-in-General.

Polichtchouk, I., T. Stockdale, P. Bechtold, M. Diamantakis, S. Malardel, I. Sandu, F. Vána, and N. Wedi, 2019: Control on stratospheric temperature in IFS: resolution and vertical advection. *ECMWF Tech. Memo.*, **847**, doi:10.21957/cz3t12t7e.

Satoh, M., T. Matsuno, H. Tomita, H. Miura, T. Nasuno, and S. Iga, 2008: Nonhydrostatic icosahedral atmospheric model (NICAM) for global cloud resolving simulations. *J. Comput. Phys.*, **227**, 3486–3514, doi:10.1016/j.jcp.2007.02.006. http://dx.doi.org/10.1016/j.jcp.2007.02.006.

Seiki, T., C. Kodama, M. Satoh, T. Hashino, Y. Hagihara, and H. Okamoto, 2015: Vertical grid spacing necessary for simulating tropical cirrus clouds with a high-resolution atmospheric general circulation model. *Geophys. Res. Lett.*, **42**, 4150–4157, doi:10.1002/2015GL064282. http://doi.wiley.com/10.1002/2015GL064282.

Takasuka, D., T. Miyakawa, M. Satoh, and H. Miura, 2015: Topographical effects on internally produced MJO-like disturbances in an aqua-planet version of NICAM. *SOLA*, **11**, 170–176, doi:10.2151/sola.2015-038. https://www.jstage.jst.go.jp/article/sola/11/0/11_2015-038/_article.

——, M. Satoh, T. Miyakawa, and H. Miura, 2018: Initiation processes of the tropical intraseasonal variability simulated in an aqua-planet experiment: what is the intrinsic mechanism for MJO onset? *J. Adv. Model. Earth Syst.*, **10**, 1047–1073, doi:10.1002/2017MS001243. http://doi.wiley.com/10.1002/2017MS001243.

Tatebe, H., and Coauthors, 2019: Description and basic evaluation of simulated mean state, internal variability, and climate sensitivity in MIROC6. *Geosci. Model Dev.*, **12**, 2727–2765,

doi:10.5194/gmd-12-2727-2019. https://www.geosci-model-dev-discuss.net/gmd-2018-155/.

Watanabe, S., K. Sato, Y. Kawatani, and M. Takahashi, 2015: Vertical resolution dependence of gravity wave momentum flux simulated by an atmospheric general circulation model. *Geosci. Model Dev.*, **8**, 1637–1644, doi:10.5194/gmd-8-1637-2015. http://www.geosci-model-dev.net/8/1637/2015/.

Williams, K. D., and Coauthors, 2013: The Transpose-AMIP II Experiment and Its Application to the Understanding of Southern Ocean Cloud Biases in Climate Models. *J. Clim.*, **26**, 3258–3274, doi:10.1175/JCLI-D-12-00429.1. https://journals.ametsoc.org/jcli/article/26/10/3258/34008/The-TransposeAMIP-II-Experiment-and-Its.

Yoshizaki, M., K. Yasunaga, S. Iga, M. Satoh, T. Nasuno, A. T. Noda, H. Tomita, and M. Fujita, 2012: Why do super clusters and Madden Julian Oscillation coexist over the equatorial region? *SOLA*, **8**, 33–36, doi:10.2151/sola.2012-009.

Step 2. Changes to homogenize the manuscript and to improve English presentation

Following the suggestions by the referees, we further revised the manuscript to homogenize it, as summarized below:

- unification of terminology (e.g., "historic" -> "historical", "revised" -> "updated", "TOA OLR" -> "OLR at the TOA" …),
- unification of usage of active and passive sentence (e.g., the first part of "Cloud microphysics" section),
- unification of usage of articles (e.g., "REF run" -> "the REF run"), and
- rearrangement of the abbreviations.

After the above homogenization, we used English text editing service by native English speakers to further improve representation of English. The most of the modifications here were grammatical ones – usage of articles, tenses, passive/active sentences, commas, abbreviations, and so on. Also, some sentences were rephrased to clarify the meanings. These modifications suggested by the text editing service were minor and did not change the meaning of the manuscript. Please confirm the final revised manuscript from the next page for the detailed changes.

The final revised manuscript

The non-hydrostatic global atmospheric model for CMIP6 HighResMIP simulations (NICAM16-S): ~~Experimental~~ experimental design, model description, and impacts of model updates~~sensitivity experiments~~

Chihiro Kodama[1], Tomoki Ohno[1], Tatsuya Seiki[1], Hisashi Yashiro[2], Akira T. Noda[1], Masuo Nakano[1], Yohei Yamada[3,1], Woosub Roh[3], Masaki Satoh[3,1], Tomoko Nitta[3], Daisuke Goto[2], Hiroaki Miura[4], Tomoe Nasuno[1], Tomoki Miyakawa[3], Ying-Wen Chen[3], and Masato Sugi[5]

[1]Japan Agency for Marine-Earth Science and Technology, Yokohama, 236-0001, Japan
[2]National Institute for Environmental Studies, Tsukuba, Ibaraki, 305-8506, Japan
[3]Atmosphere and Ocean Research Institute, The University of Tokyo, Kashiwa, 277-8564, Japan
[4]Department of Earth and Planetary Science, Graduate School of Science, The University of Tokyo, Tokyo, 113-0033, Japan
[5]Meteorological Research Institute, Tsukuba, 305-0052, Japan

Correspondence to: Chihiro Kodama (kodamac@jamstec.go.jp)

Abstract. The Non-hydrostatic ICosahedral Atmospheric Model (NICAM), a ~~nonhydrostatic~~ global ~~atmospheric~~ model with an icosahedral grid system, has been under ~~developed~~ development for nearly two decades. This paper describes NICAM16-S, the latest stable version of NICAM (NICAM.16) modified for the Coupled Model Intercomparison Project Phase 6. ~~(CMIP6)~~ High Resolution Model Intercomparison Project (HighResMIP). Major updates from NICAM.12, a previous version used for climate simulations, include updates of ~~a~~ the cloud microphysics scheme and ~~a~~ land surface model, ~~an~~ introduction of natural and anthropogenic aerosols and a subgrid-scale orographic gravity wave drag scheme, and improvement of the coupling between the cloud microphysics and the radiation schemes. External forcings were updated to follow ~~a~~ the protocol of the ~~CMIP6 High Resolution Model Intercomparison Project (~~HighResMIP~~)~~. A series of short-term sensitivity experiments were performed to determine~~check~~ and understand the impacts of the~~se~~ various model updates on the simulated mean states. The NICAM16-S simulations demonstrated ~~Improvements~~ improvements in the ice water content, ~~the~~ high cloud amount~~s~~, ~~the~~ surface air temperature over the Arctic region, ~~the~~ location and ~~the~~ strength of zonal mean subtropical jet, and shortwave radiation over ~~the~~ Africa and ~~the~~ South Asia ~~were found in the NICAM16-S simulations~~. Some long-standing biases, such as the double intertropical convergence zone and smaller low cloud amount~~s~~ still exist or are even worse~~n~~ in some cases, suggesting further necessity for understanding their mechanisms and upgrading schemes and~~/or~~ ~~their~~ parameter settings, as well as for enhancing horizontal and vertical resolutions.

1. Introduction

Moist processes play a crucial role in the formation of the Earth's climate. ~~The m~~Moist convection redistributes ~~the~~ mass, energy, and momentum of the atmosphere to form large-scale circulation. Clouds are coupled with large-scale circulation through latent and radiative heating, which can affect climate sensitivity. The accurate treatment of such interactions between clouds and circulation requires high-resolution global cloud-resolving models (Bony et al., 2015; Satoh et al., 2019). ~~Natural disasters, including heavy precipitation and strong wind associated with tropical and extratropical cyclones, are heavily involved in the moist processes.~~

~~Considering the importance of fine-scale moist processes, increasing the spatial resolution of the global atmospheric model may be a straightforward approach to improving climate simulations (Kinter et al., 2013; Roberts et al., 2018; Satoh et al., 2019; Shukla et al., 2009).~~ This, as well as an increasing demand from society to project tropical cyclones and other extreme weather, motivated us to perform ~~the first cloud-system resolving~~ climate simulations of the present-day and ~~the~~ future using the Nonhydrostatic ICosahedral Atmospheric Model (NICAM) (Tomita and Satoh, 2004; Satoh et al., 2008, 2014) with a ~~14~~ 14-km mesh ~~non-hydrostatic global atmospheric model (NICAM; Satoh et al., 2008, 2014; Tomita and Satoh, 2004)~~. Kodama et al. (2015) and Satoh et al. (2015) provided brief descriptions of the model (hereafter referred to as NICAM.12) and experimental design of the climate simulations. This unique dataset of the high-resolution climate simulation~~dataset~~, whose overall performance was reported in Kodama et al. (2015), has been used in many studies, with a focus~~ing~~ on tropical cyclones (~~Matsuoka et al., 2018;~~ Satoh et al., 2015, 2018; Yamada et al., 2017, 2019; ~~Sugi et al., 2020;~~ Matsuoka et al., 2018; Sugi et al., 2020~~Yamada et al., 2017, 2019~~), extratropical cyclones (Kodama et al., 2019; McCoy et al., 2019; Satoh et al., 2018), intraseasonal oscillations including Madden–Julian Oscillation (MJO) (Kikuchi et al., 2017; Nakano and Kikuchi, 2019), tropical synoptic-scale waves (Fukutomi et al., 2016), cloud radiative feedback (Chen et al., 2016~~; Noda et al., 2019~~; Satoh et al., 2018; Noda et al., 2019), and regional- to- global precipitation (Kilpatrick et al., 2017; Satoh et al., 2018; Na et al., 2020; ~~Satoh et al., 2018;~~ Takahashi et al., accepted~~n.d.~~).

Also, some significant climate biases have been identified in the simulation (Kodama et al., 2015), and great effort~~s~~ ~~have~~ has been devoted to improving the model for better performance of the simulated climate in a physically- consistent manner. Major updates between NICAM.12 and NICAM.16, a stable version of NICAM released in 2017, are ~~an~~ update~~ing~~ of the cloud microphysics scheme based on a comparison with Tropical Rainfall Measuring Mission (TRMM) satellite observation~~s~~ (Roh and Satoh, 2014; Roh et al., 2017~~; Roh and Satoh, 2014~~), ~~an~~ introduction of a wetland scheme in ~~a~~ the land surface model (Nitta et al., 2017), ~~an~~ implementation of the coupling between cloud microphysics and radiation that considers the non- sphericity of ice particles (Seiki et al., 2014), and introduction of a subgrid-scale orographic gravity wave drag scheme. In addition, some parameters related to the processes of surface albedo and sea ice have been revised. These model updates generally~~often (but not always)~~ reduce the biases of the simulated mean states, as discussed~~reported~~ later~~below~~. NICAM.16 has been further modified to support~~conform to~~ the external forcings of natural and anthropogenic aerosols and the solar cycle defined in the Coupled Model Intercomparison Project Phase 6 (CMIP6), High Resolution Model Intercomparison Project (HighResMIP) protocol (Haarsma et al., 2016). ~~That is, the interfaces of the CMIP6 external forcings (natural and anthropogenic aerosols and the solar cycle) have been implemented.~~ This special version of NICAM.16 for HighResMIP~~CMIP6~~ is labeled~~labelled~~ NICAM16-S, where "-S" represents the use of a single-moment cloud microphysics scheme. A double-moment cloud microphysics scheme is also available in NICAM.16 (~~Satoh et al., 2018; Seiki et al., 2014, 2015b;~~ Seiki and Nakajima, 2014; Seiki et al., 2014, 2015b; Satoh et al., 2018). However, the double-moment scheme was not used for the HighResMIP simulations and hence is not described in this paper. The DECK and CMIP historical simulations (Eyring et al., 2016) were not in this study because NICAM is an atmosphere-only model and a coupled ocean-atmosphere model, NICAM-COCO (Miyakawa et al. 2017), is being developed. ~~These model updates often (but not always) reduce the biases of the simulated mean states, as reported later.~~

This section has provided a summary ~~of the description~~ of NICAM16-S with a focus on the differences from NICAM.12. Section 2 of this paper presents the experimental design ~~(resolutions as well as initial and boundary conditions)~~ of the HighResMIP simulations and a series of sensitivity experiments by NICAM16-S. Section 3 explains the detailed model updates of NICAM16-S from NICAM.12 and their impacts on the simulated mean states. Section 4 briefly describes~~presents~~ the resolution dependency of ~~preliminary evaluations of the mean states simulated by~~ NICAM16-S. Section 5 reports on the computational aspects of the simulation. Section 6 provides a brief~~quick~~ summary of ~~this~~ the comparison results~~paper~~.

2

2. Experimental design

2.1 Spatial and temporal resolutions

Three sets of model configurations were prepared for the HighResMIP simulations, and initial and boundary conditions were

5 made for each. NICAM16-S models with specific horizontal resolutions were formally ~~labeled~~labelled NICAM16-7S (~~56~~56-km mesh), NICAM16-8S (~~28~~28-km mesh), and NICAM16-9S (~~14~~14-km mesh) in CMIP6 as source IDs. The horizontal mesh size is evaluated as a square root of the mean area of each grid cell (Satoh et al., 2014). The number *n* in ~~NICAM17~~NICAM16-*n*S is a grid division level (glevel), which denotes ~~a~~the number of subdivisions of the icosahedron to generate a mesh (Tomita et al., 2001). The physics schemes, including parameters, and the initial and boundary conditions

10 are common among different horizontal resolutions except for those explicitly noted in Sections 2 and 3.

The number of vertical levels is 38, with a model top height of around 40 km, equivalent to the previous climate simulations (Kodama et al., 2015). The interval between each vertical layer increases from 160 m to 2 km as the altitude increases from the ground to 25 km (see the "K38" setting in Figure 1 of Ohno et al. 2019). Even at such a low vertical resolution,

15 ~~Atmospheric~~atmospheric phenomena of interests, ~~may be practically well simulated~~including ~~the~~tropical cyclones, the MJO, and the diurnal precipitation cycle, may be simulated practically and accurately, as we have confirmed in the previous study (Kodama et al., 2015). As a caveat, a coarse vertical resolution in the upper atmosphere leads to an overestimation of, ~~though the vertical resolution is not sufficient to resolve~~ the cirrus ~~clouds~~cloud amount (~~Ohno et al., 2019;~~Seiki et al., 2015b; Ohno et al., 2019) and may cause a different response of high cloud amount to warmer climate (Ohno et al., 2019).

20 Also, it has been suggested that the vertical resolution should be increased when the horizontal resolution is increased in terms of atmospheric gravity waves (Lindzen and Fox-Rabinovitz, 1989; Polichtchouk et al., 2019). Such coarse vertical resolution in this study could over-produce vertical propagation of gravity waves and change zonal wind in the stratosphere~~and atmospheric gravity waves~~ (Watanabe et al., 2015).

25

The time step interval~~s~~ ~~for~~of the ~~dynamical~~dynamics (Δt in Satoh et al. 2008) ~~process are~~was set to ~~240~~4, ~~120~~2, and ~~60~~1 mins ~~for~~in NICAM16-7S, NICAM16-8S, and NICAM16-9S, respectively. ~~Diffusion coefficients of the divergence damping, the second-order Laplacian background horizontal diffusion, and the first-order Laplacian horizontal diffusion for sponge layer above 20 km are reduced appropriately as the horizontal resolution is increased (Satoh et al., 2008).~~ The time

30 loop in the model is based on the dynamics, and physics schemes with a time interval smaller or greater than that of the dynamics are subcycled or skipped, as appropriate. Specifically, ~~The~~a time step interval of 30 s was used in the cloud microphysics scheme in NICAM16-7S, NICAM16-8S, and NICAM16-9S. A time interval of ~~is 30 s and~~1 min was used in the turbulence (mainly for the planetary boundary layer) and ~~that of the~~land and ocean surface schemes in NICAM16-7S, NICAM16-8S, and NICAM16-9S~~processes including turbulence is 60 s for all the horizontal resolutions~~. The radiation

35 scheme, which requires considerable computational time, ~~is~~was executed every 40, 20, and 10 min ~~for~~in NICAM16-7S, NICAM16-8S, and NICAM16-9S, respectively. The gravity wave drag scheme was called at the same time step as that of the dynamics.

2.2 ~~Initial conditions~~HighResMIP simulations and sensitivity experiments

Table 1 shows the integration periods ~~of~~ for the HighResMIP simulations. For the Tier 1 simulations, which start from 1 January 1950, the initial condition of the atmosphere was taken from the ERA-20C reanalysis (Poli et al., 2016). The NICAM16-7S and NICAM-8S simulations ~~Strictly~~ strictly ~~following~~ followed the HighResMIP protocol and~~, the~~

5 ~~simulations~~ continued until 31 December 2014~~, using NICAM16-7S and NICAM-8S~~. The HighResMIP Tier 3 simulations using NICAM16-7S and NICAM16-8S started from 1 January 2015 as a continuation of the Tier 1 simulations and ended on 31 December 2050. The ~~Higher~~ high computational cost ~~hinders~~ hindered us from running NICAM16-9S for 100~~a hundred~~ years, and thus a time-slice approach ~~is~~ was adopted~~,~~ instead. Specifically, climate simulations were~~have been~~ performed in the following timeframes: 1950–1960, 2000–2010, and 2040–2050. For the simulations starting from 1 January 1950 or 1

10 January 2000, ~~The~~ the initial land condition**s** prescribed for NICAM16-7S, NICAM16-8S, and NICAM16-9S~~in the past and present-day simulations was~~ were taken from ~~a~~ the monthly mean climatology of the simulation by NICAM with a mesh size of 220 km (glevel- 5) under ~~a~~ present-day condition**s**. It was performed for 10 years, and the last 5 year**s** of data were used to obtain the monthly mean land climatology. This approach is the same as ~~the that~~one used in ~~the~~ previous climate simulations (Kodama et al., 2015). This could partly reduce the initial shock of the land surface model, even though it may cost more

15 than several years for some land variables, such as soil moisture, to fully settle down (not shown). The initial land condition for the future time slice run with NICAM16-9S~~a 14 km mesh~~ was obtained by interpolating the output of the NICAM16-8S simulation~~28 km mesh run~~.

In addition to the formal HighResMIP simulations, we performed a series of short-term sensitivity experiments to evaluate

20 the impacts of the model changes ~~updates~~ on the simulated climatology, as listed in Table 2. Here, the model configuration of the REFFIX run ~~experimental ID "g"~~is equivalent to that used in the formal HighResMIP ~~Tier 1 and 3~~ simulations. As noted in Section 3.6 7, we often prefer to use a slab ocean model with nudging toward the boundary sea surface temperature (SST) rather than the fixed SST condition requested by the HighResMIP protocol because of better performance in the simulated precipitation pattern (Kodama et al., 2015), particularly with a horizontal mesh size of 14 km (Section 3.7).

25 Therefore, both the fixed SST and slab ocean configurations (REFFIX and REFSLB runs, respectively) were tested in the sensitivity experiments~~(see Section 3.6)~~, and ~~,~~we used the REFFIX run with 56-km mesh and the REFSLB run with 14-km mesh as the reference (REF) runs for the other sensitivity experiments. Impacts of the model updates described in Section 3 on the simulated climate states were individually tested by switching off each update. Additionally, the DDT2M, DDT1M, RDT20M, and RDT10M runs were performed to check sensitivity of the simulated climate to the time interval of the model. ~~, and all the other configurations of the sensitivity experiments are the derivative of "g", as described in Table 2.~~ These

30 sensitivity experiments were started ~~were performed from the initial condition beginning~~ from 1 June 2004 and integrated for 1 year. An exception was the NOLND and the REF runs, which were performed for 4 years to make the land surface state settle down. The initial date was chosen to ensure consistency with~~because it was used frequently in the~~ previous NICAM studies (e.g., Kodama et al., 2012~~; Noda et al., 2016~~; Seiki et al., 2015a; Noda et al., 2016). An integration period of 1 year,

35 or even less, is sufficient to evaluate the basic state of the atmosphere, such as cloud amount, precipitation, radiation, and temperature (e.g., Phillips et al., 2004; Noda et al., 2010; Kodama et al., 2012; Williams et al., 2013; Miyakawa et al., 2018; Miyakawa and Miura, 2019; Stevens et al., 2019; Hohenegger et al., 2020), and tropical variability, including diurnal cycle, tropical cyclones, and MJO (e.g., Sato et al., 2009; Kinter et al., 2013; Stevens et al., 2019; Matsugishi et al., 2020). The interannual variability of the HighResMIP simulation by NICAM16-7S (Table 1) over 101 years was diagnosed to

40 distinguish the impacts of the model changes from internal variability in a rough manner~~The integration periods of these sensitivity experiments are 1 year in most cases.~~. The simulation data were re-gridded to the same grid of observations (Table 3~~Table 3~~) unless it is explicitly specified.

2.3 External forcings and boundary conditions

External forcings and boundary conditions of the simulations ~~basically~~ followed the HighResMIP protocol (Haarsma et al., 2016)~~; in other words, h~~. Historical and SSP585-scenario settings~~forcings~~ (O'Neill et al., 2016) were used in the Tier~~s~~ 1 and 3 simulations, respectively.

5

Daily quarter-degree ~~sea surface temperature (~~SST~~)~~ and sea ice mass (ICE) prescribed for the model were obtained from HadISST 2.2.0.0 (Kennedy et al., 2017~~; Kennedy et al., The Met Office Hadley Centre Sea Ice and Sea Surface Temperature data set, version 2.2.0.0, Technical Note, in prep~~). The SST dataset ~~is~~ was extended from 2016 to 2050 using ~~a~~ the trend obtained from a CMIP5 model ensemble mean following the RCP8.5 scenario and historical variability from 1980 to 2015

10 (Kennedy et al., 2019). Because~~Since~~ HadISST provides historical sea ice concentration (SIC), ICE was diagnosed from SIC for NICAM (see Section 3.6~~7~~). The ~~Future~~ future SIC ~~is~~ was estimated from the future SST data and ~~an~~ the observed relationship between SST and SIC (HighResMIP, 2020; Kennedy et al., 2019). Both the SST and ICE were fixed to the boundary conditions in the HighResMIP Tier~~s~~ 1 and 3 simulations. ~~In the short-term sensitivity experiments, a slab ocean model with a nudging toward the prescribed SST was also tested for a practical purpose (see Section 3.6 for its impact on the~~

15 ~~simulated climate). In the sensitivity experiments, the fixed SST condition was used in 56 km mesh run whereas and the slab ocean model with the nudging was used in 14 km mesh runs unless explicitly specified.~~

Figure 1 and Figure 2 display the decadal mean SST and ICE, respectively prescribed for the model; Figure 3 exhibits their global- mean variability. Greater warming over the maritime continent, the Indian Ocean, and the edge of the polar regions

20 are found in the 2000s compared with the 1950s, whereas cooling is noticed in the North Pacific and the North Atlantic. The SST in the 2040s has larger values almost everywhere compared with that in the 2000s, especially in the midlatitudes, the equatorial eastern Pacific, the tropical Atlantic Ocean, and the edge of the Arctic regions.~~Future change in SST is somewhat similar to the El Niño pattern, and the warming is also prominent in the midlatitudes, the tropical Atlantic Ocean, and the edge of the polar regions.~~ Similar tendencies are observed for the distribution of the SST trend (not shown). The global mean

25 SST is 17.9 °C~~°C~~ in the 1950s, 18.2 °C~~°C~~ in the 2000s, and 19.0 °C~~°C~~ in the 2040s. ICE continues to decrease from the past to the future. The global mean ICE is ~~a~~nearly halved by the 2040s compared with that in the 1950s.

The global annual mean of greenhouse gas (GHG) concentrations (Meinshausen and Vogel, 2016; Meinshausen et al., 2017; Meinshausen and Nicholls, 2018~~; Meinshausen and Vogel, 2016~~) was prescribed ~~for~~ in the model. Specifically, CO_2, CH_4,

30 N_2O, chlorofluorocarbons~~CFCs~~ (CFC-12, CFC-11, CFC-113, CFC-114, and CFC-115), hydrochlorofluorocarbons~~HCFCs~~ (HCFC-22, HCFC-141b, and HCFC-142b), hydrofluorocarbons~~HFCs~~ (HFC-134a, HFC-32, HFC-125, HFC-143a, and HFC-152a), CCl_4, CF_4, SF_6, and C_2F_6 ~~are~~ were considered as GHG~~s concentrations~~ in the model. In addition~~Also~~, historical and future monthly concentration~~ss~~ of the three-dimensional ozone field (Hegglin et al., 2016, 2018) ~~were~~ was prescribed in the model.

35

~~Natural aerosol m~~Mass and ~~the~~ number concentration~~s~~ of natural aerosols prescribed ~~for~~ in the model were obtained from a low-resolution NICAM simulation with an online aerosol module based on the Spectral Radiation-Transport Model for Aerosol Species (SPRINTARS) (Takemura et al., 2000, 2002, 2005, 2009; Goto et al., 2008, 2011). The simulated climatology of ~~the~~ aerosol~~s~~ in NICAM was~~has been~~ previously validated (Goto et al., 2018; Suzuki et al., 2008). For

40 HighResMIP~~CMIP6~~, NICAM with a mesh size of 220 km ~~mesh (glevel 5)~~ was performed for 100 years using natural aerosol emission~~s~~ with the anthropogenic aerosol module MACv2-SP (Fiedler et al., 2018; Stevens et al., 2017; see Section 3.3~~4~~) under a perpetual 2012 condition, and the data ~~of~~ for the last 90 years were averaged to obtain a monthly- mean climatology of aerosol mass ~~concentration~~ and number concentration~~s~~ of cloud condensation nuclei (CCN) from a natural

origin. A lower-bound limiter of 50 cm^{-3} was applied to the CCN prescribed for the model to avoid numerical instability in the cloud microphysics scheme. Figure 4a shows the annual mean~~s~~ of the natural aerosol optical thickness simulated by NICAM16-7S with the natural aerosol mass and~~and~~ CCN (Figure 4b) ~~simulated by and~~ prescribed ~~to~~ in the model[1]. The climatology of natural aerosol mass and CCN is invariant year by year, whereas anthropogenic aerosol~~s~~ from MACv2-SP ~~is~~

5 are time-dependent in the historical and future simulations (Fiedler et al., 2019; Stevens et al., 2017). Further, the extinction coefficient, the single scattering albedo, and the asymmetric factor~~aerosol optical properties~~ were overwritten with the stratospher~~e~~ic aerosol dataset (Thomason et al., to be submitted) above the tropopause to introduce the effect of volcanic eruptions on the radiation field in a consistent way among different models participating in the HighResMIP~~CMIP6~~.

10 Similar to the implementation of MIROC6 (Tatebe et al., 2019), historical monthly mean solar forcings (Matthes et al., 2017b, 2017a) were prescribed as total solar irradiance and solar irradiance spectra in the ~~radiative~~ radiation scheme ~~MstrnX~~ mstrnX (Sekiguchi and Nakajima, 2008). In terms of land surface processes, ~~the~~ a monthly climatology (2004–2013) of leaf area index ~~(LAI)~~ was obtained from the Moderate Resolution Imaging Spectroradiometer (MODIS) product (MCD15A2.005~~.~~, Shabanov et al., 2005; Yang et al., 2006).

15

As briefly noted in Satoh et al. (2014), a spatial filter~~smoother~~ ~~is~~ was applied to smooth the model topography to avoid ~~a model abort due to~~ numerical instability. Specifically, a hyper-diffusion ~~is~~ was repeatedly applied to the GTOPO30 (doi:10.5066/F7DF6PQS), a global digital elevation model with a horizontal spacing of approximately 1 km, to meet a specific~~certain~~ criterion ~~of~~ for the maximum elevation gradient. The maximum elevation gradient ~~is~~ was set to 0.01, 0.01414,

20 and 0.02 m m^{-1} for NICAM16-7S, NICAM16-8S, and NICAM16-9S, respectively, and the resulting topography is called "A-topography.~~"~~." Note that, in previous NICAM studies using a ~~14~~ 14-km horizontal mesh (e.g., Kodama et al., 2015), "B-topography,~~"~~," in which A-topography with~~of~~ a ~~28~~ 28-km mesh was interpolated to ~~14~~ 14-km mesh grid point~~s~~, was often used for the sake of stable integration. For HighResMIP~~CMIP6~~, A-topography was used to better represent steeper mountains and their effects on ~~the~~ atmospheric phenomena.

25

3. Model description and impact of model updates on the simulated fields

3.1 Overview

The dynamical core and numerical filters in NICAM16-S are the same as those in NICAM.12. NICAM adopts a fully compressible non-hydrostatic system as the governing equations of the dynamics (Tomita and Satoh, 2004; Satoh et al.,

30 2008). The horizontal discretization is an icosahedral grid system modified with spring dynamics for homogeneity on the sphere (Tomita et al., 2002). Divergence damping and second-order Laplacian horizontal diffusion are used to stabilize the integration (Satoh et al., 2008). Additionally, first-order Laplacian horizontal diffusion is applied above an altitude of 20 km to avoid spurious wave reflection at the model top.

35 Table 4 gives~~shows~~ a summary of the physics schemes used in NICAM16-S and NICAM.12. ~~Dynamical core and horizontal and vertical diffusion, including the planetary boundary layer schemes in NICAM16-S, are the same as those of NICAM.12~~

---

[1] ~~Note that a~~An error was found in the natural aerosol forcing prescribed ~~to~~ in the model, as recently reported in ES-DOC Errata website (https://errata.es-doc.org/static/view.html?uid=ada34e91-4a94-d668-a491-fe16556aaf46). Its influence on the results presented in this paper seems to be negligible, according to an additional 56 km mesh experiment with the corrected natural aerosol forcing (not shown).

except for some minor updates. A single-moment bulk cloud microphysics scheme, NICAM Single-moment Water 6 (NSW6), that solves mass concentrations for six water categories – vapor, cloud water, cloud ice, rain, snow, and graupel (Tomita, 2008; Roh and Satoh, 2014; Roh et al., 2017; Roh and Satoh, 2014) – is used instead of a combination of convection and large-scale condensation schemes to explicitly represent interactions between clouds and circulation.

Although most climate models continue to use convection and large-scale condensation schemes even for a mesh size around 14 km, we believe that being free from development and tuning of such complex parameterizations can be another wise option to focus more on investigating the nature of the simulation with explicit cloud microphysics when we expect to proceed toward global cloud resolving climate simulation in the future. While most climate models use convection and large-scale condensation schemes even for a mesh size around 14 km, we used the cloud microphysics scheme to represent interactions between clouds and circulation in an explicit way. This not only lowers the cost of model development but also reduces the uncertainty in the results arising from highly arbitrary tuning. This approach has also been tested by other researchers besides the NICAM group (Maher et al., 2018; Hohenegger et al., 2020). Furthermore, gGlobal mean precipitation is constrained by radiative cooling in a large-scale clear-sky regions, which can be captured by a model with the relatively coarse resolution run without the convection and large-scale condensation schemes. Although our choice leads to a patchy behaviour of precipitation in the simulation, tThe simulated climatology of the precipitation pattern, even by with the lowest resolution setting (NICAM16-7S), is comparable with the observed patternsation, as shown below, although our choice leads to patchy precipitation behaviour and dry/wet bias in the middle/lower troposphere in the simulation (Miyakawa et al., 2018) (see Section 4). Similar precipitation behaviour was also reported in a climate model study with a mesh size of around $O(10^2$ km) without a convection scheme (Maher et al., 2018). In terms of clouds, Seiki et al., (2015b) conducted NICAM simulations with 28- and 14-km meshes to study the impact of the vertical resolution on the simulated cirrus clouds. They found a similar vertical resolution dependency between the 14- and 28-km meshes. Ohno et al., (2019) used a 28-km mesh NICAM and found a high cloud response to SST increases that is comparable with results using 7- and 14-km meshes (Iga et al., 2007). In terms of MJO, Takasuka et al., (2018) performed an aqua planet experiment with a 56-km mesh NICAM to investigate MJO-like disturbances. Yoshizaki et al. (2012) and Takasuka et al. (2015) even performed NICAM with a mesh size larger than 100 km without the convection and large-scale condensation schemes and found MJO-like disturbances in the simulation.

A modified version of the Mellor–Yamada level 2 scheme (Nakanishi and Niino, 2006; Noda et al., 2010) is used to simulate planetary boundary layer. The radiation scheme, mstrnX (Sekiguchi and Nakajima, 2008), is a broadband model with 29 radiation bands as used here. The land surface model, Minimal Advanced Treatments of Surface Interaction and RunOff (MATSIRO) (Takata et al., 2003) solves land states such as soil temperature, soil moisture, and land surface fluxes. Ocean surface fluxes are calculated following Louis (1979) with a modified roughness length for strong surface wind conditions (Fairall et al., 2003; Moon et al., 2007). The conventional orographic gravity wave drag scheme (McFarlane, 1987) is used to introduce the effect of vertically propagating subgrid-scale orographic gravity waves on the momentum tendency of the atmosphere. Though we did not fine-tune the model due to heavy computational cost, we crudely turned parameters of sea ice thickness with NICAM16-7S (Section 3.7) and the gravity wave drag scheme with NICAM16-9S (Section 3.8). We did not return the model at each resolution under the principles of the HighResMIP.

As we discuss in Section 2.2 and Table 2, A a series of short-term sensitivity experiments were performed to monitor impacts of several model updates on the simulated climatology. Figure 55 (right part of each panel) summarizes Table 2 offers a full list of sensitivity experiments, and Table 4 presents observations for comparisons with the model . Some of their impacts of the model changes on the global means mean climate. All the significant impacts of the model changes shown here could be qualitatively reproduced even when the analysis period was limited to the last 6 months (not shown). The

7

REFFIX and REFSLB runs with each horizontal mesh and the observations are shown on the left in each panel in Figure 5~~5 are summarized in Table 5, and comparisons with observations along with impacts of the horizontal resolutions are shown in Table 6 for reference. Unless explicitly specified, the simulation data are re gridded to the same grid of observations Table 4 or to 2.5° in latitude and longitude.~~ We will discuss these impacts along with the details of the model

5   updates later in this section.~~As noted in Section 3.6, we often prefer to use a slab ocean model with nudging toward the boundary SST rather than the fixed SST condition requested by the HighResMIP protocol because of better performance in the simulated precipitation pattern (Kodama et al., 2015). Therefore, both the fixed SST and slab ocean configurations were tested in the sensitivity experiments (see Section 3.6).~~

10 **3.2~~1~~ Cloud microphysics**

~~Climate simulations with NICAM16-S were performed with a single moment bulk cloud microphysics scheme with six water categories (hereafter referred to as NSW6).~~ Recently, Roh and Satoh (2014) and Roh et al. (2017) ~~have~~ significantly revised the NSW6 scheme based on comparisons with ~~the~~ TRMM observation~~s~~. We used the revised version of the NSW6 scheme in NICAM16-S ~~and found~~to show ~~the~~ improvements in the simulated climatology ~~of the NICAM simulation~~, as

15 shown below.

The NSW6 scheme ~~was~~ originated with Lin et al. (1983) and Rutledge and Hobbs (1984). ~~After their works,~~ Tomita (2008) modified their cloud microphysics scheme to ensure consistency with ~~the~~ thermodynamics used in NICAM~~.~~; Tomita (2008)~~Tomita~~ also simplified it to reduce ~~the~~ calculation cost for ~~global~~ high-resolution global simulations. ~~The~~ NSW6 was

20 evaluated by comparing the simulated optical properties with satellite observations (Satoh et al., 2010; Kodama et al., 2012; Hashino et al., 2013, 2016; Roh and Satoh, 2014, 2018; Roh et al., 2017) using satellite simulators, specifically, the ~~(~~CFMIP Observational Simulator Package ~~developed by~~ (Haynes et al., 2007; Chepfer et al., 2008; Bodas-Salcedo et al., 2008, 2011) and ~~, or~~ Joint Simulator ~~developed by~~ (Matsui et al., 2009; Masunaga et al., 2010; Hashino et al., 2013). It was revised in each stage of the version management of NICAM (Kodama et al., 2012; Roh and Satoh, 2014; Roh et al., 2017). The

25 revision of the NSW6 scheme by Roh and Satoh (2014) and Roh et al. (2017) represents a significant change between NICAM.12 and ~~is the key in this updated version of the NICAM (~~NICAM16-S~~)~~.

Table 5 summarizes key changes in the NSW6 scheme by Roh and Satoh (2014) and Roh et al. (2017)~~-~~. In short, the revision aimed to enhance organizations of tropical convective cloud systems by assuming lighter precipitation of graupel and snow

30 and by ~~moderately~~ moderating the ~~developing~~ development of cloud ice. Finally, they ~~achieved~~ successful~~ly~~ ~~reproduction~~ reproduced ~~of~~ the vertical structures of shallow, congestus, and deep convective clouds over the tropics, ~~comparing~~ compared to TRMM and CloudSat satellite observations. They also used microwave satellite observations to evaluate the simulated results (Roh and Satoh, 2018)~~.; hence~~ Therefore, improvements in tropical cloud systems with the revised scheme are robust in terms of optical signals (see the original papers for more details). Note that ~~a~~ the separation of convective and

35 stratiform systems in Roh and Satoh (2014) was omitted in this study because of its small impact (not shown) despite the high computational cost.

The sensitivity experiments with and without the update of the cloud microphysics scheme (the REF and NOCLD runs, respectively) were compared. ~~Table 5a shows the global mean impact of the updated cloud microphysics scheme on the~~

40 ~~simulated mean values.~~ The most noticeable impact ~~is~~ was ~~on~~ an increase in ice water content (IWC) by more than twofold~~twice~~ (Figure 5~~5~~, e), and this mostly accounts for ~~a~~ the snow category in the cloud microphysics scheme. Figure 6 shows the meridional-height cross section of the observed and simulated zonal mean IWC~~ice water content (IWC)~~ and its

8

breakdown into the categories of cloud ice, snow~~,~~ and graupel in the <u>NOCLD and REF runs</u>~~simulation~~. The simulated IWC is largely underestimated using the model <u>without</u>~~before~~ the update<u>d</u> ~~of~~ cloud microphysics scheme <u>(the NOCLD run)</u>, as also shown in Seiki et al. (2015a), and it becomes comparable with ~~the~~ CloudSat observation<u>s</u> ~~after~~ <u>with</u> the update <u>(the REF run)</u>. A noticeable increase in the snow category ~~is~~ <u>was</u> seen in the tropical upper troposphere and <u>midlatitude</u> storm-track region. Cloud ice ~~and graupel are~~<u>is</u> also increased in the upper troposphere~~.,~~ <u>and g</u>~~G~~raupel <u>is</u> increased in the tropical middle troposphere <u>but</u>~~rather~~ decreased in the storm-track region. As a result, global mean column-integrated cloud ice and snow ~~are~~ increased by 24 % and 399 %<u>, respectively,</u> and that of graupel <u>is</u> decreased by 8.4 %. The <u>net</u> increase in IWC is consistent with the decelerated development of <u>IWC</u>~~ice water content~~ by the modified mass and diameter relationship of snow, <u>which</u>~~that~~ reduces the snow density (Table 5<u>,</u> d), by the diminished efficiency of accretion of cloud ice by snow (Table 5<u>,</u> g), and by ignoring ~~an~~ <u>the</u> accretion of snow and cloud ice by graupel (Table 5<u>,</u> f). Differences in cloud processes (convection vs. synoptic system) may <u>cause different signs of the impact of the model update</u> ~~vary increasing/decreasing in~~<u>on</u> graupel ~~by the model update~~.

Despite the drastic increase in mass concentrations of snow and cloud ice, the amount of high cloud<u>s</u>, particularly, optically thin cloud<u>s</u>, is ~~somewhat~~ reduced <u>by the update (Figure 5, g)</u>. Consistently, global mean <u>outgoing longwave radiation (OLR)</u> is increased by about 4 W m^{-2} (<u>a</u>~~a~~Figure 5<u>5</u>~~,~~ c), opposite to that found in Roh et al. (2017). In addition, <u>the</u> decrease in <u>top-of-atmosphere (TOA)</u> brightness temperature by the update ~~(Figure 7)~~ is very small <u>(Figure 7)</u> compared with that in Roh et al. (2017). These differences between Roh et al. (2017) and this study can be mostly explained by the new coupling procedure between cloud microphysics and radiative transfer<u>,</u> as described in Section 3.<u>2</u>~~3~~<u>,</u> and be partially explained by the different treatment of <u>the</u> terminal velocity of cloud ice <u>in the reference runs between Roh et al. (2017) and this study. Eventually,</u> <u>T</u>~~t~~he cloud ice terminal velocity <u>was set to zero in both Roh et al. (2017) and this study. Unlike this study, Roh et al. (2017) performed their reference run with non-zero cloud ice terminal velocity, as</u> diagnosed by Heymsfield and Donner (1990)<u>, and their comparison before and after the scheme update includes the effects of reduced cloud ice terminal velocity.</u> ~~was replaced with zero in Roh et al. (2017) whereas it was zero and unchanged in this study.~~ The reduction of the cloud ice <u>descent</u>~~fall~~ speed, as in Roh et al. (2017), could increase and elevate ~~the~~ high cloud<u>s</u> and decrease<u>s</u> the OLR <u>(Kodama et al., 2012)</u>~~, as also seen in Kodama et al. (2012)~~. <u>A</u> ~~The~~ low cloud amount ~~is~~ increased <u>(Figure 5i)</u> as a result of <u>the</u> compensation between an increase in ~~a~~ medium and ~~a~~ thick cloud<u>s</u> and a decrease in ~~a~~ thin cloud<u>s</u>. These results indicate that the clouds grow thicker on average by updating the cloud microphysics scheme in this study.

3.<u>3</u>~~2~~ Coupling between cloud microphysics and radiative transfer

In NICAM16-S, <u>the</u> cloud microphysics scheme<u>s</u> ~~are~~ <u>is</u> fully coupled with <u>the radiation scheme</u>~~a broadband radiative transfer model, named~~ ~~MstrnX~~ <u>mstrnX</u> (Sekiguchi and Nakajima, 2008). The effective ~~radii~~ <u>radius r_e</u> of hydrometeors ~~are~~ <u>is</u> calculated with the same assumption of the particle size distribution function as <u>the</u> cloud microphysics <u>scheme,</u>~~.~~ including indirect effect<u>s</u>~~,~~ and then passed to the ~~MstrnX~~<u>mstrnX</u> scheme. In contrast, fixed effective radii <u>of 8 μm for liquid hydrometeors and 40 μm for ice hydrometeors</u> were assumed in NICAM.12 ~~(8 and 40 μm were assumed for liquid and solid hydrometeors, respectively)~~.

The use of consistent assumptions <u>of coupling</u> between cloud microphysics and radiative transfer can reduce ~~a~~ <u>the</u> model bias in the radiation budget (Seiki et al., 2015a) and has non-negligible impacts on ~~a~~ climate projection (Chen et al., 2016). In addition, the coupling provides model developers with a better understanding of the origins of model biases (Hashino et al., 2016). ~~The following section summarizes the changes in the radiation budget by the coupling between cloud microphysics and radiative transfer as well as details of the update.~~

The MstrnX mstrnX scheme requires the a database of single scattering properties of hydrometeors (RADPARA), including parameters such as the volume extinction coefficient, absorption coefficient, asymmetry factor, and the second moment of phase function (Nakajima et al., 2000). In NICAM-16-S we used the RADPARA database revised by Seiki et al., (2014). The RADPARA database of liquid hydrometeors was pre-calculated according to the Mie theory. The non-spherical RADPARA database developed by Fu (1996) and Fu et al. (1998) was applied to solid hydrometeors. The RADPARA database was then compiled as a lookup table of the effective radii from 1 μm to 1 mm to cover the size range of most of the hydrometeors in global simulations (Seiki et al., 2014). The effects of precipitating hydrometeors on the radiation budget are detectable, specifically over the intertropical convergence zone (ITCZ) and storm-track region (e.g., Waliser et al., 2011; Li et al., 2014, 2016; Chen et al., 2018; Li et al., 2014, 2016; Michibata et al., 2019; Waliser et al., 2011). The revised RADPARA database was evaluated in depth by comparing it with balloon-borne sonde observations in a midlatitude cirrus case (Seiki et al., 2014), and its effectiveness for global simulations was evaluated in several studies (Satoh et al., 2018; Seiki et al., 2015a, 2015b; Satoh et al., 2018).

Because of non-sphericity, the effective radius of ice particles has a controversial definition, whereas the effective radius is well defined in the case of spherical particles. According to Fu (1996), the effective radius, r_e, of solid hydrometeors is defined as follows:

$$r_{e,j} = \frac{3}{4\rho_{ice}} \frac{\rho q_j}{\int_0^\infty A_j(D_j) N_j(D_j) dD_j} \quad (j = i, s, g), \tag{1}$$

where $j = i, s, g$ are cloud ice, snow, and graupel, respectively; ρ is the air density; $\rho_{ice} = 916.7$ kg m^{-3}; q_j is specific content; A_j is the projected area of a particle to flow, ; and D_j is diameter and $\rho_{ice} = 916.7$ kg m^{-3}. The integral in equation (1) is analytically calculated using the assumed particle size distribution functions $N_j(D_j)$ and a sponge-like spherical shape for in the case of cloud ice and graupel. In contrast, snow has two-dimensional fractal shapes; hence, the numerator–denominator ratio becomes almost constant. Thus, the effective radius of snow is assumed to be constant ($r_{e,is} = 125$ μm with $A_s = 0.45 D_s^{2.0}$), and it which is derived by approximating the A–D relationship of aggregates compiled by Mitchell (1996).

The impacts of the coupling procedure and the non-spherical scattering were examined by comparing the REF run with the NONSI run using the fixed effective radii and the spherical RADPARA database. The impacts of non-spherical scattering alone could be seen from the comparison between the REF and NONS runs using the spherical RADPARA database. a set of seasonal simulations with NICAM-16S (g run in Table 2), NICAM-16S except for the spherical RADPARA database (g9 run in Table 2), and NICAM-16S except for the fixed effective radii and the spherical RADPARA database (g9a in Table 2). Figure 8 shows the zonal mean values of the OLR and the reflected outgoing shortwave radiation (OSR) at the TOA from the sensitivity experiments. Given the substantial increase in cloud ice and snow from the revised new NSW6 scheme (cf. Section 3.12), ice optical thickness increases proportionately to the increases in the ice water path (IWP) with the fixed effective radii. As a result, both the longwave and shortwave radiation budgets are for both the longwave and shortwave is strongly biased in the NONSI g9a run. A major portion of the biases in OLR is drastically offset in the g9 NONS run by assuming larger effective radii in the coupling procedure. Thus, the coupling procedure automatically prevents artificial biases originating from the inconsistent parameter settings between the cloud microphysics and radiative transfer with at the model update. The use of the non-spherical RADPARA database slightly increases OSR over the tropics to the midlatitude of the summer hemisphere because the assumed asymmetry factor for non-spherical particles is smaller than the that one for spherical particles (cf. Seiki et al., 2014).

Finally, NICAM16-S still shows strong negative biases in OLR over the tropical to subtropical regions and OSR over the subtropical high-pressure belt at the TOA compared with the Clouds and Earth's Radiant Energy Systems (CERES) product (Figure 8, black vs. red curves), and these biases are qualitatively similar to those simulated in NICAM.12 (Kodama et al., 2015). The former OLR bias can be solved by increasing vertical resolution to 400 m near the tropopause with 74 vertical layers (Seiki et al., 2015b). The latter OSR bias mainly stem from the underestimation of low-level clouds, and the current updates in the cloud microphysics scheme do not improve the results for warm clouds. The coupling procedure strengthens the negative biases in OSR at TOA in the midlatitudes (see Figure 8, green vs. blue curves) because, in NICAM.12, high clouds associated with extratropical cyclones are artificially brightened and, therefore, conceal the biases due to low-level clouds (cf. Fig. 4 in Kodama et al., 2012). Unlike NICAM.12, a strong negative bias of OSR at the TOA is also prominent over the Arctic region, and this seems to relate to the update (reduction) of the surface albedo introduced in Section 3.6.

3.3 Aerosols in the cloud microphysics and radiation schemes

In NICAM.12, the direct radiative effect of aerosol is not considered in the radiation scheme, and the number concentration of CCN is set to a constant value of 50 cm^{-3}, a typical value over the ocean, in the cloud microphysics scheme. In NICAM16-S, both the direct and indirect effects of aerosols are considered by prescribing a distribution of aerosol mass concentration in the radiation scheme and CCN in the cloud microphysics scheme. The dataset of natural aerosols in the troposphere and stratosphere is described in Section 2.3. For anthropogenic aerosols in the troposphere, a simple plume model, MACv2-SP (Stevens et al., 2017; Fiedler et al., 2019), is used to diagnose the vertical profile of the aerosol optical depth, single scattering albedo, and asymmetry factor and factor of CCN increase arising from anthropogenic aerosols. This means that the magnitude of the anthropogenic increase in CCN depends on CCN from natural origins.

The sensitivity experiments with and without the update of the aerosol treatment (the REF and NOAER runs) are compared in Figure 9. The aerosol update reduces the net downward shortwave radiation at the surface over most of the continents, particularly over Africa and South Asia (Figure 9, b and d), leading to a reduction of the excess insolation there (not shown). The reduced insolation at the surface is partly cancelled out by a reduction in the upward longwave radiation over Africa (Figure 9, a and c) in association with a decrease in surface air temperature (not shown). Meanwhile, an enhancement of the surface net downward shortwave radiation is dominant over the ocean, particularly in the NICAM16-9S (14-km mesh) run (Figure 9, b and d), in association with a thinning of cloud optical depth and a decrease in cloud amount (not shown). This links to a decrease in the liquid water path with the aerosol update (Figure 5f), which was also found in an online aerosol experiment with the 14-km mesh NICAM (Sato et al., 2018). As a result of these compensations, the global mean net surface radiation change arising from aerosol forcing is around –2.0 W m^{-2} in NICAM16-7S and +0.4 W m^{-2} in NICAM16-9S in this study. Such a reverse from a decrease to an increase between the resolutions might be related to the resolution dependency of the low and middle cloud amount in the REF run (left panels of Figure 5, h and i), and a detailed analysis is needed to properly understand the mechanism.

3.~~5~~4 Land surface model

~~The~~A land surface model ~~named as minimal advanced treatments of surface interaction and runoff~~ (MATSIRO~~;~~ (Takata et al., 2003) is used in NICAM. Recently, a wetland scheme was implemented in MATSIRO of NICAM16-S to represent the storage of snowmelt while considering the subgrid-scale terrain complexity (Nitta et al., 2017)~~; it was implemented in NICAM.16-S~~. The wetland scheme reduces the summertime warm and dry bias over much of Western Eurasia and North America through delayed snowmelt runoff in MIROC5 (Nitta et al., 2017). In addition, the effect of ~~a~~ decrease~~d in~~ surface albedo associated with the accumulation of water on land ice was implemented in NICAM~~.~~16-S.

Figure 10 shows the impact~~s~~ of the land surface model update on soil moisture~~, precipitation, and surface air temperature in~~ during boreal summer~~s~~. The soil moisture is increased over most of the Eurasian and ~~the~~ North American continents, as expected from Nitta et al. (2017), particularly in ~~the~~ Siberia and ~~the area~~ around the Great Lakes. Though it is expected from Nitta et al. (2017) that increased soil moisture leads to an increase in ~~Consistently, albeit noisier,~~ precipitation ~~is increased~~ and a decrease in surface air temperature ~~is decreased on average in the Siberia and the area around the Great Lakes in summer~~, the actual impacts on precipitation and surface air temperature are still unclear (not shown). It is difficult to show robust reduction of the biases at this stage, and~~.~~ ~~l~~Longer integration is needed to assess these impacts ~~quantitatively~~appropriately.

3.~~5~~6 Surface albedo

Surface albedo values were updated~~revised~~ based on ~~the~~ observations. In NICAM.12~~the past~~, they were tuned to reduce the TOA radiation imbalance, and this~~which~~ caused a higher bias of surface albedo over the Arctic compared with that seen in ~~a~~ satellite observation~~s~~ (Hashino et al., 2016). Table 6 shows the ~~revised and previous values of~~ surface albedo values used in NICAM16-S and NICAM.12. ~~In most cases, t~~The albedo values of the sea ice for the visible and near-infrared wavelengths and of fresh snow over land for the visible wavelengths ~~are~~ were set to be smaller in NICAM16-S than those in NICAM.12. In addition to the update~~changes~~ in Table 6, an artificial ~~the~~ elevated~~ion of the~~ ocean surface albedo for the direct visible wave~~length~~ by a factor of 1.35 ~~times~~ for the radiation scheme~~calculation~~ in NICAM.12~~the previous simulations~~ ~~is~~was discarded in NICAM16-S ~~because this is a highly artificial factor~~.

~~Consistent with the reduced albedo and the increased net upward shortwave radiation,~~ The sensitivity experiments with and without the albedo update ~~using NICAM16-7S~~ (the REF and NOALB runs, respectively) show that the use of the new surface albedo values~~configuration~~ tends to reduce the surface air temperature bias over ~~the~~ land ice compared with the previous~~old one~~ ~~bias~~ (Figure 11, a, vs. Figure 11, ~~bc~~. and ~~black~~green vs. red~~green~~ curves~~lines~~ in Figure 11, d). Specifically, the cold bias in Greenland, the Himalayas, and the Antarctic is reduced. This is consistent with the reduced surface albedo for the visible wavelengths and the resulting decreased net upward shortwave radiation at the surface (Figure 5, k). Global mean ~~Upward~~ net downward longwave radiation at the surface is increased (Figure 5~~5~~, j). The increase is attributed primarily to a decrease~~d in~~ upward longwave radiation over the ocean (not shown), consistent with the increased surface albedo for the infrared wavelengths~~(i.e., less blackbody)~~ over the ocean. In terms of the TOA radiation budget, OSR worsens by a few watts per square meter (Figure 5~~5~~, d), which arises from the polar regions (Figure 12~~12~~, b; green vs. red curves). ~~Warm bias still exists in the Arctic in the new configuration, and this will be reduced by changing a sea ice configuration, as explained in Section 3.6.~~

3.67 Treatment of oceans

A mixed-layer slab ocean model similar to that in McFarlane et al. (1992) had beenwas implemented in NICAM. The model predicts SST, ICE, snow over sea ice, and snow temperature by solving a the heat balance between the ocean, sea ice, snow, and the atmosphere. A The depth of the slab ocean model is set to 15 m, considering the better performance of the simulated precipitation pattern (Kodama et al., 2015) and MJO (Grabowski, 2006). A simple nudging technique is used to force the predicted SST and ICE toward their a reference statesSST with a a relaxation time of τ_{SST}7 and τ_{ICE}, respectivelydays. Specifically, $\tau_{SST} = 7$ days and $\tau_{ICE} = 0$ (i.e., ICE was fixed to the boundary condition) were used in the slab ocean experiments of this study and in the previous climate simulation with NICAM.12 (Kodama et al., 2015). Both τ_{SST} and τ_{ICE} were set to zero in the fixed SST/ICE experiments, including the HighResMIP simulations.

In the slab ocean model implemented in NICAM.12 and NICAM-16-S, SIC is diagnosed from ICE, as,

$$
\text{SIC} = \begin{cases} \sqrt{\dfrac{\text{ICE}}{\text{SICCRT}}}, & \text{for ICE} < \text{SICCRT}, \\ 1, & \text{for ICE} \geq \text{SICCRT} \end{cases} \tag{2}
$$

where SICCRT is a parameter inset to 300 kg m^{-2}.

In many cases, including the HighResMIP protocol, only the SST and SIC data are provided from CMIP6 to run the model, and, therefore, the ICE data prescribed for the model should be diagnosed from SIC data. In NICAM.12 and NICAM16-S, ICE is diagnosed simply as,

$$
\text{ICE} = \text{SICCRT} \times \text{SIC}^2. \tag{3}
$$

In the previous study using NICAM.12, we often set a the value of SICCRT to 300 kg m^{-2}. considering for Eq. (3), the same as that used in Eq. (2). However, this situation leads tocauses an underestimation of ICE over most of the sea ice areas and causesand leads to a warm bias over the Arctic (Kodama et al., 2015); Figure 11, b; blue curve in Figure 11, d). Based on an ocean model result (H. Tatebe, personal communication), we performed a series of preliminary annual-scale experiments using NICAM16-7S, with SICCRT values of 1,600 and 3,200, to improve the surface air temperature over the Arctic. As a result of this crude tuning, and sensitivity experiments (Figure 10c), SICCRT is set to 1,600 kg m^{-2} for Eq. (3) in NICAM16-S. to diagnose ICE from SIC. This led to a significant reduction in the warm bias (Figure 11, b, vs. Figure 11, c; blue vs. red curves in Figure 11, d) and an excess of OLR at TOA (blue vs. red curves in Figure 1212, a) over the Arctic.

In the HighResMIP protocol, SST and SIC in the model are fixed to the time-varying boundary external conditions. This fixed SST/SIC condition is achieved by nudging SST and ICE toward the prescribed external condition with a zero relaxation time in the slab ocean model. However, fixed SST simulation is known to cause severe bias in the precipitation pattern in the tropics (Kodama et al., 2015), and thus the use of the slab ocean model with a 7 day relaxation time is often preferred. e and Figure 11 summarize the comparisons of the simulations between the fixed SST condition and the slab ocean model and nudging. Overall, the global mean impact of the slab ocean model is not very large (circles vs. rectangles in Figure 55). Compared with the fixed SST runs, In the simulation with slab ocean model, global mean precipitation and OLR showeds a slight increases in the slab ocean runs, and OLR shows an increase, which is are associated with a slightly warmer surface air temperature. In terms of the local climate, however, the fixed SST simulation is known to cause severe bias in the horizontal distribution of clouds and precipitation systems in the tropics (Kodama et al., 2015; Figure 13), and thus the use of the slab ocean model with a 7-day relaxation time is often preferred. The introduction of the slab ocean model considerably affects affected the horizontal distribution of the clouds and precipitation systems (Figure 13). A Double double ITCZ bias is was more prominent in the precipitation, as well as, the high cloud fraction, and OLR fields (not shown) in the fixed SST

runs compared with the slab ocean runs, particularly in the high-resolution run. ~~As far as o~~Our investigation ~~shows~~showed ~~;~~ that NICAM16-9S with the slab ocean model best ~~simulates~~simulated the ITCZ peak precipitation and the precipitation pattern. Although ~~an~~ the importance of the short-term SST variation driven by the atmosphere ~~on~~ for the precipitation pattern ~~of the precipitation~~ is apparent from Figure 13, the introduction of the slab ocean model alone does not resolve ~~its~~the bias ~~of~~

5 ~~the precipitation pattern~~. Further analysis is necessary to understand the physical mechanisms of the bias, ~~notably~~ perhaps the timescale of the convection in particular~~,~~.

3.~~7~~8 Orographic gravity wave drag

No gravity wave drag scheme is used in NICAM.12. In NICAM16-S, the conventional orographic gravity wave drag scheme

10 (McFarlane, 1987) is used~~tested~~ to better simulate the location and strength of the subtropical jet. The wave generation parameter ~~(~~α~~)~~, which is proportional to the product of wave generation efficiency and representative horizontal wavenumber (Eq. 3.1b in McFarlane 1987), was tuned first for NICAM16-9S to improve zonal mean zonal wind and then roughly halved as the horizontal mesh size was doubled~~is roughly doubled as the horizontal mesh size is halved~~. Specifically, α ~~is~~was set to 3.38×10^{-5} for NICAM16-7S~~56 km mesh~~, 7.12×10^{-5} for NICAM16-8S~~28 km mesh~~, and 1.46×10^{-4} for NICAM16-

15 9S~~14 km mesh, respectively~~. Figure 14 and Figure 15 show the zonal mean zonal wind in boreal summer and winter, as simulated with and without the gravity wave drag scheme (the REF and NOGWD runs, respectively). The zonal mean zonal wind simulated without the gravity wave drag scheme ~~is~~was biased poleward in both the NICAM16-9S and NICAM16-7S~~56 km and 14 km mesh~~ runs. The gravity wave drag scheme ~~decelerates~~decelerated the zonal mean zonal wind at the poleward flank of the subtropical jet, especially ~~during~~in northern hemisphere~~NH~~ winter, reducing the locational bias of the

20 jet. The impact of the gravity wave drag scheme is larger in NICAM16-7S~~the 56 km mesh model~~ than ~~that~~ in NICAM16-9S~~the 14 km mesh model~~. The pattern of the zonal wind response ~~of~~to the gravity wave drag scheme~~the zonal mean zonal wind to the orographic gravity wave drag scheme~~ is similar to that of previous studies (e.g.,~~ Iwasaki et al., 1989;~~ McFarlane, 1987; Iwasaki et al., 1989).

25 Although it is believed that even a mesh size of 14 km ~~mesh~~ is insufficient to explicitly simulate the effects of the orographic gravity wave drag on the mean field (Nappo, 2012), introducing such a gravity wave drag scheme will not necessarily lead to an improvement of the simulated climate ~~it may not be a wise choice to introduce such a gravity wave drag scheme to~~in the global non-hydrostatic model. The ~~Gravity~~gravity wave drag scheme introduces the ~~uncertain~~ parameter α, which is uncertain and tuned to best simulate the climatology of the zonal wind for each resolution in general, although we did not

30 tune α for each resolution. There is no solid guideline ~~to~~for ~~determine~~determining α, including the dependency of the wave generation efficiency and representative horizontal wavenumber on the horizontal and vertical resolutions. Therefore, the use of a gravity wave drag scheme may hinder the pure resolution dependency of the mean field and suppress the advantages of the high-resolution model for simulating large-scale circulation in a seamless manner. Nevertheless, we ~~determined~~decided to use the orographic gravity wave drag scheme for HighResMIP~~CMIP6~~ to reduce the locational bias of the subtropical jet to

35 ~~so that an~~ improve~~ment~~ results for ~~of~~ the tropical cyclone track region~~would ensue~~. It is important to recognize the merits and demerits involved in the use of a gravity wave drag scheme and reconsider its use depending on the main purpose of the simulation.

4. Horizontal and temporal resolution dependency ~~Preliminary evaluations with observations including dependency of horizontal resolution~~

Understanding the dependency of horizontal resolution is a central interest of the HighResMIP. Figure 16 shows the global mean climate in NICAM16-7S (56-km mesh; blue circle), NICAM16-8S (28-km mesh; green circle), and NICAM16-9S (14-km mesh; red circle), along with its sensitivity to the time step interval of the models' dynamics (including the gravity wave drag scheme) and radiation scheme. Note that the dependency of the interval of the radiation scheme on the global mean climate is negligible.

~~G~~Table 6 shows the summary of the comparisons between NICAM16-S simulations and the observations along with a dependency of horizontal resolution. In terms of the global mean energy budget of the atmosphere, most of the bias features are similar to the previous NICAM climate simulations with 14-km mesh (Kodama et al., 2015), meaning that both OLR and OSR are underestimated. In the past, a high cloud amount was overestimated in the NICAM simulations. Now, a high cloud amount is comparable with the ISCCP observation in terms of global mean, although higher altitudes and thinner optical depth (not shown) are simulated, leading to the underestimation of OLR. ~~The most noticeable change from the previous simulation in terms of the global mean is the IWP. As described in Section 3.1, IWP is drastically increased by the update of cloud microphysics scheme.~~ Global mean precipitation and TOA OLR ~~are~~ decreased as the horizontal resolution ~~is~~ increased (Figure 16, b and c), consistent with a previous NICAM study using 3.5- to ~~14~~ 14-km mesh~~es~~ ~~NICAM~~ (Miyakawa and Miura, 2019). The results did not strongly depend on the time step interval of the model. As seen in Figure 13, the precipitation pattern in the tropics depends strongly on the resolution: more-dominant double-ITCZ patterns and less-intense local precipitation are simulated as the horizontal resolution is increased. The intense precipitation occurs less frequently in the higher-resolution runs (Figure 17), consistent with Noda et al. (2012) using older NICAM with 14- and 7-km meshes. The intense precipitation occurs more frequently in the model compared with the Global Precipitation Climatology Project (GPCP) product (Noda et al., 2012), and it is consistent with the results of Maher et al. (2018), who compared precipitation in global climate models without a convection scheme with precipitation in the GPCP product. (Na et al., (2020) showed that the frequency of intense precipitation in the GPCP product is lower than that in the TRMM product, and the 14-km mesh NICAM without a convection scheme could realistically reproduce the intense precipitation observed by the TRMM satellite.

The ~~L~~low ~~level~~ cloud amount ~~is~~ was substantially underestimated, especially in the NICAM16-7S and NICAM16-8S runs (Figure 16, i), leading to ~~the~~ an underestimation of the OSR at the TOA (Figure 16, d). Consistently, the net downward shortwave radiation at the surface decreased (Figure 16, k) and the ~~Surface~~ surface air temperature ~~is~~ slightly decreased (Figure 16, a) as the horizontal resolution ~~is~~ increased ~~in association with an increase in total cloud fraction~~. ~~The most noticeable change from the previous simulation in terms of the global mean is the IWP. As described in Section 3.1, IWP is drastically increased by the update of cloud microphysics scheme.~~ This dependency of the low cloud amount and its related variables, in terms of global mean, on horizontal resolution could be reproduced by changing the time step interval of the dynamics in the model. The low cloud amount was rather greater in the 56-km mesh run than that in the 14-km mesh run under the fixed time step interval of the dynamics (red circle in the REFFIX run vs. blue circle in the DDT1M run in Figure 16, i). Also, the simulated OSR at the TOA is greater and closer to that of the CERES product in the 56-km mesh run compared with the 14-km mesh run with the same temporal resolution, though the better performance in the simulated global mean OSR at the TOA in the 56-km mesh run is a result of a strong compensation between a negative bias off the subtropical west coasts of continents and the southern hemisphere storm-track region and a positive bias in the rest of the lower latitudes (not shown). Such a result of dependency of OSR at the TOA on horizontal resolution with a fixed temporal resolution is similar to that found by Goto et al. (2020), who executed 14-km and 56-km mesh online-aerosol NICAM with the same time step intervals of 60 s for the dynamics, turbulence, and surface schemes and 10 s for the cloud microphysics

scheme. In HighResMIP, there is no protocol for the temporal resolution of the model, and the horizontal resolution dependency may include the effect of the temporal resolution change in the HighResMIP models.

5. Computational aspects

5.1 Simulations

Table 7 ~~shows~~ describes the computational setting and the simulation year per wall-clock day (SYPD)~~elapsed time and the file size~~ of the NICAM16-S simulations ~~by NICAM16-7S~~run, ~~NICAM16-8S and NICAM16-9S~~ on the Earth Simulator 3 ~~(NEC SX-ACE)~~. The Earth Simulator 3 is an NEC SX-ACE system with 5,120 nodes in total for computation, and each computation node has 4 cores. We often used 10, 40, and 160 computation nodes to run NICAM16-7S, NICAM16-8S, and NICAM-9S, respectively, to obtain a balance between computational efficiency and wall clock time. An exception was NICAM16-8S for the HighResMIP simulation, for which 160 computation nodes were used to perform a 101-year simulation within a realistic clock time. A ~~File~~file-staging option was used in the NICAM16-8S and NICAM16-9S simulations, whereas the file was directly read and written from ~~the~~a global file system in the NICAM16-7S simulation to reduce~~save time for~~ queuing time. T~~The~~he actual SYPD~~wall clock time, including queuing time,~~ was a few times smaller~~greater~~ than that~~SYPD~~ shown in Table 7 for NICAM16-8S and NICAM16-9S ~~depending on the congestion of the Earth Simulator 3. For the product run of NICAM16-8S, 160 nodes are used to finish a 101-year simulation within a realistic time.~~

Figure 18 breaks down the total elapsed time ~~into~~for each component of the model. Unlike a previous evaluation using the K computer (Yashiro et al., 2016), the measurement ~~included~~includes ~~an~~the initial setup and input/output processes. Physics contributes~~is~~ a major part ~~that contributes~~to the total elapsed time. Among the several physics components, the radiation scheme primarily contributes to the total elapsed time, followed by the cloud microphysics scheme, consistent with Yashiro et al. (2016) on the K computer. As the resolution ~~increases~~increased, the percentage of time consumed by ~~the~~dynamics ~~is~~ increased and the time consumed by~~that of~~ the cloud microphysics and turbulence ~~near surface~~ processes ~~decreases~~ decreased because of their invariant time step interval ~~of the cloud microphysics and near-surface processes is set to be invariant throughout~~among the models with different resolutions. An increase in the percentage of the land surface scheme in the simulations with higher resolution and greater number of computational nodes seems to be caused by the node imbalance associated with land–ocean distribution. Because the dynamics involves communication at every time step, some parts of the elapsed time counted as the dynamics can actually be a waiting time due to the ~~because of~~node imbalance occurring in other processes.

5.2 Post-~~processes~~processing

The data are output ~~in~~on the model's native~~an~~ icosahedral grid on the height above sea level (ASL) or on the standard pressure. The vertical interpolation from the terrain-following height to the ASL height or standard pressure is performed online using second-order Lagrange interpolation during the simulation.

Post-~~processes~~processing ~~are~~is performed in the following order: *ico2ll*, *roughen*, and *z2pre*.
(1) *ico2ll*

All the native icosahedral grid data are converted to high-resolution latitude–longitude grid data by area–weight averaging. The interval of latitude and longitude is determined so that the longitudinal interval is close to the average interval of the icosahedral grid (Satoh et al., 2014) on the equator. Specifically, the interval of longitude and latitude is 0.56° for NICAM16-7S, 0.28° for NICAM16-8S, and 0.14° for NICAM16-9S.

5 (2) *roughen*

All ~~The~~ the high-resolution latitude–longitude grid data are coarsened to low-resolution latitude–longitude grid data by area–weight averaging. It is often necessary to reduce the amount of data ~~size~~ by such coarsening, although HighResMIP~~CMIP6~~ does not ~~request~~ ask us to coarsen the data. We prepare~~d~~ 1.0°, 1.25°, and 2.5° data for analysis.

(3) *z2pre*

10 Several three-dimensional variables are converted from the ASL height to the standard pressure at this point by linear interpolation, if it is necessary.

After post-processing steps (1)–(3), monthly mean data are created.

15 The ~~Pressure~~ pressure velocity is obtained~~diagnosed~~ from the vertical velocity and temperature after *ico2ll*~~,~~ under the ~~assuming~~ assumption of hydrostatic balance. The ~~Geopotential~~ geopotential height is calculated from the linear interpolation of vertical levels using logarithms of pressure, with an ~~assuming~~ assumption of constant gravity acceleration regardless ~~irrespective~~ of height, which is a ~~consistent~~ treatment consistent with the model configuration.

20 Note that the high-resolution data requested by HighResMIP are or will be available through the Earth System Grid Federation (ESGF). All the other data such as low resolution, monthly mean, and special variables are available on request from the corresponding author.

6. Summary

25 This paper ~~described~~ describes the experimental design, the latest stable version of NICAM prepared for the HighResMIP (NICAM16-S),~~model description~~ and impacts of ~~the model~~NICAM updates on the simulated climatology using NICAM16-S at different resolutions~~prepared for CMIP6 HighResMIP (NICAM16-S)~~. The major updates and their impacts on simulation results are summarized as follows:

- ~~Update~~ update of the cloud microphysics scheme: Snow and cloud ice was increase~~d in the atmosphere~~, leading to
30   decreased ~~less~~ high cloud amount and increased ~~more~~ OLR at the TOA.
- ~~Implementation~~ implementation of the coupling between cloud microphysics and radiation schemes: The negative OLR bias ~~is~~ was reduced in association with a~~the~~ larger cloud ice effective radius.
- ~~Update~~ update of treatment of natural and anthropogenic aerosols: The ~~Local~~ local surface radiation budget ~~is~~ was improved, especially over Africa and South Asia.
35 - ~~Update~~ update of land surface model: Overall, the soil moisture ~~and the precipitation increase and the surface air temperature decreases~~ over most of the Eurasian and the North American continents was increased~~over the continent~~.
- update~~Revision~~ of the surface albedo values: The ~~Cold~~ cold bias in the Greenland, the Himalayas, and the Antarctic ~~is~~ was ~~reduced~~decreased.
- modification of~~Change in~~ the ~~diagnostics of~~ ICE diagnostics: The ~~W~~warm bias over the Arctic region ~~is reduced~~was
40   decreased.

17

- ~~Introduction~~ introduction of the orographic gravity wave drag scheme: The location and strength of the zonal mean jet ~~are~~ were improved.

Comprehensive evaluations and future projections using full HighResMIP data by NICAM16-S will be presented in a forthcoming paper.

5

Code and data availability

The exact model source code, input data ~~or~~ and scripts to generate them, and scripts for the simulations and ~~the~~ post-~~processes~~ processing used to produce the results presented in this paper are archived on Zenodo (doi:10.5281/zenodo.3727329). The model source ~~codes~~ code ~~are~~ is shared ~~by~~ with the NICAM community and available for
10 those who are interested as long as ~~a~~ the user follows the terms and conditions described ~~in~~ at http://www.nicam.jp/hiki/?Research+Collaborations. Most of the input data are freely accessible from input4MIPs (https://esgf-node.llnl.gov/projects/input4mips/) for ocean boundary conditions, GHG concentrations, and ozone and solar forcing~~,~~; from the ECMWF website (https://apps.ecmwf.int/datasets/data/era20c-daily/) for ERA-20C reanalysis~~,~~; from supplemental materials of MACv2-SP description papers (Fiedler et al., 2019; Stevens et al., 2017) for anthropogenic aerosol
15 data~~,~~; and from the U.S. Geological Survey website (https://doi.org/10.5066/F7DF6PQS) for GTOPO30 data. The other input data, obtained from ftp://iacftp.ethz.ch/pub_read/luo/CMIP6/MIROC3.2_29/ for volcanic aerosols and from https://lpdaac.usgs.gov/ ~~–~~for the leaf area index, are available on request from the corresponding author. HighResMIP product run ~~Tier 1 (3) simulation~~ data are ~~or are (and~~ will be~~)~~ distributed freely through the ~~Earth System Grid Federation~~ (~~ESGF~~). ~~Data on a series of~~The sensitivity ~~experiments~~ experiment data are available on request from the corresponding
20 author.

Author contributions

CK and ATN managed the overall HighResMIP~~CMIP6~~ activity in the NICAM group and prepared the initial and boundary conditions, and MS managed development and scientific activity in the NICAM group. CK added interfaces of the initial and
25 boundary conditions to NICAM~~,~~. ~~and~~ TO added a function to output variables requested by HighResMIP~~CMIP6~~ and converted the output data using CMOR3. CK, TO, TS, HY, MN, and YY contributed to the development of NICAM16-S, including de~~bugging~~bug fixes, and WS, TN, and DG provided their schemes and/or parameters for the development. CK performed all the HighResMIP simulations~~product runs~~ and ~~all~~the sensitivity experiments ~~described here~~, transferred the data to ESGF, and wrote a major part of this paper. TS wrote most ~~part~~ of Sections 3.1 and 3.2 and TS, ATN, DG, HM, and
30 TN modified the manuscript. All the authors provided advice for the development of NICAM16-S and/or experimental design and reviewed the manuscript.

Competing interests

The authors declare that they have no conflict of interest.

35

18

Acknowledgment

References

Adler, R. F., Huffman, G. J., Chang, A., Ferraro, R., Xie, P.-P., Janowiak, J., Rudolf, B., Schneider, U., Curtis, S., Bolvin, D., Gruber, A., Susskind, J., Arkin, P. and Nelkin, E.: The version-2 global precipitation climatology project (GPCP) monthly precipitation analysis (1979–present), J. Hydrometeorol., 4(6), 1147–1167, doi:10.1175/1525-

5   7541(2003)004<1147:TVGPCP>2.0.CO;2, 2003.

Aoki, T., Kuchiki, K., Niwano, M., Kodama, Y., Hosaka, M. and Tanaka, T.: Physically based snow albedo model for calculating broadband albedos and the solar heating profile in snowpack for general circulation models, J. Geophys. Res., 116(D11), D11114, doi:10.1029/2010JD015507, 2011.

Armstrong, R. L. and and Brun, E., Eds.: Snow and climate: Physical processes, surface energy exchange and modeling,

10   Cambridge Univ. Press, Cambridge, U. K., 2008.

Austin, R. T. and Stephens, G. L.: Retrieval of stratus cloud microphysical parameters using millimeter-wave radar and visible optical depth in preparation for CloudSat: 1. Algorithm formulation, J. Geophys. Res. Atmos., 106(D22), 28233–28242, doi:10.1029/2000JD000293, 2001.

Austin, R. T., Heymsfield, A. J. and Stephens, G. L.: Retrieval of ice cloud microphysical parameters using the CloudSat

15   millimeter-wave radar and temperature, J. Geophys. Res., 114, D00A23, doi:10.1029/2008JD010049, 2009.

Bodas-Salcedo, A., Webb, M. J., Brooks, M. E., Ringer, M. A., Williams, K. D., Milton, S. F. and Wilson, D. R.: Evaluating cloud systems in the Met Office global forecast model using simulated CloudSat radar reflectivities, J. Geophys. Res., 113, D00A13, doi:10.1029/2007JD009620, 2008.

Bodas-Salcedo, A., Webb, M. J., Bony, S., Chepfer, H., Dufresne, J.-L., Klein, S. A., Zhang, Y., Marchand, R., Haynes, J.

20   M., Pincus, R. and John, V. O.: COSP: Satellite simulation software for model assessment, Bull. Am. Meteorol. Soc., 92(8), 1023–1043, doi:10.1175/2011BAMS2856.1, 2011.

Bony, S., Stevens, B., Frierson, D. M. W., Jakob, C., Kageyama, M., Pincus, R., Shepherd, T. G., Sherwood, S. C., Siebesma, A. P., Sobel, A. H., Watanabe, M. and Webb, M. J.: Clouds, circulation and climate sensitivity, Nat. Geosci., 8(4), 261–268, doi:10.1038/ngeo2398, 2015.

25   Chen, Y.-W., Seiki, T., Kodama, C., Satoh, M., Noda, A. T. and Yamada, Y.: High Cloud Responses to Global Warming Simulated by Two Different Cloud Microphysics Schemes Implemented in the Nonhydrostatic Icosahedral Atmospheric Model (NICAM), J. Clim., 29(16), 5949–5964, doi:10.1175/JCLI-D-15-0668.1, 2016.

Chen, Y.-W., Seiki, T., Kodama, C., Satoh, M. and Noda, A. T.: Impact of precipitating ice hydrometeors on longwave radiative effect estimated by a global cloud-system resolving model, J. Adv. Model. Earth Syst., 10(2), 284–296,

30   doi:10.1002/2017MS001180, 2018.

Chepfer, H., Bony, S., Winker, D., Chiriaco, M., Dufresne, J.-L. and Sèze, G.: Use of CALIPSO lidar observations to evaluate the cloudiness simulated by a climate model, Geophys. Res. Lett., 35(15), L15704, doi:10.1029/2008GL034207, 2008.

Eyring, V., Bony, S., Meehl, G. A., Senior, C. A., Stevens, B., Stouffer, R. J. and Taylor, K. E.: Overview of the Coupled

35   Model Intercomparison Project Phase 6 (CMIP6) experimental design and organization, Geosci. Model Dev., 9(5), 1937–1958, doi:10.5194/gmd-9-1937-2016, 2016.

Fairall, C. W., Bradley, E. F., Hare, J. E., Grachev, A. A. and Edson, J. B.: Bulk parameterization of air–sea fluxes: updates and verification for the COARE algorithm, J. Clim., 16(4), 571–591, doi:10.1175/1520-0442(2003)016<0571:BPOASF>2.0.CO;2, 2003.

40   Fiedler, S., Stevens, B., Gidden, M., Smith, S. J., Riahi, K. and van Vuuren, D.: First forcing estimates from the future CMIP6 scenarios of anthropogenic aerosol optical properties and an associated Twomey effect, Geosci. Model Dev., 12(3), 989–1007, doi:10.5194/gmd-12-989-2019, 2019.

Field, P. R., Hogan, R. J., Brown, P. R. A., Illingworth, A. J., Choularton, T. W. and Cotton, R. J.: Parametrization of ice-particle size distributions for mid-latitude stratiform cloud, Q. J. R. Meteorol. Soc., 131(609), 1997–2017, doi:10.1256/qj.04.134, 2005.

Fu, Q.: An accurate parameterization of the solar radiative properties of cirrus clouds for climate models, J. Clim., 9(9), 2058–2082, doi:10.1175/1520-0442(1996)009<2058:AAPOTS>2.0.CO;2, 1996.

Fu, Q., Yang, P. and Sun, W. B.: An accurate parameterization of the infrared radiative properties of cirrus clouds for climate models, J. Clim., 11(9), 2223–2237, doi:10.1175/1520-0442(1998)011<2223:AAPOTI>2.0.CO;2, 1998.

Fukutomi, Y., Kodama, C., Yamada, Y., Noda, A. T. and Satoh, M.: Tropical synoptic-scale wave disturbances over the western Pacific simulated by a global cloud-system resolving model, Theor. Appl. Climatol., 124(3–4), 737–755, doi:10.1007/s00704-015-1456-4, 2016.

Gilmore, M. S., Straka, J. M. and Rasmussen, E. N.: Precipitation uncertainty due to variations in precipitation particle parameters within a simple microphysics scheme, Mon. Weather Rev., 132(11), 2610–2627, doi:10.1175/MWR2810.1, 2004.

Goto, D., Takemura, T. and Nakajima, T.: Importance of global aerosol modeling including secondary organic aerosol formed from monoterpene, J. Geophys. Res., 113(D7), D07205, doi:10.1029/2007JD009019, 2008.

Goto, D., Nakajima, T., Takemura, T. and Sudo, K.: A study of uncertainties in the sulfate distribution and its radiative forcing associated with sulfur chemistry in a global aerosol model, Atmos. Chem. Phys., 11(21), 10889–10910, doi:10.5194/acp-11-10889-2011, 2011.

Goto, D., Nakajima, T., Tie, D., Yashiro, H., Sato, Y., Suzuki, K., Uchida, J., Misawa, S., Yonemoto, R., Trieu, T. T. N., Tomita, H. and Satoh, M.: Multi-scale simulations of atmospheric pollutants using a non-hydrostatic icosahedral atmospheric model, in Land-Atmospheric Research Applications in South and Southeast Asia, edited by K. Vadrevu, T. Ohara, and C. Justice, pp. 277–302, Springer International Publishing., 2018.

Goto, D., Sato, Y., Yashiro, H., Suzuki, K., Oikawa, E., Kudo, R., Nagao, T. M. and Nakajima, T.: Global aerosol simulations using NICAM.16 on a 14-km grid spacing for a climate study: Improved and remaining issues relative to a lower-resolution model, Geosci. Model Dev. Discuss., doi:10.5194/gmd-2020-34, 2020.

Grabowski, W. W.: Impact of explicit atmosphere–ocean coupling on MJO-like coherent structures in idealized aquaplanet simulations, J. Atmos. Sci., 63(9), 2289–2306, doi:10.1175/JAS3740.1, 2006.

Haarsma, R. J., Roberts, M. J., Vidale, P. L., Senior, C. A., Bellucci, A., Bao, Q., Chang, P., Corti, S., Fučkar, N. S., Guemas, V., von Hardenberg, J., Hazeleger, W., Kodama, C., Koenigk, T., Leung, L. R. R., Lu, J., Luo, J.-J., Mao, J., Mizielinski, M. S., Mizuta, R., Nobre, P., Satoh, M., Scoccimarro, E., Semmler, T., Small, J. and von Storch, J.-S.: High Resolution Model Intercomparison Project (HighResMIP v1.0) for CMIP6, Geosci. Model Dev., 9(11), 4185–4208, doi:10.5194/gmd-9-4185-2016, 2016.

Hashino, T., Satoh, M., Hagihara, Y., Kubota, T., Matsui, T., Nasuno, T. and Okamoto, H.: Evaluating cloud microphysics from NICAM against CloudSat and CALIPSO, J. Geophys. Res. Atmos., 118(13), 7273–7292, doi:10.1002/jgrd.50564, 2013.

Hashino, T., Satoh, M., Hagihara, Y., Kato, S., Kubota, T., Matsui, T., Nasuno, T., Okamoto, H. and Sekiguchi, M.: Evaluating Arctic cloud radiative effects simulated by NICAM with A-train, J. Geophys. Res. Atmos., 121(12), 7041–7063, doi:10.1002/2016JD024775, 2016.

Haynes, J. M., Marchand, R. T., Luo, Z., Bodas-Salcedo, A. and Stephens, G. L.: A multipurpose radar simulation package: QuickBeam, Bull. Am. Meteorol. Soc., 88(11), 1723–1728, doi:10.1175/BAMS-88-11-1723, 2007.

Hegglin, M., Kinnison, D., Lamarque, J.-F. and Plummer, D.: CCMI ozone in support of CMIP6 - version 1.0. Version 20160711., 2016.

Hegglin, M., Kinnison, D., Lamarque, J.-F. and Plummer, D.: input4MIPs.CMIP6.ScenarioMIP.UReading.UReading-CCMI-ssp585-1-0, Version 20181101., 2018.

Heymsfield, A. J. and Donner, L. J.: A scheme for parameterizing ice-cloud water content in general circulation models, J. Atmos. Sci., 47(15), 1865–1877, doi:10.1175/1520-0469(1990)047<1865:ASFPIC>2.0.CO;2, 1990.

HighResMIP: PRIMAVERA-H2020 / HighResMIP-futureSSTSeaice, HighResMIP [online] Available from: https://github.com/PRIMAVERA-H2020/HighResMIP-futureSSTSeaice (Accessed 17 August 2020), 2020.

5 Hohenegger, C., Kornblueh, L., Klocke, D., Becker, T., Cioni, G., Engels, J. F., Schulzweida, U. and Stevens, B.: Climate statistics in global simulations of the atmosphere, from 80 to 2.5 km grid spacing, J. Meteorol. Soc. Japan., 98(1), 73–91, doi:10.2151/jmsj.2020-005, 2020.

Hong, S.-Y., Dudhia, J. and Chen, S.-H.: A revised approach to ice microphysical processes for the bulk parameterization of clouds and precipitation, Mon. Weather Rev., 132(1), 103–120, doi:10.1175/1520-

10 0493(2004)132<0103:ARATIM>2.0.CO;2, 2004.

Iga, S., Tomita, H., Tsushima, Y. and Satoh, M.: Climatology of a nonhydrostatic global model with explicit cloud processes, Geophys. Res. Lett., 34(22), L22814, doi:10.1029/2007GL031048, 2007.

Iwasaki, T., Yamada, S. and Tada, K.: A parameterization scheme of orographic gravity wave drag with two different vertical partitionings Part I: impacts on medium-range forecasts, J. Meteorol. Soc. Japan., 67(1), 11–27,

15 doi:10.2151/jmsj1965.67.1_11, 1989.

Kato, S., Rose, F. G., Rutan, D. A., Thorsen, T. J., Loeb, N. G., Doelling, D. R., Huang, X., Smith, W. L., Su, W. and Ham, S.-H.: Surface irradiances of edition 4.0 Clouds and the Earth's Radiant Energy System (CERES) Energy Balanced and Filled (EBAF) data product, J. Clim., 31(11), 4501–4527, doi:10.1175/JCLI-D-17-0523.1, 2018.

Kennedy, J., Titchner, H., Rayner, N. and Roberts, M.: input4MIPs.MOHC.SSTsAndSeaIce.HighResMIP.MOHC-HadISST-

20 2-2-0-0-0, Version 20170201, Earth System Grid Federation., 2017.

Kennedy, J., Titchner, H., Rayner, N. and Roberts, M.: input4MIPs.CMIP6.HighResMIP.MOHC.MOHC-highresSST-future-1-0-1, Version 20190215., 2019.

Kikuchi, K., Kodama, C., Nasuno, T., Nakano, M., Miura, H., Satoh, M., Noda, A. T. and Yamada, Y.: Tropical intraseasonal oscillation simulated in an AMIP-type experiment by NICAM, Clim. Dyn., 48(7–8), 2507–2528,

25 doi:10.1007/s00382-016-3219-z, 2017.

Kilpatrick, T., Xie, S.-P. and Nasuno, T.: Diurnal convection-wind coupling in the Bay of Bengal, J. Geophys. Res. Atmos., 122(18), 9705–9720, doi:10.1002/2017JD027271, 2017.

Kinter, J. L., Cash, B., Achuthavarier, D., Adams, J., Altshuler, E., Dirmeyer, P., Doty, B., Huang, B., Jin, E. K. K., Marx, L., Manganello, J., Stan, C., Wakefield, T., Palmer, T., Hamrud, M., Jung, T., Miller, M., Towers, P., Wedi, N., Satoh, M.,

30 Tomita, H., Kodama, C., Nasuno, T., Oouchi, K., Yamada, Y., Taniguchi, H., Andrews, P., Baer, T., Ezell, M., Halloy, C., John, D., Loftis, B., Mohr, R. and Wong, K.: Revolutionizing climate modeling with Project Athena: a multi-institutional, international collaboration, Bull. Am. Meteorol. Soc., 94(2), 231–245, doi:10.1175/BAMS-D-11-00043.1, 2013.

Knapp, K. R., Ansari, S., Bain, C. L., Bourassa, M. A., Dickinson, M. J., Funk, C., Helms, C. N., Hennon, C. C., Holmes, C. D., Huffman, G. J., Kossin, J. P., Lee, H.-T., Loew, A. and Magnusdottir, G.: Globally gridded satellite observations for

35 climate studies, Bull. Am. Meteorol. Soc., 92(7), 893–907, doi:10.1175/2011BAMS3039.1, 2011.

Knight, C. A., Cooper, W. A., Breed, D. W., Paluch, I. R., Smith, P. L. and Vali, G.: Microphysics, in Hailstorms of the Central High Plains, edited by C. Knight and P. Squires, pp. 151–193, Colorado Associated University Press. [online] Available from: https://opensky.ucar.edu/islandora/object/books%3A140, 1982.

Kobayashi, S., Ota, Y., Harada, Y., Ebita, A., Moriya, M., Onoda, H., Onogi, K., Kamahori, H., Kobayashi, C., Endo, H.,

40 Miyaoka, K. and Takahashi, K.: The JRA-55 reanalysis: general specifications and basic characteristics, J. Meteorol. Soc. Japan., 93(1), 5–48, doi:10.2151/jmsj.2015-001, 2015.

Kodama, C., Noda, A. T. T. and Satoh, M.: An assessment of the cloud signals simulated by NICAM using ISCCP, CALIPSO, and CloudSat satellite simulators, J. Geophys. Res. Atmos., 117(D12), doi:10.1029/2011JD017317, 2012.

Kodama, C., Yamada, Y., Noda, A. T., Kikuchi, K., Kajikawa, Y., Nasuno, T., Tomita, T., Yamaura, T., Takahashi, H. G., Hara, M., Kawatani, Y., Satoh, M., Sugi, M. and Satoh, M.: A 20-year climatology of a NICAM AMIP-type simulation, J. Meteorol. Soc. Japan., 93(4), 393–424, doi:10.2151/jmsj.2015-024, 2015.

Kodama, C., Stevens, B., Mauritsen, T., Seiki, T. and Satoh, M.: A new perspective for future precipitation change from intense extratropical cyclones, Geophys. Res. Lett., 46(21), 12435–12444, doi:10.1029/2019GL084001, 2019.

Lang, S., Tao, W.-K., Simpson, J., Cifelli, R., Rutledge, S., Olson, W. and Halverson, J.: Improving simulations of convective systems from TRMM LBA: easterly and westerly Regimes, J. Atmos. Sci., 64(4), 1141–1164, doi:10.1175/JAS3879.1, 2007.

Li, J.-L. F., Forbes, R. M., Waliser, D. E., Stephens, G. and Lee, S.: Characterizing the radiative impacts of precipitating snow in the ECMWF Integrated Forecast System global model, J. Geophys. Res. Atmos., 119(16), 9626–9637, doi:10.1002/2014JD021450, 2014.

Li, J.-L. F., Lee, W.-L., Waliser, D., Wang, Y.-H., Yu, J.-Y., Jiang, X., L'Ecuyer, T., Chen, Y.-C., Kubar, T., Fetzer, E. and Mahakur, M.: Considering the radiative effects of snow on tropical Pacific Ocean radiative heating profiles in contemporary GCMs using A-Train observations, J. Geophys. Res. Atmos., 121(4), 1621–1636, doi:10.1002/2015JD023587, 2016.

Lin, Y.-L., Farley, R. D. and Orville, H. D.: Bulk Parameterization of the Snow Field in a Cloud Model, J. Clim. Appl. Meteorol., 22(6), 1065–1092, doi:10.1175/1520-0450(1983)022<1065:BPOTSF>2.0.CO;2, 1983.

Lindzen, R. S. and Fox-Rabinovitz, M.: Consistent vertical and horizontal resolution, Mon. Weather Rev., 117(11), 2575–2583, doi:10.1175/1520-0493(1989)117<2575:CVAHR>2.0.CO;2, 1989.

Loeb, N. G., Doelling, D. R., Wang, H., Su, W., Nguyen, C., Corbett, J. G., Liang, L., Mitrescu, C., Rose, F. G. and Kato, S.: Clouds and the Earth's Radiant Energy System (CERES) Energy Balanced and Filled (EBAF) Top-of-Atmosphere (TOA) edition-4.0 data product, J. Clim., 31(2), 895–918, doi:10.1175/JCLI-D-17-0208.1, 2018.

Louis, J.-F.: A parametric model of vertical eddy fluxes in the atmosphere, Boundary-Layer Meteorol., 17(2), 187–202, doi:10.1007/BF00117978, 1979.

Maher, P., Vallis, G. K., Sherwood, S. C., Webb, M. J. and Sansom, P. G.: The impact of parameterized convection on climatological precipitation in atmospheric global climate models, Geophys. Res. Lett., 45(8), 3728–3736, doi:10.1002/2017GL076826, 2018.

Masunaga, H., Matsui, T., Tao, W., Hou, A. Y., Kummerow, C. D., Nakajima, T., Bauer, P., Olson, W. S., Sekiguchi, M. and Nakajima, T. Y.: Satellite data simulator unit, Bull. Am. Meteorol. Soc., 91(12), 1625–1632, doi:10.1175/2010BAMS2809.1, 2010.

Matsugishi, S., Miura, H., Nasuno, T. and Satoh, M.: Impact of latent heat flux modifications on the reproduction of a Madden–Julian Oscillation event during the 2015 pre-YMC campaign using a global cloud-system-resolving model, SOLA, 16A(Special_Edition), 12–18, doi:10.2151/sola.16A-003, 2020.

Matsui, T., Zeng, X., Tao, W.-K., Masunaga, H., Olson, W. S. and Lang, S.: Evaluation of long-term cloud-resolving model simulations using satellite radiance observations and multifrequency satellite simulators, J. Atmos. Ocean. Technol., 26(7), 1261–1274, doi:10.1175/2008JTECHA1168.1, 2009.

Matsuoka, D., Nakano, M., Sugiyama, D. and Uchida, S.: Deep learning approach for detecting tropical cyclones and their precursors in the simulation by a cloud-resolving global nonhydrostatic atmospheric model, Prog. Earth Planet. Sci., 5(1), 80, doi:10.1186/s40645-018-0245-y, 2018.

Matthes, K., Funke, B., Kruschke, T. and Wahl, S.: input4MIPs.SOLARIS-HEPPA.solar.CMIP.SOLARIS-HEPPA-3-2. Version 20170103., 2017a.

Matthes, K., Funke, B., Andersson, M. E., Barnard, L., Beer, J., Charbonneau, P., Clilverd, M. A., Dudok de Wit, T., Haberreiter, M., Hendry, A., Jackman, C. H., Kretzschmar, M., Kruschke, T., Kunze, M., Langematz, U., Marsh, D. R., Maycock, A. C., Misios, S., Rodger, C. J., Scaife, A. A., Seppälä, A., Shangguan, M., Sinnhuber, M., Tourpali, K., Usoskin,

I., van de Kamp, M., Verronen, P. T. and Versick, S.: Solar forcing for CMIP6 (v3.2), Geosci. Model Dev., 10(6), 2247–2302, doi:10.5194/gmd-10-2247-2017, 2017b.

McCoy, D. T., Field, P. R., Elsaesser, G. S., Bodas-Salcedo, A., Kahn, B. H., Zelinka, M. D., Kodama, C., Mauritsen, T., Vanniere, B., Roberts, M., Vidale, P. L., Saint-Martin, D., Voldoire, A., Haarsma, R., Hill, A., Shipway, B. and Wilkinson, J.: Cloud feedbacks in extratropical cyclones: insight from long-term satellite data and high-resolution global simulations, Atmos. Chem. Phys., 19(2), 1147–1172, doi:10.5194/acp-19-1147-2019, 2019.

McFarlane, N. A.: The effect of orographically excited gravity wave drag on the general circulation of the lower stratosphere and troposphere, J. Atmos. Sci., 44(14), 1775–1800, doi:10.1175/1520-0469(1987)044<1775:TEOOEG>2.0.CO;2, 1987.

McFarlane, N. A., Boer, G. J., Blanchet, J.-P. and Lazare, M.: The Canadian Climate Centre second-generation general circulation model and its equilibrium climate, J. Clim., 5(10), 1013–1044, doi:10.1175/1520-0442(1992)005<1013:TCCCSG>2.0.CO;2, 1992.

Meinshausen, M. and Nicholls, Z. R. J.: UoM-REMIND-MAGPIE-ssp585-1-2-1 GHG concentrations. Version 20181127., 2018.

Meinshausen, M. and Vogel, E.: input4MIPs.UoM.GHGConcentrations.CMIP.UoM-CMIP-1-2-0. Version 20160830., 2016.

Meinshausen, M., Vogel, E., Nauels, A., Lorbacher, K., Meinshausen, N., Etheridge, D. M., Fraser, P. J., Montzka, S. A., Rayner, P. J., Trudinger, C. M., Krummel, P. B., Beyerle, U., Canadell, J. G., Daniel, J. S., Enting, I. G., Law, R. M., Lunder, C. R., O&apos;Doherty, S., Prinn, R. G., Reimann, S., Rubino, M., Velders, G. J. M., Vollmer, M. K., Wang, R. H. J. and Weiss, R.: Historical greenhouse gas concentrations for climate modelling (CMIP6), Geosci. Model Dev., 10(5), 2057–2116, doi:10.5194/gmd-10-2057-2017, 2017.

Michibata, T., Suzuki, K., Sekiguchi, M. and Takemura, T.: Prognostic precipitation in the MIROC6-SPRINTARS GCM: description and evaluation against satellite observations, J. Adv. Model. Earth Syst., 11(3), 839–860, doi:10.1029/2018MS001596, 2019.

Mitchell, D. L.: Use of mass- and area-dimensional power laws for determining precipitation particle terminal velocities, J. Atmos. Sci., 53(12), 1710–1723, doi:10.1175/1520-0469(1996)053<1710:UOMAAD>2.0.CO;2, 1996.

Miyakawa, T. and Miura, H.: Resolution dependencies of tropical convection in a global cloud/cloud-system resolving model, J. Meteorol. Soc. Japan., 97(3), 745–756, doi:10.2151/jmsj.2019-034, 2019.

Miyakawa, T., Noda, A. T. and Kodama, C.: The impact of hybrid usage of a cumulus parameterization scheme on tropical convection and large-scale circulations in a global cloud-system resolving model, J. Adv. Model. Earth Syst., 10(11), 2952–2970, doi:10.1029/2018MS001302, 2018.

Moon, I.-J., Ginis, I., Hara, T. and Thomas, B.: A physics-based parameterization of air–sea momentum flux at high wind speeds and its impact on hurricane intensity predictions, Mon. Weather Rev., 135(8), 2869–2878, doi:10.1175/MWR3432.1, 2007.

Na, Y., Fu, Q. and Kodama, C.: Precipitation probability and its future changes from a global cloud-resolving model and CMIP6 simulations, J. Geophys. Res. Atmos., 125(5), doi:10.1029/2019JD031926, 2020.

Nakajima, T., Tsukamoto, M., Tsushima, Y., Numaguti, A. and Kimura, T.: Modeling of the radiative process in an atmospheric general circulation model, Appl. Opt., 39(39), 4869–4878, 2000.

Nakanishi, M. and Niino, H.: An improved Mellor–Yamada level-3 model: Its numerical stability and application to a regional prediction of advection fog, Boundary-Layer Meteorol., 119(2), 397–407, doi:10.1007/s10546-005-9030-8, 2006.

Nakano, M. and Kikuchi, K.: Seasonality of intraseasonal variability in global climate models, Geophys. Res. Lett., 46(8), 4441–4449, doi:10.1029/2019GL082443, 2019.

Nappo, C.: An introduction to atmospheric gravity waves, 2nd ed., Academic Press., 2012.

Nitta, T., Yoshimura, K. and Abe-Ouchi, A.: Impact of Arctic Wetlands on the Climate System: Model Sensitivity Simulations with the MIROC5 AGCM and a Snow-Fed Wetland Scheme, J. Hydrometeorol., 18(11), 2923–2936, doi:10.1175/JHM-D-16-0105.1, 2017.

Niwano, M., Aoki, T., Kuchiki, K., Hosaka, M., Kodama, Y., Yamaguchi, S., Moytoyoshi, H. and Iwata, Y.: Evaluation of updated physical snowpack model SMAP, Bull. Glaciol. Res., 32, 65–78, doi:10.5331/bgr.32.65, 2014.

Noda, A. T., Oouchi, K., Satoh, M., Tomita, H., Iga, S. and Tsushima, Y.: Importance of the subgrid-scale turbulent moist process: Cloud distribution in global cloud-resolving simulations, Atmos. Res., 96(2–3), 208–217, doi:10.1016/j.atmosres.2009.05.007, 2010.

Noda, A. T., Oouchi, K., Satoh, M. and Tomita, H.: Quantitative assessment of diurnal variation of tropical convection simulated by a global nonhydrostatic model without cumulus parameterization, J. Clim., 25(14), 5119–5134, doi:10.1175/JCLI-D-11-00295.1, 2012.

Noda, A. T., Seiki, T., Satoh, M. and Yamada, Y.: High cloud size dependency in the applicability of the fixed anvil temperature hypothesis using global nonhydrostatic simulations, Geophys. Res. Lett., doi:10.1002/2016GL067742, 2016.

Noda, A. T., Kodama, C., Yamada, Y., Satoh, M., Ogura, T. and Ohno, T.: Responses of clouds and large-scale circulation to global warming evaluated from multidecadal simulations using a global nonhydrostatic model, J. Adv. Model. Earth Syst., 11(9), 2980–2995, doi:10.1029/2019MS001658, 2019.

O'Neill, B. C., Tebaldi, C., van Vuuren, D. P., Eyring, V., Friedlingstein, P., Hurtt, G., Knutti, R., Kriegler, E., Lamarque, J.-F., Lowe, J., Meehl, G. A., Moss, R., Riahi, K. and Sanderson, B. M.: The Scenario Model Intercomparison Project (ScenarioMIP) for CMIP6, Geosci. Model Dev., 9(9), 3461–3482, doi:10.5194/gmd-9-3461-2016, 2016.

Ohno, T., Satoh, M. and Noda, A.: Fine vertical resolution radiative-convective equilibrium experiments: roles of turbulent mixing on the high-cloud response to sea surface temperatures, J. Adv. Model. Earth Syst., 11(6), 1637–1654, doi:10.1029/2019MS001704, 2019.

Poli, P., Hersbach, H., Dee, D. P., Berrisford, P., Simmons, A. J., Vitart, F., Laloyaux, P., Tan, D. G. H., Peubey, C., Thépaut, J.-N., Trémolet, Y., Hólm, E. V., Bonavita, M., Isaksen, L. and Fisher, M.: ERA-20C: an atmospheric reanalysis of the twentieth century, J. Clim., 29(11), 4083–4097, doi:10.1175/JCLI-D-15-0556.1, 2016.

Polichtchouk, I., Stockdale, T., Bechtold, P., Diamantakis, M., Malardel, S., Sandu, I., Vána, F. and Wedi, N.: Control on stratospheric temperature in IFS: resolution and vertical advection, ECMWF Tech. Memo., 847, doi:10.21957/cz3t12t7e, 2019.

Roh, W. and Satoh, M.: Evaluation of precipitating hydrometeor parameterizations in a single-moment bulk microphysics scheme for deep convective systems over the tropical central Pacific, J. Atmos. Sci., 71(7), 2654–2673, doi:10.1175/JAS-D-13-0252.1, 2014.

Roh, W. and Satoh, M.: Extension of a multisensor satellite radiance-based evaluation for cloud system resolving models, J. Meteorol. Soc. Japan., 96(1), 55–63, doi:10.2151/jmsj.2018-002, 2018.

Roh, W., Satoh, M. and Nasuno, T.: Improvement of a cloud microphysics scheme for a global nonhydrostatic model using TRMM and a satellite simulator, J. Atmos. Sci., 74(1), 167–184, doi:10.1175/JAS-D-16-0027.1, 2017.

Rossow, W. B. and Schiffer, R. A.: Advances in understanding clouds from ISCCP, Bull. Am. Meteorol. Soc., 80(11), 2261–2287, doi:10.1175/1520-0477(1999)080<2261:AIUCFI>2.0.CO;2, 1999.

Rutledge, S. A. and Hobbs, P. V.: The mesoscale and microscale structure and organization of clouds and precipitation in midlatitude cyclones. XII: a diagnostic modeling study of precipitation development in narrow cold-frontal rainbands, J. Atmos. Sci., 41(20), 2949–2972, doi:10.1175/1520-0469(1984)041<2949:TMAMSA>2.0.CO;2, 1984.

Sato, T., Miura, H., Satoh, M., Takayabu, Y. N. and Wang, Y.: Diurnal cycle of precipitation in the tropics simulated in a global cloud-resolving model, J. Clim., 22(18), 4809–4826, doi:10.1175/2009JCLI2890.1, 2009.

Sato, Y., Goto, D., Michibata, T., Suzuki, K., Takemura, T., Tomita, H. and Nakajima, T.: Aerosol effects on cloud water amounts were successfully simulated by a global cloud-system resolving model, Nat. Commun., 9(1), 985, doi:10.1038/s41467-018-03379-6, 2018.

Satoh, M., Matsuno, T., Tomita, H., Miura, H., Nasuno, T. and Iga, S.: Nonhydrostatic icosahedral atmospheric model (NICAM) for global cloud resolving simulations, J. Comput. Phys., 227(7), 3486–3514, doi:10.1016/j.jcp.2007.02.006, 2008.

Satoh, M., Inoue, T. and Miura, H.: Evaluations of cloud properties of global and local cloud system resolving models using CALIPSO and CloudSat simulators, J. Geophys. Res., 115, D00H14, doi:10.1029/2009JD012247, 2010.

Satoh, M., Tomita, H., Yashiro, H., Miura, H., Kodama, C., Seiki, T., Noda, A. T., Yamada, Y., Goto, D., Sawada, M., Miyoshi, T., Niwa, Y., Hara, M., Ohno, T., Iga, S., Arakawa, T., Inoue, T. and Kubokawa, H.: The non-hydrostatic icosahedral atmospheric model: Description and development, Prog. Earth Planet. Sci., 1(1), 18, doi:10.1186/s40645-014-0018-1, 2014.

Satoh, M., Yamada, Y., Sugi, M., Kodama, C. and Noda, A. T. T.: Constraint on future change in global frequency of tropical cyclones due to global warming, J. Meteor. Soc. Japan, 93(4), 489–500, doi:10.2151/jmsj.2015-025, 2015.

Satoh, M., Noda, A. T., Seiki, T., Chen, Y.-W., Kodama, C., Yamada, Y., Kuba, N. and Sato, Y.: Toward reduction of the uncertainties in climate sensitivity due to cloud processes using a global non-hydrostatic atmospheric model, Prog. Earth Planet. Sci., 5(1), 67, doi:10.1186/s40645-018-0226-1, 2018.

Satoh, M., Stevens, B., Judt, F., Khairoutdinov, M., Lin, S.-J., Putman, W. M. and Düben, P.: Global cloud-resolving models, Curr. Clim. Chang. Reports, 5(3), 172–184, doi:10.1007/s40641-019-00131-0, 2019.

Seiki, T. and Nakajima, T.: Aerosol effects of the condensation process on a convective cloud simulation, J. Atmos. Sci., 71(2), 833–853, doi:10.1175/JAS-D-12-0195.1, 2014.

Seiki, T., Satoh, M., Tomita, H. and Nakajima, T.: Simultaneous evaluation of ice cloud microphysics and nonsphericity of the cloud optical properties using hydrometeor video sonde and radiometer sonde in situ observations, J. Geophys. Res. Atmos., 119(11), 6681–6701, doi:10.1002/2013JD021086, 2014.

Seiki, T., Kodama, C., Noda, A. T. and Satoh, M.: Improvement in global cloud-system-resolving simulations by using a double-moment bulk cloud microphysics scheme, J. Clim., 28(6), 2405–2419, doi:10.1175/JCLI-D-14-00241.1, 2015a.

Seiki, T., Kodama, C., Satoh, M., Hashino, T., Hagihara, Y. and Okamoto, H.: Vertical grid spacing necessary for simulating tropical cirrus clouds with a high-resolution atmospheric general circulation model, Geophys. Res. Lett., 42(10), 4150–4157, doi:10.1002/2015GL064282, 2015b.

Sekiguchi, M. and Nakajima, T.: A k-distribution-based radiation code and its computational optimization for an atmospheric general circulation model, J. Quant. Spectrosc. Radiat. Transf., 109(17–18), 2779–2793, doi:10.1016/j.jqsrt.2008.07.013, 2008.

Shabanov, N. V., Dong Huang, Wenze Yang, Tan, B., Knyazikhin, Y., Myneni, R. B., Ahl, D. E., Gower, S. T., Huete, A. R., Aragao, L. E. O. C. and Shimabukuro, Y. E.: Analysis and optimization of the MODIS leaf area index algorithm retrievals over broadleaf forests, IEEE Trans. Geosci. Remote Sens., 43(8), 1855–1865, doi:10.1109/TGRS.2005.852477, 2005.

Stevens, B., Fiedler, S., Kinne, S., Peters, K., Rast, S., Müsse, J., Smith, S. J. and Mauritsen, T.: MACv2-SP: a parameterization of anthropogenic aerosol optical properties and an associated Twomey effect for use in CMIP6, Geosci. Model Dev., 10(1), 433–452, doi:10.5194/gmd-10-433-2017, 2017.

Stevens, B., Satoh, M., Auger, L., Biercamp, J., Bretherton, C., Düben, P., Judt, F., Khairoutdinov, M., Klocke, D., Kornblueh, L., Kodama, C., Neumann, P., Lin, S., Putman, W. M., Röber, N., Shibuya, R., Vidale, P. and Wedi, N.: DYAMOND: The DYnamics of the Atmospheric general circulation Modeled On Non-hydrostatic Domains, Prog. Earth Planet. Sci, 1–18, 2019.

Sugi, M., Yamada, Y., Yoshida, K., Mizuta, R., Nakano, M., Kodama, C. and Satoh, M.: Future changes in the global frequency of tropical cyclone seeds, SOLA, 16, 70–74, doi:10.2151/sola.2020-012, 2020.

Suzuki, K., Nakajima, T., Satoh, M., Tomita, H., Takemura, T., Nakajima, T. Y. and Stephens, G. L.: Global cloud-system-resolving simulation of aerosol effect on warm clouds, Geophys. Res. Lett., 35(19), L19817, doi:10.1029/2008GL035449, 2008.

Takahashi, H. G., Kamizawa, N., Nasuno, T., Yamada, Y., Kodama, C., Sugimoto, S. and Satoh, M.: Response of the Asian summer monsoon precipitation to global warming in a high-resolution global nonhydrostatic model, J. Clim., accepted, doi:10.1175/JCLI-D-19-0824.1, 2020.

Takasuka, D., Miyakawa, T., Satoh, M. and Miura, H.: Topographical effects on internally produced MJO-like disturbances in an aqua-planet version of NICAM, SOLA, 11, 170–176, doi:10.2151/sola.2015-038, 2015.

Takasuka, D., Satoh, M., Miyakawa, T. and Miura, H.: Initiation processes of the tropical intraseasonal variability simulated in an aqua-planet experiment: what is the intrinsic mechanism for MJO onset?, J. Adv. Model. Earth Syst., 10(4), 1047–1073, doi:10.1002/2017MS001243, 2018.

Takata, K., Emori, S. and Watanabe, T.: Development of the minimal advanced treatments of surface interaction and runoff, Glob. Planet. Change, 38(1–2), 209–222, doi:10.1016/S0921-8181(03)00030-4, 2003.

Takemura, T., Okamoto, H., Maruyama, Y., Numaguti, A., Higurashi, A. and Nakajima, T.: Global three-dimensional simulation of aerosol optical thickness distribution of various origins, J. Geophys. Res. Atmos., 105(D14), 17853–17873, doi:10.1029/2000JD900265, 2000.

Takemura, T., Nakajima, T., Dubovik, O., Holben, B. N. and Kinne, S.: Single-scattering albedo and radiative forcing of various aerosol species with a global three-dimensional model, J. Clim., 15(4), 333–352, doi:10.1175/1520-0442(2002)015<0333:SSAARF>2.0.CO;2, 2002.

Takemura, T., Nozawa, T., Emori, S., Nakajima, T. Y. and Nakajima, T.: Simulation of climate response to aerosol direct and indirect effects with aerosol transport-radiation model, J. Geophys. Res., 110(D2), D02202, doi:10.1029/2004JD005029, 2005.

Takemura, T., Egashira, M., Matsuzawa, K., Ichijo, H., O'ishi, R. and Abe-Ouchi, A.: A simulation of the global distribution and radiative forcing of soil dust aerosols at the Last Glacial Maximum, Atmos. Chem. Phys., 9(9), 3061–3073, doi:10.5194/acp-9-3061-2009, 2009.

Tatebe, H., Ogura, T., Nitta, T., Komuro, Y., Ogochi, K., Takemura, T., Sudo, K., Sekiguchi, M., Abe, M., Saito, F., Chikira, M., Watanabe, S., Mori, M., Hirota, N., Kawatani, Y., Mochizuki, T., Yoshimura, K., Takata, K., O'ishi, R., Yamazaki, D., Suzuki, T., Kurogi, M., Kataoka, T., Watanabe, M. and Kimoto, M.: Description and basic evaluation of simulated mean state, internal variability, and climate sensitivity in MIROC6, Geosci. Model Dev., 12(7), 2727–2765, doi:10.5194/gmd-12-2727-2019, 2019.

Thomason, L., Vernier, J.-P., Bourassa, A., Arfeuille, F., Bingen, C., Peter, T. and Luo, B.: Stratospheric Aerosol Data Set (SADS Version 2) prospectus, Prep. Geosci. Model Dev. [online] Available from: http://www.wcrp-climate.org/images/modelling/WGCM/CMIP/CMIP6Forcings_StratosphericAerosolDataSet_InitialDescription_150131.pdf (Accessed 28 July 2020), 2015.

Thompson, G., Field, P. R., Rasmussen, R. M. and Hall, W. D.: Explicit forecasts of winter precipitation using an improved bulk microphysics scheme. Part II: implementation of a new snow parameterization, Mon. Weather Rev., 136(12), 5095–5115, doi:10.1175/2008MWR2387.1, 2008.

Tomita, H.: New microphysical schemes with five and six categories by diagnostic generation of cloud ice, J. Meteorol. Soc. Japan, 86A, 121–142, doi:10.2151/jmsj.86A.121, 2008.

Tomita, H. and Satoh, M.: A new dynamical framework of nonhydrostatic global model using the icosahedral grid, Fluid Dyn. Res., 34(6), 357–400, doi:10.1016/j.fluiddyn.2004.03.003, 2004.

Tomita, H., Tsugawa, M., Satoh, M. and Goto, K.: Shallow water model on a modified icosahedral geodesic grid by using spring dynamics, J. Comput. Phys., 174(2), 579–613, doi:10.1006/jcph.2001.6897, 2001.

Tomita, H., Satoh, M. and Goto, K.: An optimization of the icosahedral grid modified by spring dynamics, J. Comput. Phys., 183(1), 307–331, doi:10.1006/jcph.2002.7193, 2002.

Waliser, D. E., Li, J.-L. F., L'Ecuyer, T. S. and Chen, W.-T.: The impact of precipitating ice and snow on the radiation balance in global climate models, Geophys. Res. Lett., 38(6), doi:10.1029/2010GL046478, 2011.

5   Watanabe, S., Sato, K., Kawatani, Y. and Takahashi, M.: Vertical resolution dependence of gravity wave momentum flux simulated by an atmospheric general circulation model, Geosci. Model Dev., 8(6), 1637–1644, doi:10.5194/gmd-8-1637-2015, 2015.

Yamada, Y., Satoh, M., Sugi, M., Kodama, C., Noda, A. T., Nakano, M. and Nasuno, T.: Response of tropical cyclone activity and structure to global warming in a high-resolution global nonhydrostatic model, J. Clim., 30(23), 9703–9724,

10   doi:10.1175/JCLI-D-17-0068.1, 2017.

Yamada, Y., Kodama, C., Satoh, M., Nakano, M., Nasuno, T. and Sugi, M.: High-resolution ensemble simulations of intense tropical cyclones and their internal variability during the El Niños of 1997 and 2015, Geophys. Res. Lett., 46(13), 7592–7601, doi:10.1029/2019GL082086, 2019.

Yamazaki, T., Taguchi, B. and Kondo, J.: Estimation of the heat balance in a small snow-covered forested catchment basin,

15   Tenki (in Japanese), 41(2), 71–77, 1994.

Yang, W., Tan, B., Huang, D., Rautiainen, M., Shabanov, N. V., Wang, Y., Privette, J. L., Huemmrich, K. F., Fensholt, R., Sandholt, I., Weiss, M., Ahl, D. E., Gower, S. T., Nemani, R. R., Knyazikhin, Y. and Myneni, R. B.: MODIS leaf area index products: from validation to algorithm improvement, IEEE Trans. Geosci. Remote Sens., 44(7), 1885–1898, doi:10.1109/TGRS.2006.871215, 2006.

20   Yashiro, H., Terai, M., Yoshida, R., Iga, S., Minami, K. and Tomita, H.: Performance analysis and optimization of Nonhydrostatic ICosahedral Atmospheric Model (NICAM) on the K Computer and TSUBAME2.5, in Proceedings of the Platform for Advanced Scientific Computing Conference on - PASC '16, pp. 1–8, ACM Press, New York, New York, USA., 2016.

Yoshizaki, M., Iga, S. and Satoh, M.: Eastward-propagating property of large-scale precipitation systems simulated in the

25   coarse-resolution NICAM and an explanation of its appearance, SOLA, 8, 21–24, doi:10.2151/sola.2012-006, 2012.

Tables

Table 1: List of HighResMIP simulations.

Source ID	HighResMIP Tier	Integration period	Initial atmospheric condition	Initial land condition
NICAM16-7S	1 & 3	1950–2050 (101-yr)	ERA-20C (Poli et al., 2016)	NICAM climatology
NICAM16-8S	1 & 3	1950–2050 (101-yr)	ERA-20C	NICAM climatology
NICAM16-9S	1	1950–1960 (11-yr)	ERA-20C	NICAM climatology
NICAM16-9S	1	2000–2010 (11-yr)	ERA-20C	NICAM climatology
NICAM16-9S	3	2040–2050 (11-yr)	The NICAM16-8S Tier 3 run08f_1950	The NICAM16-8S Tier 3 run08f_1950 run, 1st January 2040

Table 2: List of sensitivity experiments.

~~Experimental ID~~Run name	Descriptions
~~g~~	~~Same as NICAM16-S.~~
REFFIX	Same as NICAM16-S (with the fixed SST condition; Section 3.7).
REFSLB	Same as NICAM16-S but with the slab ocean model and nudging technique (Section 3.7).
REF	Alias name of the REFFIX run for 56 km mesh and the REFSLB run for 14 km mesh.
~~g3~~NOCLD	Same as ~~the g~~ REF run but for using the previous cloud microphysics scheme used in NICAM.12 (Table 5; ~~Section~~ Section 3.~~1~~2).
NONS	Same as the REF run but for assuming the spherical particle in the radiation table (Section 3.3).
NONSI	Same as the NONS run but for using the fixed effective radii of 8 µm for liquid hydrometeors and 40 µm for ice hydrometeors (Section 3.3).
~~g6~~NOAER	Same as ~~the g~~ REF run but for prescribing zero natural and anthropogenic aerosol mass concentration for the radiation scheme and constant CCN of 50 cm^{-3} for the cloud microphysics scheme (Section 3.~~3~~4).
NOANTAER	Same as the REF run but for prescribing zero anthropogenic aerosol mass concentrations for the radiation scheme (Section 2.3).
NOLND~~g4~~	Same as ~~the g~~ REF run but for omitting the effects of wetland and water accumulation ~~of water~~ on land ice (Section 3.~~4~~5).
NOALB	Same as the REF run but for using the previous surface albedo values (Table 6; Section 3.6).
NOSIC	Same as the REF run but for using the previous SICCRT value of 300 kg m^{-2} (Section 3.7).
~~g8~~NOGWD	Same as ~~the g~~ REF run but for switching off the subgrid-scale orographic gravity wave drag scheme (Section 3.~~7~~8).
~~g9~~	~~Same as g but for considering only the spherical particle in the radiation table (Section 3.2).~~
~~g9a~~	~~Same as g9 but for removing the interaction between radiation and cloud microphysics (Section 3.2).~~
~~f1d~~	~~Same as g but for a previous configuration of aerosol effective radii#.~~
~~f1~~	~~Same as f1d but for using the previous SICCRT value of 300 kg m^{-2} (Section 3.6).~~
~~f~~	~~Same ad f1 but for using the previous surface albedo values (Table 6; Section 3.5).~~
DDT2M	Same as the REF run but for setting the time step interval of the dynamics and gravity wave drag scheme to 2 min.
DDT1M	Same as the REF run but for setting the time step interval of the dynamics and including gravity wave drag scheme to 1 min.
RDT20M	Same as the REF run but for setting the time step interval of the radiation scheme to 20 min.
RDT10M	Same as the REF run but for setting the time step interval of the radiation scheme to 10 min.

~~# In the f1d run, the aerosol effective radii of soil dust and seasalt are set to 4 µm and 2 µm, respectively, following the older MstrnX (Nakajima et al., 2000). In the g (=NICAM16-S) runs, those of soil dust and seasalt are set to 1.6 µm (Mahowald et al., 2014; Omar, 2005) and a function of relative humidity (considering hygroscopity).~~

5

Table 3: List of observational datasetss

Short name	Full name	Resolution	Reference
CERES	Clouds and Earth's Radiant Energy System (CERES) Energy Balanced and Filled (EBAF) TOA/SFC Edition 4.0 (Ed4.0)	1.0°×1.0°, monthly-mean	Kato et al. (2018), Loeb et al. (2018)
CloudSat	CloudSat level 2B radar-only cloud water content (2B-CWC-RO)	0.25°×0.25°	Austin et al. (2009), Austin and Stephens (2001)
GPCP	Global Precipitation Climatology Project (version 2.2)	2.5°×2.5°, monthly-mean	Adler et al. (2003)
GridSat	Gridded Satellite Data – B1	0.07°×0.07°, three-hourly	Knapp et al. (2011)
ISCCP	International Satellite Cloud Climatology Project	2.5° × 2.5°, monthly-mean	Rossow and Schiffer (1999)
JRA-55	Japanese 55-year reanalysis	1.25° × 1.25°, monthly-mean	Kobayashi et al. (2015)

	a. Modification of cloud microphysics (3.1)		b. Introduction of aerosol (3.3)		c. Modification of surface albedo (3.5)	d. Modification of SICCRT (3.6)	e. Impact of slab ocean (3.6)			f. Introduction of orographic gravity wave drag (3.7)
Experimental ID (Table 2)	g-g3		g-g6		f1-f	f1d-f1	g	g	g	g-g8
Horizontal mesh size	14 km*	56 km	14 km*	56 km	56 km	56 km	56 km	28 km	14 km	56 km
Surface air temperature, ℃	-0.30	-0.10	-0.04	-0.06	+0.08	-0.21	+0.10	+0.15	+0.15	-0.16
Precipitation, mm day^{-1}	+0.08	+0.08	-0.02	-0.02	+0.04	-0.01	+0.02	+0.03	+0.02	-0.01
TOA OLR, W m^{-2}	+4.47	+4.03	+0.01	-0.02	-0.52	-0.47	+0.30	+0.27	+0.34	-0.24
TOA OSR, W m^{-2}	-2.52	-1.83	-2.17	+0.24	-2.03	+0.05	+0.07	+0.38	+0.60	-0.01
IWP, g m^{-2}	+46.03	+51.24	-0.74	-0.67	+0.26	-0.04	-0.19	-0.51	-0.75	-0.23
LWP, g m^{-2}	+0.50	+0.09	-4.14	-2.58	+1.07	-0.33	+0.31	+1.13	+1.19	-0.28
ISCCP high visible cloud amount, %	-6.25	-5.35	+0.09	-0.12	-0.28	+0.07	+0.17	+0.19	+0.16	-0.09
ISCCP middle visible cloud amount, %	+0.28	+1.03	+0.09	-0.04	+0.18	+0.06	+0.10	+0.20	+0.34	-0.06
ISCCP low visible cloud amount, %	+1.81	+1.89	-0.85	-0.35	+0.59	-0.03	-0.47	-0.33	-0.20	+0.18
SFC net LW, downward pos., W m^{-2}	+0.40	+1.03	+0.61	+0.67	+2.00	+0.26	+0.37	+0.69	+0.73	+0.07
SFC net SW, downward pos., W m^{-2}	+1.23	+0.44	-0.25	-2.68	+2.12	-0.00	-0.32	-0.79	-1.07	+0.07
SFC latent heat flux, upward pos., W m^{-2}	+2.19	+2.35	-0.61	-0.66	+1.16	-0.33	+0.70	+1.04	+0.75	-0.38
SFC sensible heat flux, upward pos., W m^{-2}	+1.03	+1.07	-1.24	-1.20	+0.25	+0.17	-0.11	-0.15	-0.15	+0.37

*slab ocean model with nudging toward the SST boundary condition is used instead of fixed SST condition.

CMIP6 formal model label (if any)	NICAM16-S			Observations
	NICAM16-7S	NICAM16-8S	NICAM16-9S	
Horizontal mesh size	56 km	28 km	14 km	
Surface air temperature, °C	14.32	14.20	13.78	14.59a
Precipitation, mm day^{-1}	2.96	2.88	2.85	2.71b
TOA OLR, W m^{-2}	238.12	237.66	235.52	240.20c
TOA OSR, W m^{-2}	83.48	82.20	91.33	99.11c
IWP, g m^{-2}	88.44	87.86	81.55	
LWP, g m^{-2}	43.02	39.37	46.35	
ISCCP high visible cloud amount, %	21.54	23.23	22.73	22.58d
ISCCP middle visible cloud amount, %	11.67	11.16	13.32	20.04d
ISCCP low visible cloud amount, %	10.73	10.18	16.95	23.17d
SFC net LW, downward pos., W m^{-2}	-59.12	-60.23	-56.61	-52.91c
SFC net SW, downward pos., W m^{-2}	184.32	186.06	176.48	163.87c
SFC latent heat flux, upward pos., W m^{-2}	85.82	83.44	82.67	
SFC sensible heat flux, upward pos., W m^{-2}	17.58	18.80	20.63	

a: JRA55. b: GPCP. c: CERES. d: ISCCP.

Table 4: Physics schemes in NICAM16-S and NICAM.12.

Model	NICAM16-S (NICAM.16 for ~~CMIP6~~HighResMIP)	NICAM.12
Cloud microphysics	NICAM Single-moment Water 6 (NSW6) (Tomita, 2008; Roh and Satoh, 2014; Roh et al., 2017)	NSW6 (Tomita, 2008; Kodama et al., 2012)
Cumulus convection and ~~laege~~large-scale condensation	Not used	Not used
Radiation	~~MstrnX~~ mstrnX (Sekiguchi and Nakajima, 2008), updated radiation table (Seiki et al., 2014), and coupling with cloud microphysics	~~MstrnX~~ mstrnX (Sekiguchi and Nakajima, 2008)
Turbulence	Mellor-Yamada Nakanishi-Niino level 2~~(MYNN2)~~ (Nakanishi and Niino, 2006; Noda et al., 2010)	Same
Gravity wave	Orographic gravity wave drag (McFarlane, 1987)	Not used
Land surface	Minimal Advanced Treatments of Surface Interaction and RunOff (MATSIRO) (Takata et al., 2003) with wetland scheme (Nitta et al., 2017)~~ and albedo modification~~	MATSIRO (Takata et al., 2003)
Ocean surface flux	Bulk surface scheme (Louis, 1979); surface roughness is evaluated following Fairall et al. (2003) and Moon et al. (2007)	Same
Ocean ~~model~~treatment	Fixed to observations (or single layer slab ocean with a nudging toward observations)	Single layer slab ocean with a nudging toward observations

Table 5: Summary of the key changes in the NSW6 scheme by Roh and Satoh (2014) and Roh et al. (2017)[#].

	NSW6 in NICAM.16-S (Roh and Satoh, 2014; Roh et al., 2017)	NSW6 in NICAM.12 (Tomita, 2008; Kodama et al., 2012)
a. Production of cloud ice	Ice nucleation and vapor deposition are calculated explicitly following Hong et al. (2004).	Cloud water and cloud ice are produced or reduced by saturation adjustment (Tomita, 2008).
b. Terminal velocity of cloud ice (no change between the two)	0	0 (same)
c. Size distribution of snow	A bi-modal shape of the rescaled particle size distribution of snow is assumed following Thompson et al., (2008), who used aircraft observations by Field et al. (2005).	Marshall Palmer distributions are assumed for rain, snow, and graupel with global constants of N_0 following Lin et al. (1983) and Rutledge and Hobbs (1984), as follow: $N_j(D_j) = N_{0,j}\exp(-\lambda_j D_j), (j = r,s,g).$
d. Mass and diameter (M-D) relationship of snow	The mass (m) and maximum dimension (D) relationship of snow assumes two-dimensional fractal shapes ($m_s = 0.069\,D_s^2$) with variable snow density following Thompson et al., (2008).	Ice hydrometeors are assumed as the spherical shape with fixed bulk densities following Rutledge and Hobbs (1984).
e. Intercept parameter in the M-D relationship of graupel	The intercept parameter of graupel $N_{0g} = 4 \times 10^8$ [m^{-4}] is used (Gilmore et al., 2004; Knight et al., 1982).	The intercept parameter of graupel $N_{0g} = 4 \times 10^6$ [m^{-4}] is used following Rutledge and Hobbs (1984), assuming midlatitude cyclones.
f. Accretion of snow and cloud ice by graupel	Accretion of snow and cloud ice by graupel is ignored following Lang et al. (2007).	Accretion of snow and cloud ice by graupel occurs.
g. Efficiency of accretion of cloud ice by snow	0.25.	1.0.

The particle size distribution of for rain was also revised in the original paper, but the revision is not used in the latest version because it had a small impact and reduced of the computational efficiency against its small impact on improvements.

5   In addition, the assumption that cloud ice does not precipitate is inconsistent with some of the other ice cloud microphysics assumptions, but it is used to reproduce tune the model to the observed high cloud signals over the tropics ad hoc.

Table 6: Surface albedo in NICAM16-S and NICAM.12.

	NICAM16-S	NICAM.12
Sea ice, VIS and NIR	0.5 and 0.5 (Hashino et al., 2016)	0.8 and 0.6
Snow over sea ice, IR	0.02 (Armstrong and and Brun, 2008; Niwano et al., 2014)	0
Fresh snow over land, VIS	0.90 (e.g. Aoki et al. 2011; Yamazaki et al. 1994)	0.98
Open ocean, IR	0.05	0.005

VIS, NIR, and IR stand for visible, near-infrared, and infrared bands, respectively.

	NICAM16-S	NICAM.12
Sea ice, VIS and NIR	0.5 and 0.5 (Hashino et al., 2016)	0.8 and 0.6
Snow over sea ice, IR	0.02 (Armstrong and and Brun, 2008; Niwano et al., 2014)	0
Fresh snow over land, VIS	0.90 (e.g. Aoki et al. 2011; Yamazaki et al. 1994)	0.98
Open ocean, IR	0.05	0.005

Table 7: ~~Technical~~ Computational aspects of the simulations on the Earth Simulator 3. They are sampled from 6-month simulations (1 July 2004–31 December 2004).

Source ID	NICAM16-7S	NICAM16-8S	NICAM16-9S
Number of nodes	10	40 / 160	160
Number of MPI processes	40	160 / 640	640
File staging	No	Yes / Yes	Yes
Simulation year per wall-clock day (SYPD)	0.42	0.37 / 0.63	0.22
~~Output size in latitude-longitude grid per year, TB~~	~~0.64~~	~~2.4~~	~~9.5~~

Figures
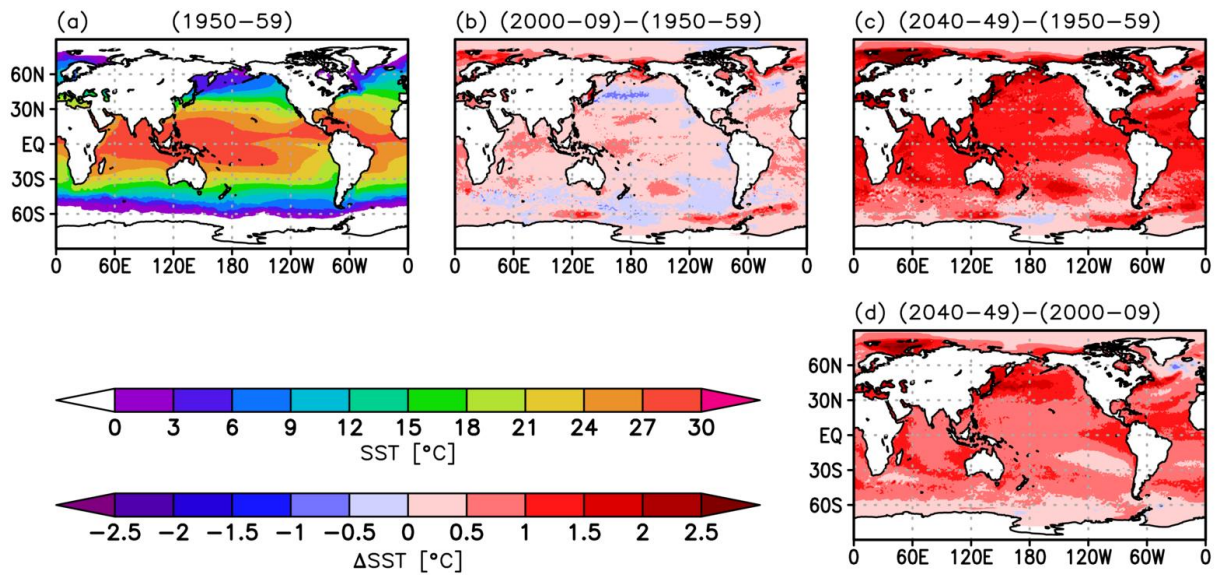
Figure 1: Decadal mean horizontal distribution of sea surface temperature (SST) prescribed ~~for~~ in the model averaged ~~in~~ for the 1950s (a). Differences between the 2000s and the 1950s (b), the 2040s and the 1950s (c), and the 2040s and the 2000s (d) are also shown. ~~Their u~~Units ~~is~~ are °C~~in degrees Celsius~~.
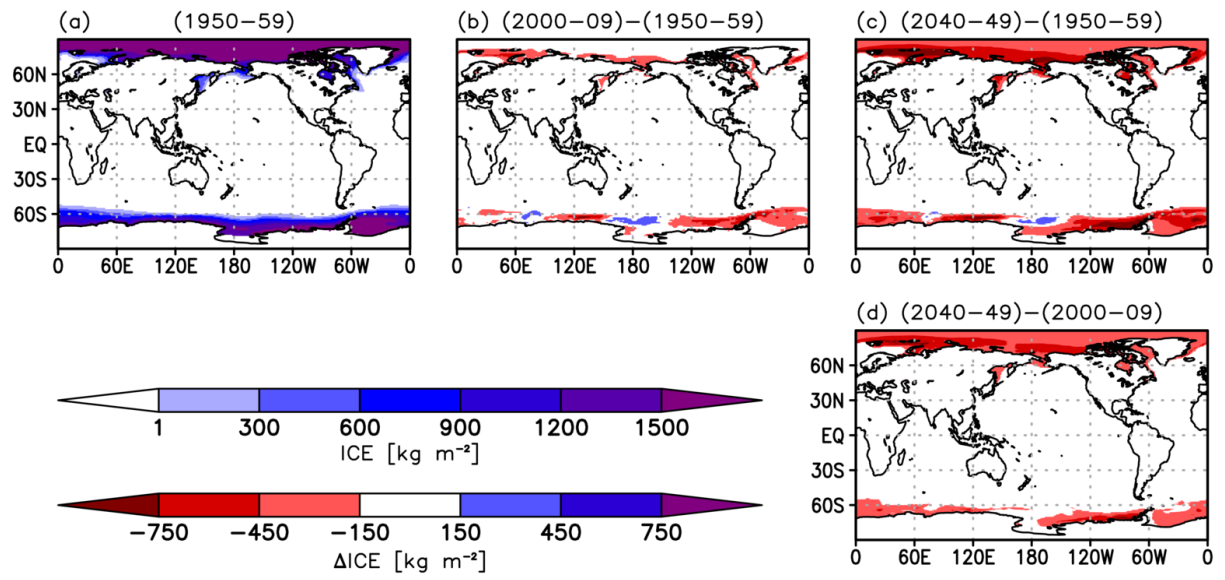
Figure 2: ~~The s~~Same as Figure 1 but for sea ice mass (ICE) in kg m^{-2}.
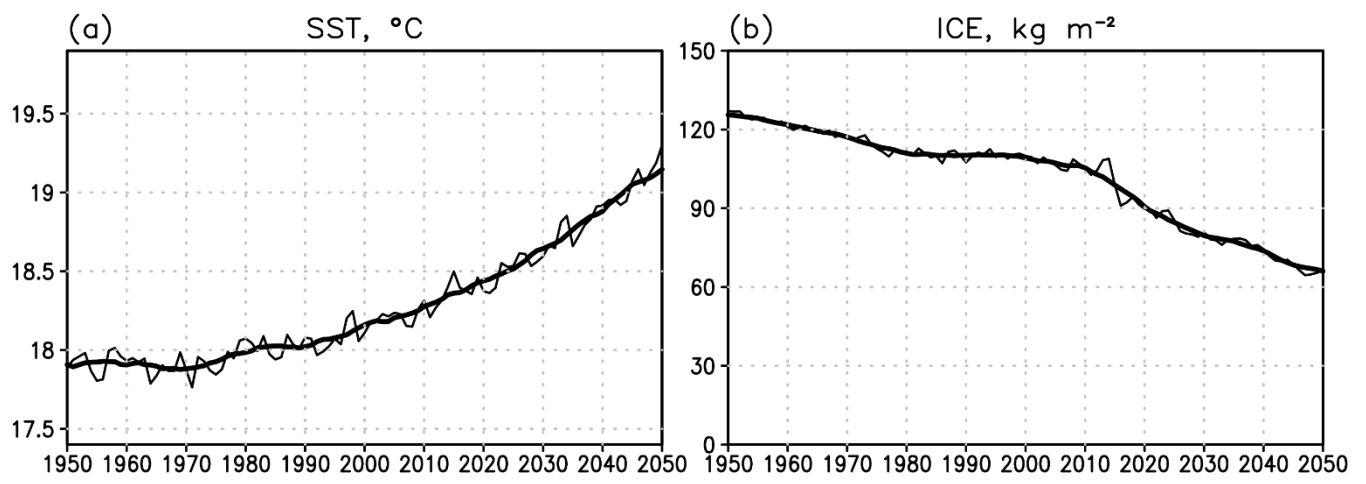
Figure 3: Global mean SST (a; in °C) and ICE (b; in kg m⁻²) prescribed ~~in~~for the model. Annual mean (thin ~~curve~~line) and decadal running mean (thick ~~line~~curve) ~~means~~ are shown.
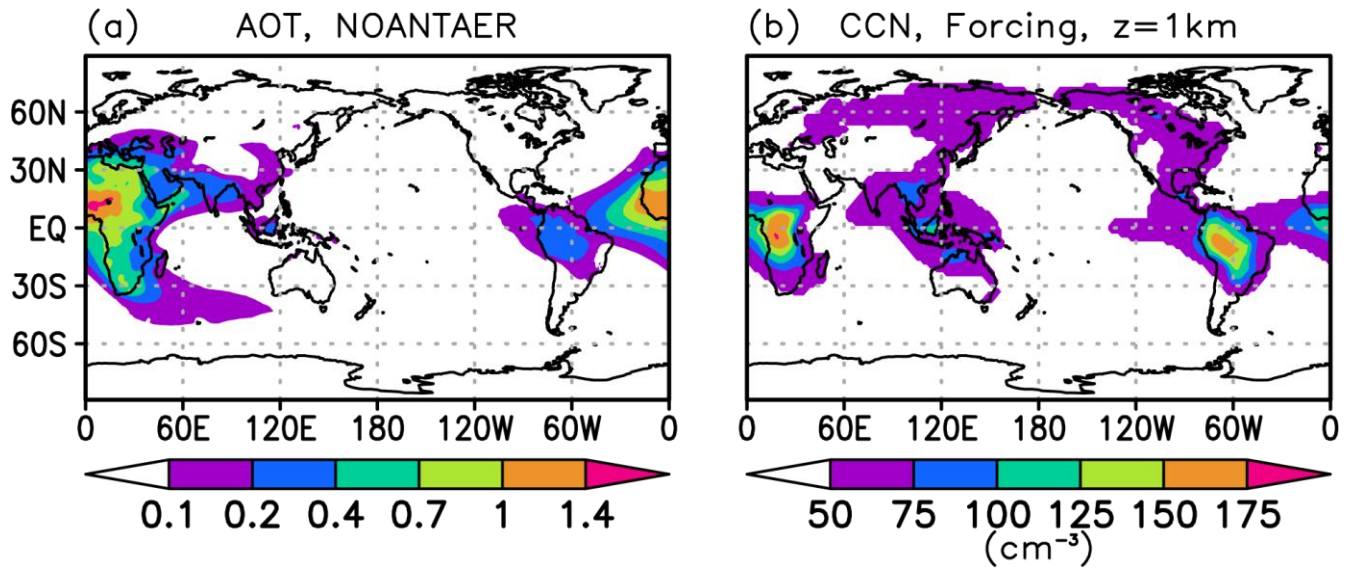
Figure 4: (a) Annual mean natural aerosol optical thickness <u>averaged for June 2004–May 2005 as</u> simulated by NICAM16-7<u>S</u> <u>(NOANTAER run in Table 2). The data are gridded at 0.56° in longitude and latitude. ~~The simulation, starting from 1 June 2004,~~ ~~was conducted for one year without anthropogenic aerosol.~~</u> **(b)** The annual mean number concentration of cloud condensation nuclei (CCN) from the natural origin at 1 km above sea level prescribed for the model. <u>The data are gridded at 2° in longitude and latitude and</u> ~~T~~<u>t</u>he unit is cm^{-3}<u>.</u>~~,~~ The lower bound of CCN<u>,</u> ~~is~~ 50 cm^{-3} <u>(Section 2.3)</u>~~, is shown in white (no shading).~~

41
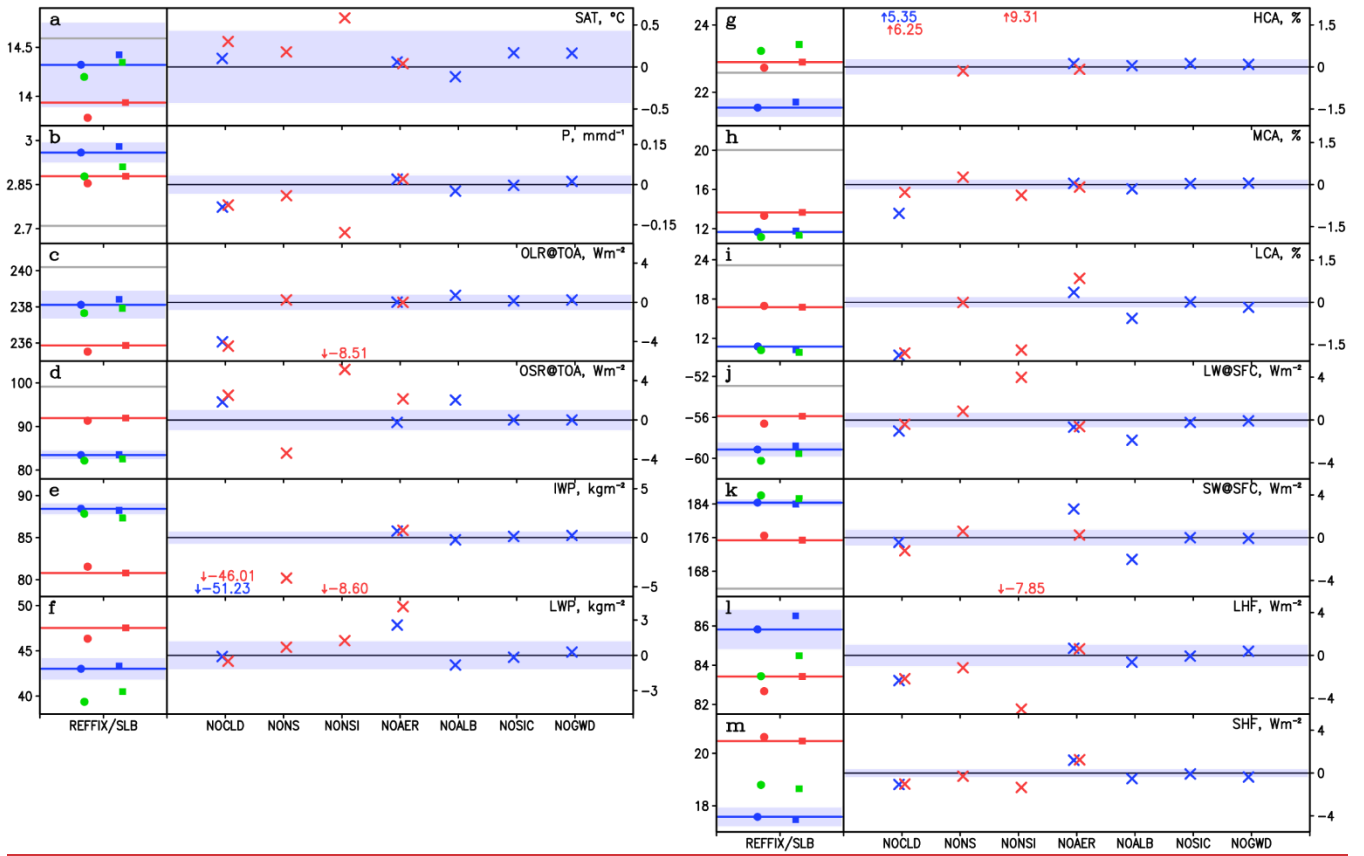
Figure 5: Global annual means of surface air temperature (a), precipitation (b), top-of-atmosphere (TOA) outgoing longwave radiation (OLR) (c), TOA outgoing shortwave radiation (OSR) (d), ice water path (e), liquid water path (f), high cloud amount (g), middle cloud amount (h), low cloud amount (i), surface net downward longwave radiation (j), surface net downward shortwave radiation (k), surface latent heat flux (l), and surface sensible heat flux (m). They are averaged over June 2004–May 2005, and their units are shown at the upper-right corner of each panel. Blue shading shows the interannual variability (2σ, detrended) estimated from the HighResMIP NICAM16-7S run over 1950–2050 (**Table 1**). In the left part of each panel contains plots of global annual means simulated by NICAM16-7S (56-km mesh; blue), NICAM16-8S (28-km mesh; green), and NICAM16-9S (14-km mesh; red), which were performed under the fixed SST condition (filled circles; REFFIX run in **Table 2**) and with the slab ocean condition (filled squares; REFSLB run in **Table 2**). Blue and red lines are the reference (REF) runs with 56-km mesh and 14-km mesh, respectively. Observational values taken from the JRA-55 reanalysis (surface air temperature), GPCP (precipitation), CERES (radiation), and ISCCP (cloud amount) are shown as gray lines. The right part of each panel shows differences between the REF run and each sensitivity run (NOCLD, NONS, NONSI NOAER, NOALB, NOSIC, and NOGWD runs in **Table 2**). Results outside the scale range are shown with digits.
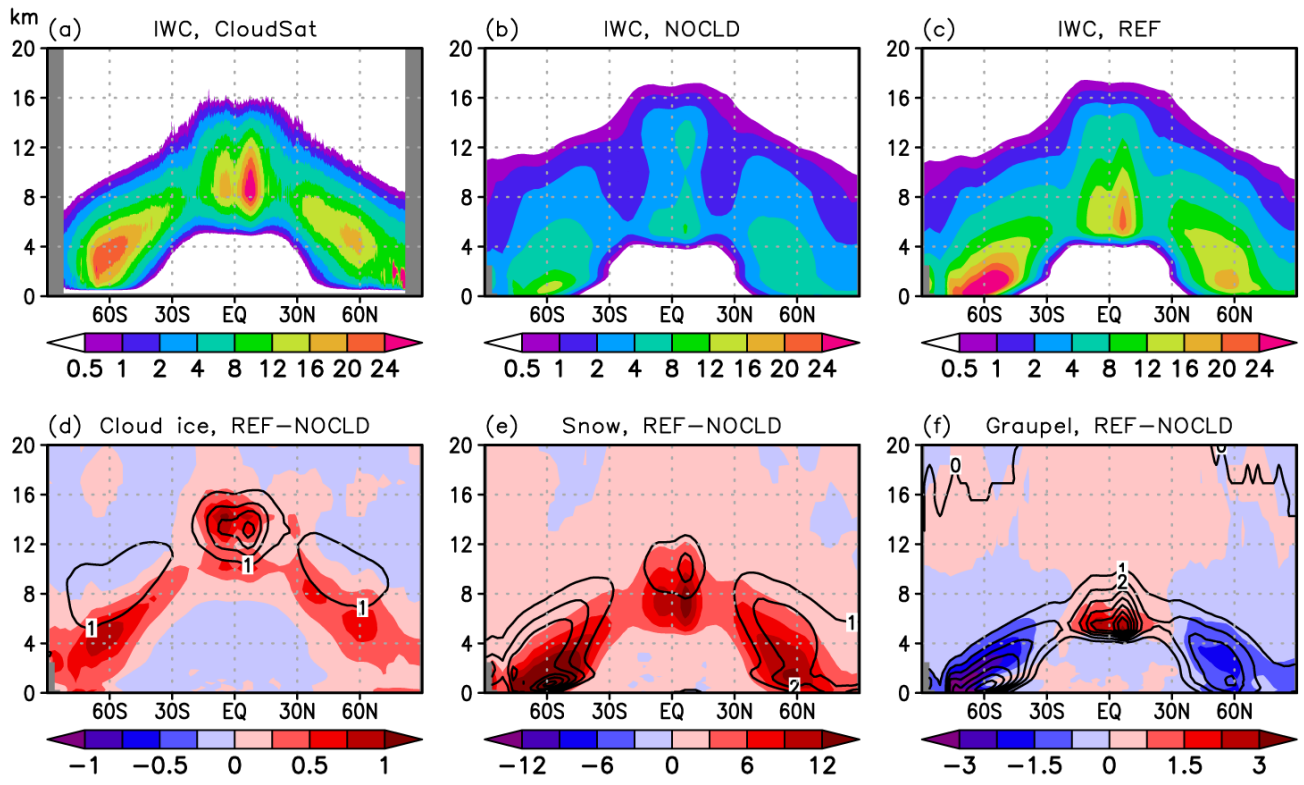
Figure 6: Annual mean of the zonal mean ice water content (~~IWC; unit in~~ 10⁻⁶ kg m⁻³) in CloudSat observations (a~~), ~~) and the NOCLD (b) and ~~14 km mesh~~ REF ~~NICAM simulations using the cloud microphysics scheme of NICAM.12 (b) and that of NICAM16-9S~~ (c) runs by NICAM16-9S ~~(Table 7; g3 and g runs in Table 2)~~. Breakdown of the simulated ice water content (IWC) into cloud ice (d), snow (e), and graupel (f) is shown ~~on~~ in the bottom panels. The contours show~~s~~ the NOCLD run,~~simulation using the cloud microphysics schemes before the update~~ and shading shows the difference between the REF and NOCLD runs~~simulations using the cloud microphysics schemes before and after the update~~. The analysis data are 0.25° (a) and 2.5° (b–f) gridded data, and the vertical axis is the altitude in km above sea level.

43
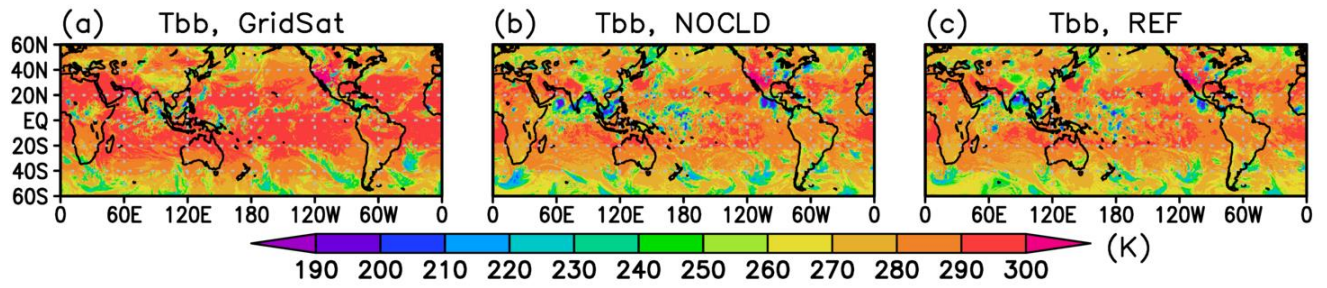
Figure 7: ~~Top-of-the-atmosphere (~~TOA~~)~~ brightness temperature near 11 μm at 00:00 UTC June 6, 2004, from <u>the</u> GridSat product (a) <u>and</u> ~~and~~ the NOCLD (b) and REF (c) runs by NICAM16-9S~~NICAM using the cloud microphysics scheme of NICAM.12 (b; g3 run in Table 2) and that of NICAM16-9S (c; g run in Table 2)~~. The display style follows Figure 1 of Roh et al. (2017). Grid interval <u>in (b) and (c)</u>~~of the NICAM data~~ is 0.14°.
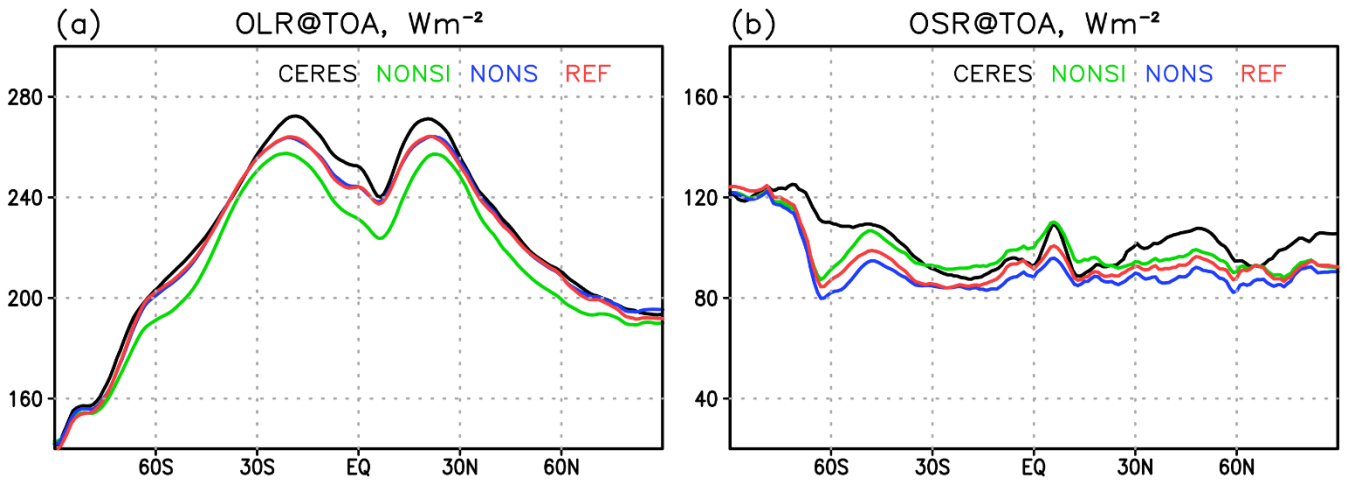
Figure 8: ~~Annual mean of~~TOA ~~outgoing longwave radiation (~~OLR~~)~~ (a) and ~~outgoing shortwave radiation (~~OSR~~)~~ (b) at the TOA~~, in~~ (W m⁻²)~~, averaged over June-July-August in 2004~~ for ~~the~~ CERES product (black) and ~~14 km mesh~~ NICAM~~16-9S simulations~~. Green, blue, and red ~~lines~~ curves show ~~the~~ NONSI~~g9a~~, NONS~~g9~~, and ~~g~~REF runs~~, respectively~~ ~~in Table 2~~.

5
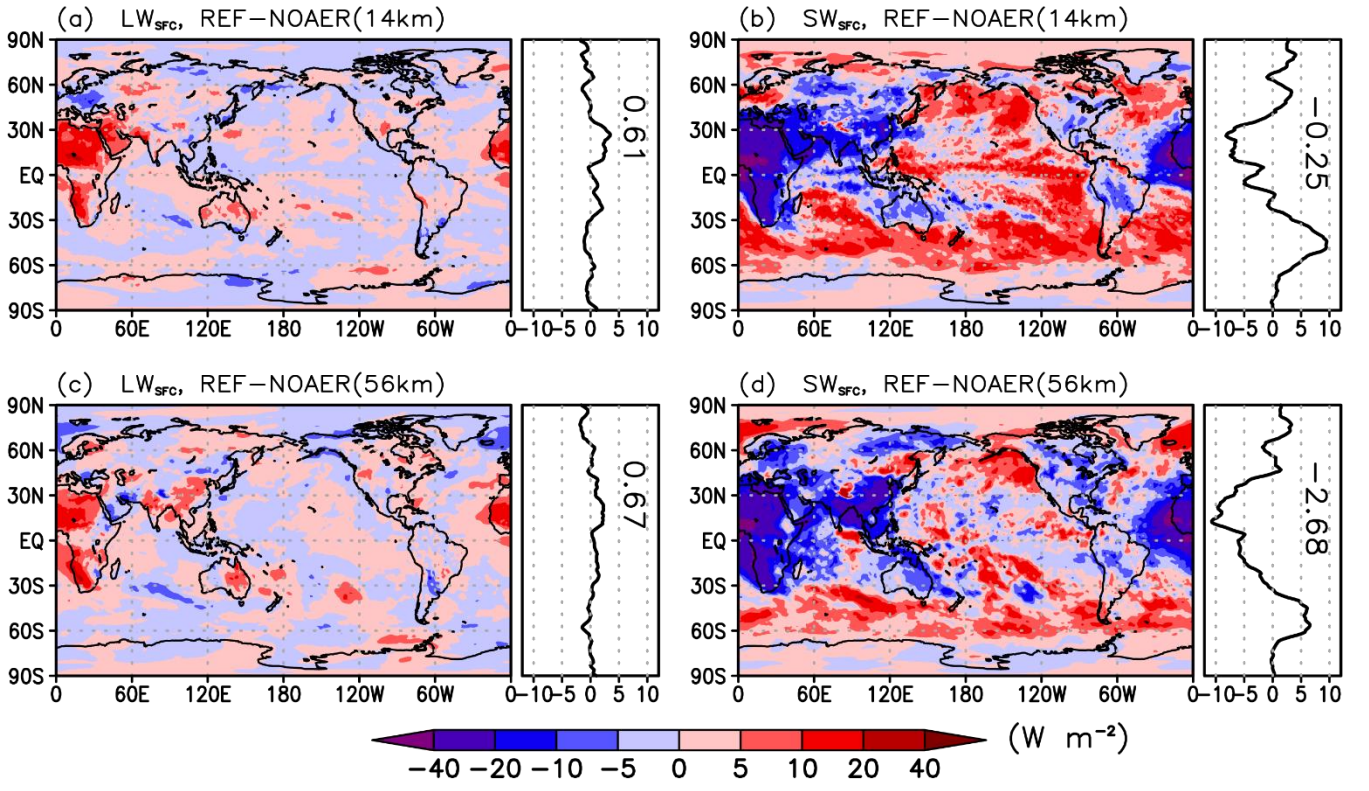
Figure 9: Impact of the update of the aerosol treatment ~~described in Section 3.3~~ (the gREF run minus the ~~g6~~ NOAER run~~in Table 2~~). 2-D distribution, zonal, and global means of the net longwave (a, c~~left~~) and shortwave (b, d~~right~~) radiation at the surface are shown for the NICAM16-9S~~56 km~~ (a, b~~top~~) and NICAM16-7S~~14 km mesh simulation~~ s (c, d~~bottom~~) runs. The data are gridded at 1° in longitude and latitude, and ~~Tt~~he sign of the radiation is downward positive.
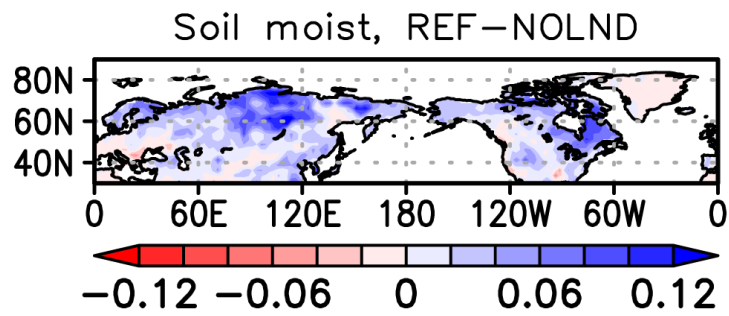
Figure 10: Impact of the update of the land ~~surface~~ model ~~described in Section 3.4 and Table 2~~ (the REF run minus the NOLND ~~rung4~~ g) on the simulated soil moisture at the uppermost land surface model level ~~(a), precipitation (b), and surface air temperature (c)~~. Simulations using NICAM16-7S~~56 km NICAM~~ were performed for ~~four~~ 4 years, and ~~last three~~ June-July-August data for the last 3 years are averaged. The data are gridded at 2.5° in longitude and latitude.
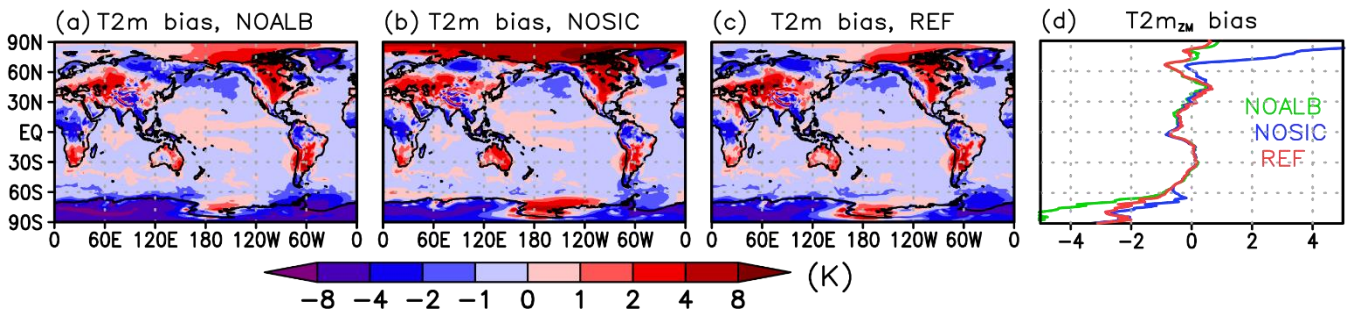
Figure 11: Bias in the simulated surface air temperature (K) by NICAM16-7S against JRA-55 reanalysis averaged for June 2004— May 2005. ~~The NOALB (a).~~ ~~Old albedo configuration and SICCRT = 300 (the f run in Table 2).~~ NOSIC (b), and ~~New albedo configuration and SICCRT = 30REF 0 (the f1 run in Table 2). (c) runs are shownNew albedo configuration and SICCRT = 1600 (the f1d run in Table 2). (d)~~ The zonal mean bias~~es~~ of the surface air temperature for the NOALB (green), NOSIC (blue), and REF (red) runs are shown in (d).

48
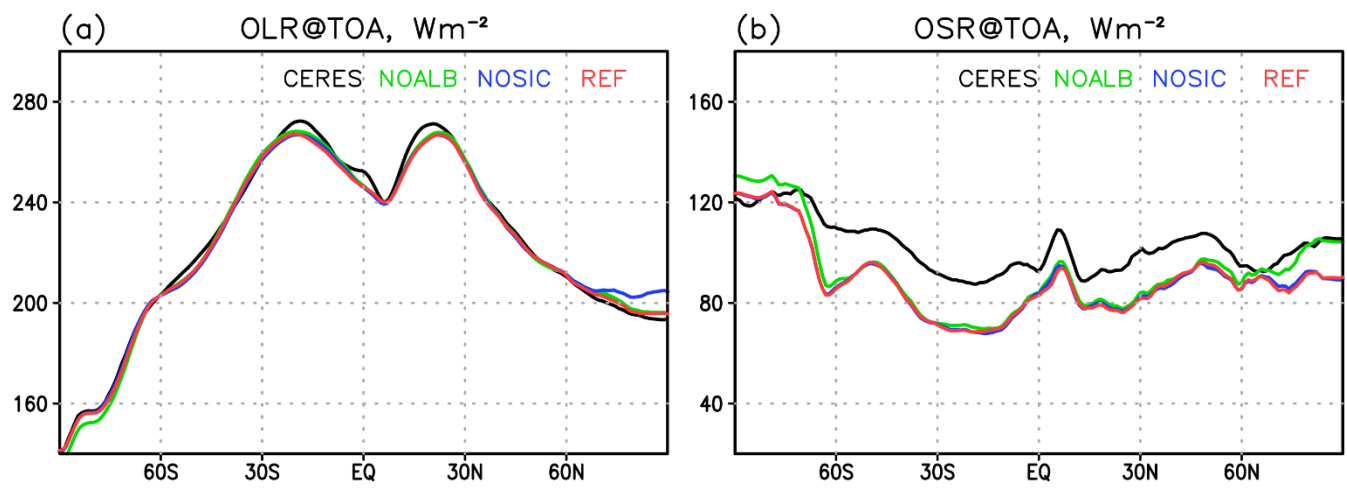
Figure 12: Same as Figure 8 but for the NOALB (green), NOSIC (blue), and REF (red) runs by NICAM16-7S.
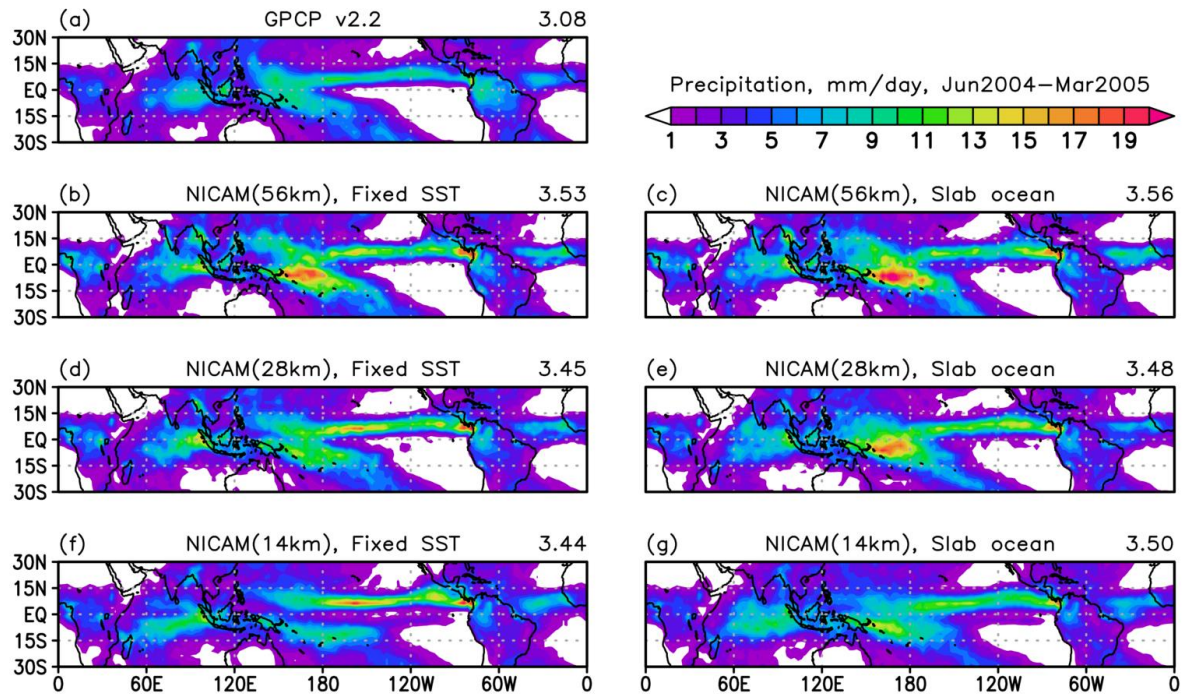
Figure 13: Annual mean precipitation during June 2004—May 2005 for ~~the~~ GPCP product (a), ~~the REFFIX NICAM with the SST boundary condition fixed to the prescribed~~runs SST (~~e~~b, ~~e~~d, ~~g~~f), and ~~the REFSLB runs~~NICAM with the slab ocean model nudged toward the prescribed SST (~~d~~c, ~~f~~e, ~~h~~g). Results from NICAM16-7S (~~e~~b, ~~d~~c), NICAM16-8S (~~e~~d, ~~f~~e), and NICAM16-9S (~~g~~f, ~~h~~g) are shown, and tropical mean precipitation ~~are~~ is noted at the top-right corner of each panel.
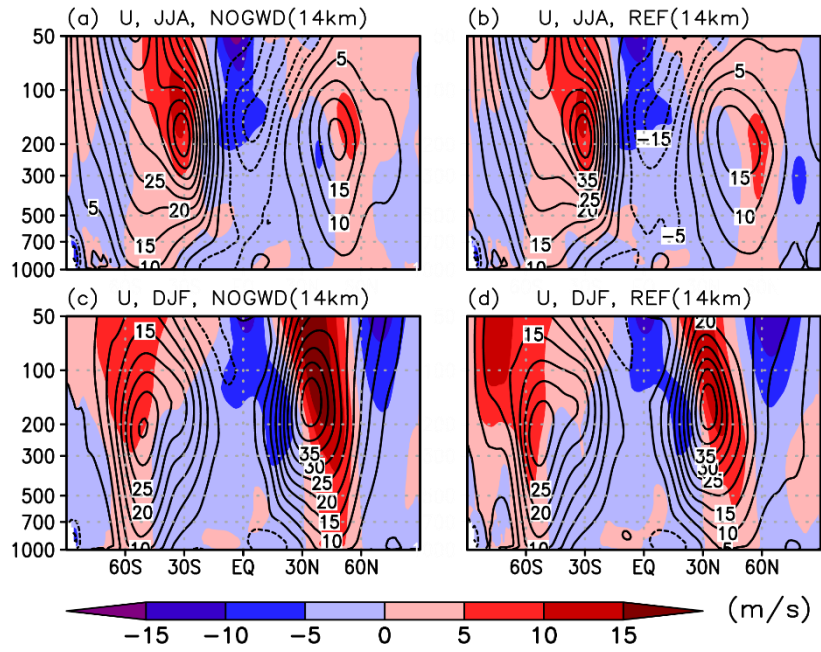
Figure 14: Zonal mean zonal wind (contour~~s~~) and its bias from JRA-55 reanalysis (~~shaded~~shadings) for June~~—~~August 2004 (a, b) and December 2004~~—~~February 2005 ~~as~~ simulated by NICAM16-9S~~14 km mesh model~~ without (a, c~~; NOGWD run~~) and with ~~the gravity wave drag scheme~~ (b, d~~; the REF run~~) the gravity wave drag scheme.

5
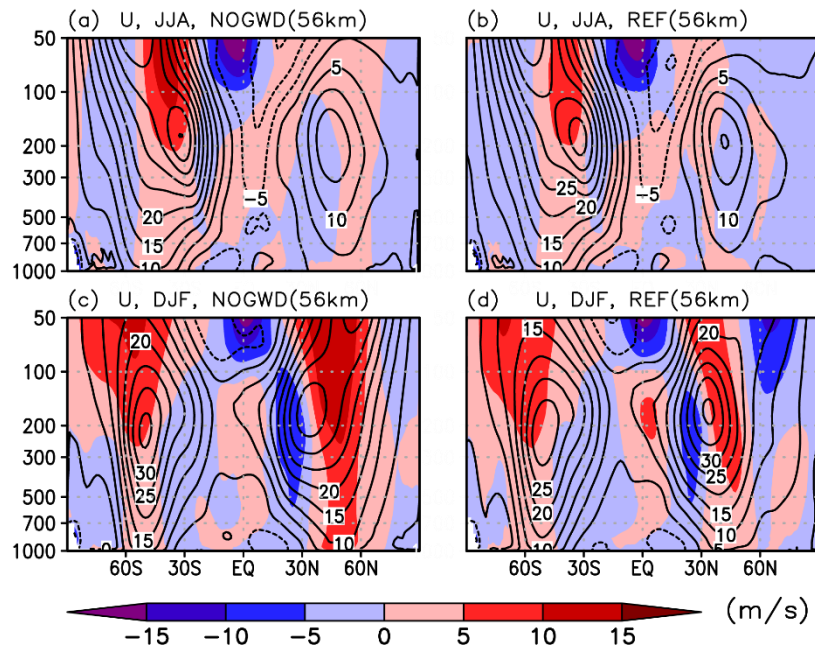
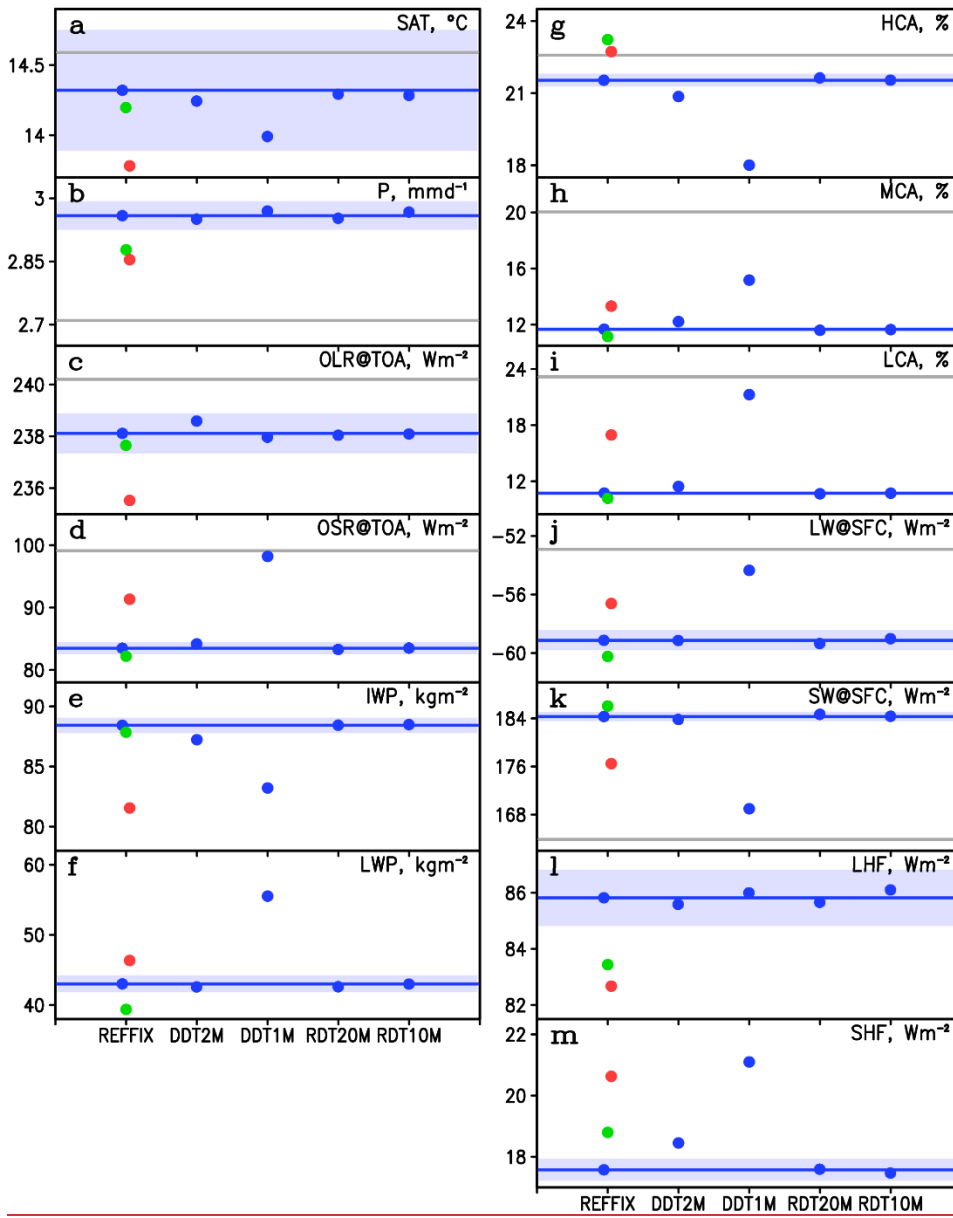**Figure 15: Same as Figure 14 but for the simulation by NICAM16-7S~~56 km mesh model~~.**

Figure 16: Same as the left part of Figure 5 but for the REFFIX, DDT2M, DDT1M, RDT20M, and RDT10M runs.
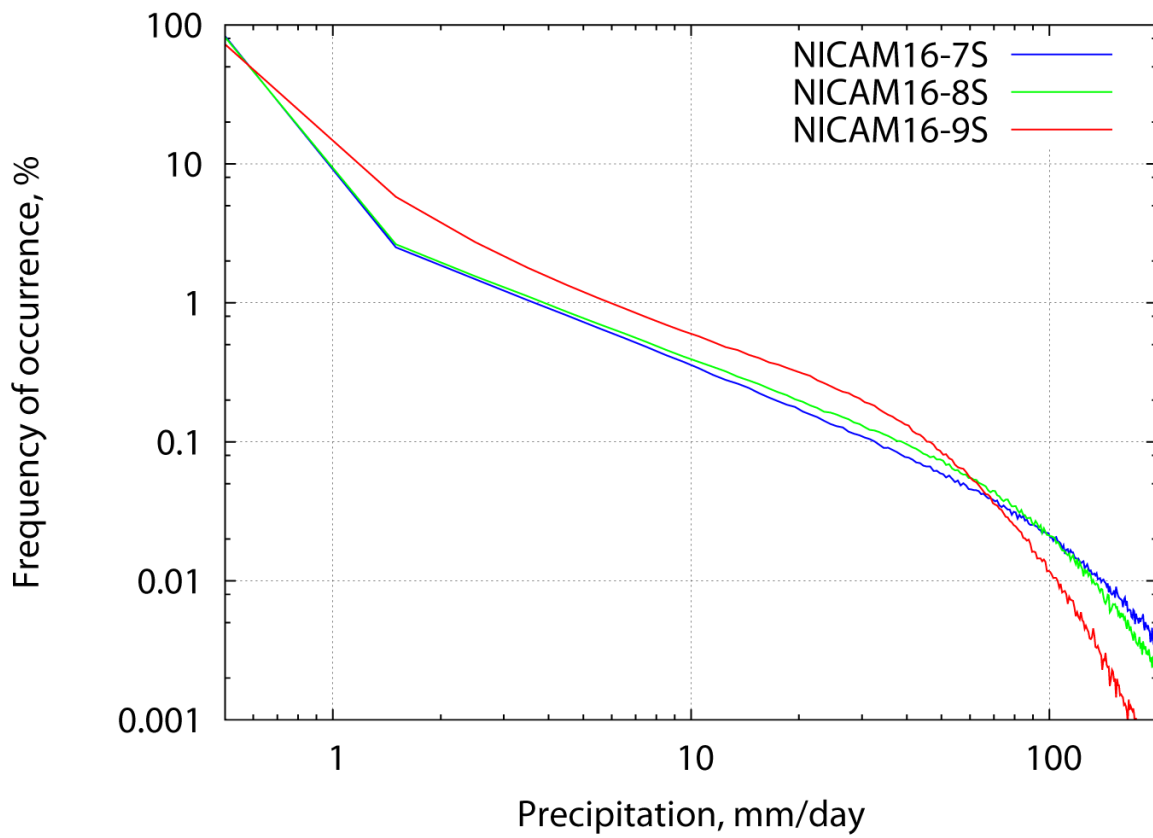
5

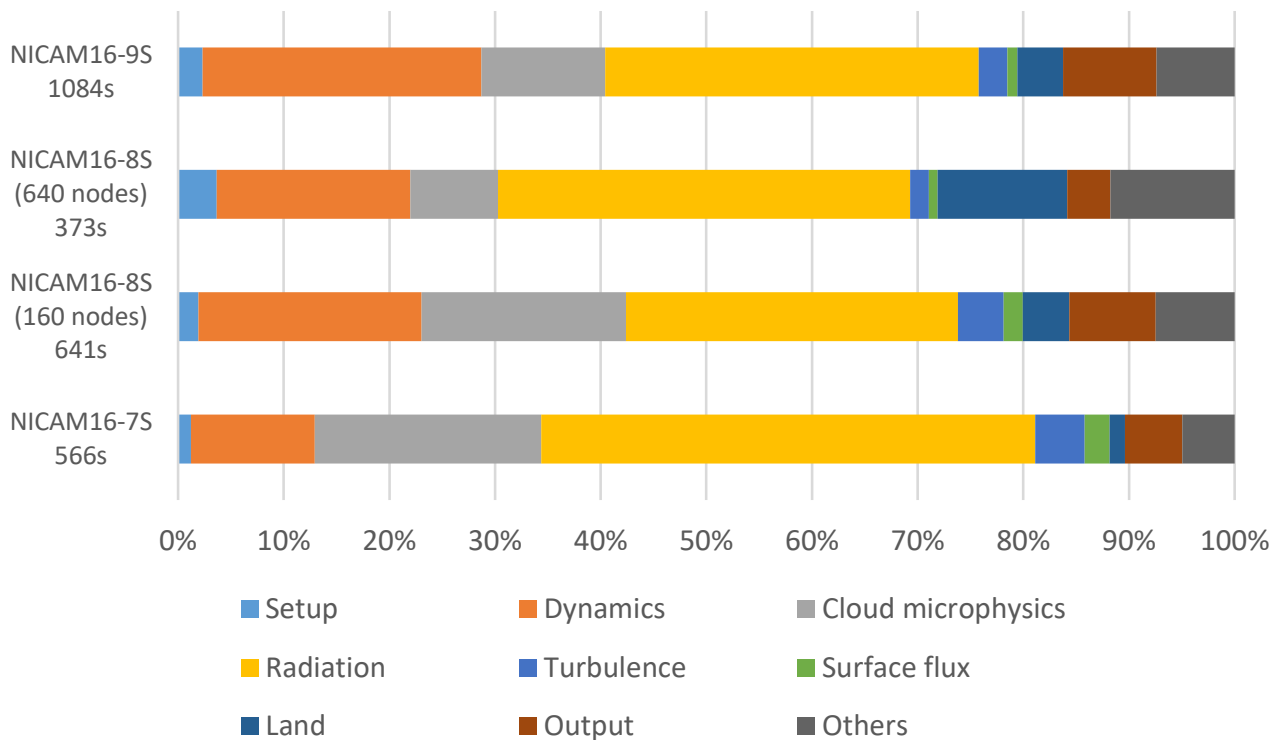Breakdown of the elapsed time
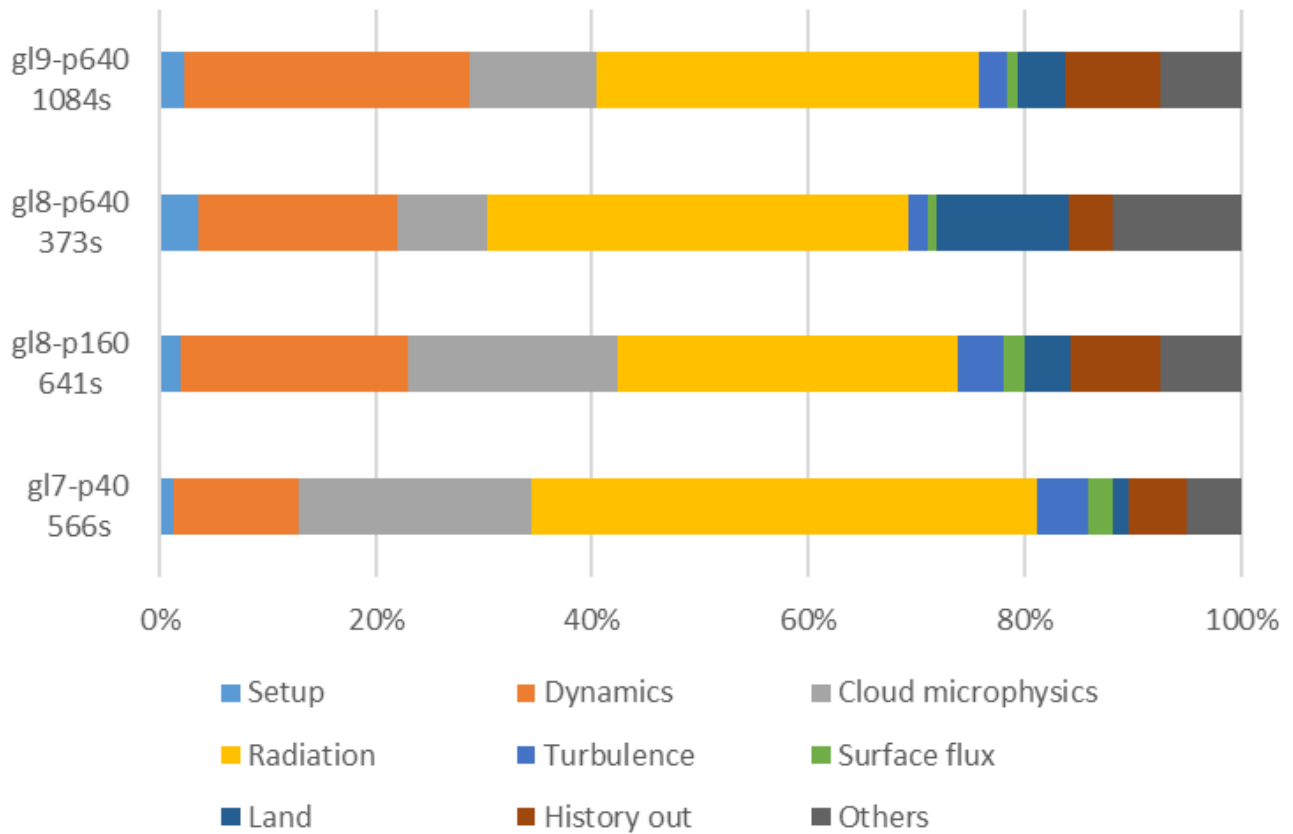
Elapsed time

Figure 18: Percentage of ~~the~~ **elapsed time for each component of NICAM16-S on the Earth Simulator 3.** ~~Times~~ ~~They a~~**we**~~re~~ **sampled from** ~~6~~ **6-month simulations (1 July 2004–31 December 2004). The computational time per** ~~1~~ **1-day integration is shown on the left.**